

**The Role of Age in Cellular Responses to  
Microenvironmental Cues as a Breast Cancer  
Susceptibility Factor**

*Fanny Pélissier*

DISSERTATION FOR THE DEGREE OF PHILOSOPHIAE DOCTOR (PHD) AT  
THE UNIVERSITY OF BERGEN



supervised by

Prof. James LORENS

University of Bergen, Norway

And Dr. Mark LABARGE

Lawrence Berkeley National Laboratory, Berkeley, California

Public defense date: May 9<sup>th</sup> 2016

Opponent: Prof. Thorarinn GUDJONSSON, University of Iceland

Opponent: Prof. Karl-Johan MALMBERG, University of Oslo

Committee Member: As. Prof. Camilla KRAKSTAD, University of Bergen

© Copyright Fanny Pélissier

The material in this publication is protected by copyright law.

Year: 2016

Title: The Role of Age in Cellular Responses to Microenvironmental Cues as  
a Breast Cancer Susceptibility Factor

Author: Fanny Pélissier

Print: AiT Bjerch AS / University of Bergen

*This dissertation is dedicated to my fiancé Thibault whose unconditional love and encouragement have been my source of inspiration and motivation, and have heartened me to pursue an academic career.*

## Acknowledgements

Foremost, I would like to express my sincere gratitude to my advisor Prof. Jim Lorens whose selfless time and care were sometimes all that kept me going. I am thankful for his creative ideas and infallible motivation. I am deeply grateful for the unique and marvelous collaborations that I had the chance to take part in, and for the huge amount of freedom and trust conferred.

In addition, I deeply thank my co-supervisor Dr. Mark LaBarge for everything he has done for me as a mentor. I would not have been able to do this research and achieve learning in the same manner without his help and support. I could not have imagined having better supervisors for my PhD training.

My sincere thanks also go to Prof. Bernd Bodenmiller who provided me an opportunity to join his team, and who gave access to his laboratory and research facilities to learn the mass cytometry technique. Without his and his team's precious support it would not have been possible to conduct this research.

Besides my advisors, I would like to thank the rest of my committee members: Prof. Thorarinn Gudjonsson, Prof. Karl-Johan Malmberg, and As. Prof. Camilla Krakstad, for accepting to be my opponents and my committee member to widen my research horizons from various perspectives.

I thank my fellow labmates for the stimulating discussions, for teaching me numerous lab techniques, and for all the fun we have had in the last four

years. In particular, I am grateful to Sissel Vik Berge for an invaluable technical assistance. I also thank Kasia for the animal training, Brith from the Molecular Imaging Center and Agata for their help with my experiments and their friendship. I thank Ana for the invaluable scientific discussions. I also thank Dr. Amra Grudic-Feta for her help in the PhD submission process.

There are no words sufficient enough to thank my friend Cédric for his unyielding support.

I would also like to thank my family: my parents and my brothers for supporting me spiritually throughout my PhD and my expat life in general.

Finally, I thank Thibault for the invaluable statistical and scientific discussion and guidance. You would deserve to be a co-author in all of my publications. We make a great team!

*In memory of Simone Péliissier (1934-2014) and Juliette Philippe (1929-2014)*

## Scientific Environment

This work was a collaboration between the Department of Biomedicine at the University of Bergen, Norway, and the Lawrence Berkeley National Laboratory (LBNL), Berkeley, California, under the supervision of Prof. James Lorens and Dr. Mark LaBarge during the period 2012-2016. Financial support was provided by a research fellowship from the University of Bergen. A financial support for a stay abroad was obtained to collaborate with Prof. Bernd Bodenmiller at the University of Zürich (UZH).



---

## Abbreviations

AMOT	Angiomotin
ANKRD1	Ankryn repeat domain 1
ARF	Alternate reading frame protein
AT	Ataxia telangiectasia
Atg7	Autophagy-related gene 7
BMP	Bone morphogenic protein
BRCA1	Breast cancer 1
<i>C. elegans</i>	<i>Caenorhaditis elegans</i>
CTGF	Connective tissue growth factor
Cyr61	cystein-rich angiogenic inducer 61
D1	CyclinD1/CDK2
DDR	DNA damage response
DSB	Double-strand break
ECM	Extracellular matrix
EMT	Epithelial to Mesenchymal transition
ER	Estrogen receptor
ER	Endoplasmic reticulum
FA	Focal adhesion
FACS	Fluorescence activated cell sorting
F-actin	Filamentous actin
FAK	Focal adhesion kinase
Gla	Gamma-carboxyglutamic acid
GSC	Germline stem cell
HER2-E	HER2-Enriched
HMEC	Human mammary epithelial cell
Hpo	Hippo
HSC	Hematopoietic stem cell
ICP-TOF-MS	Inductively coupled plasma time-of-flight mass spectrometry
IL	Interleukin
iPSC	Induced-pluripotent stem cell
JNK	Jun N-terminal kinase
K	Cytokeratin
LATS	Large tumor suppressor kinase
LEP	Luminal epithelial

lrECM	Laminin-rich ECM
LSK	Lin-Sca-1+cKit+
MCB	Mass-tag cellular barcoding
MEP	Myoepithelial
MLC	Myosin light chain
MMP	Matrix metalloproteinase
MPP	Multipotent progenitor
MSC	Mesenchymal stem cell
MST	Mammalian Ste20-like kinase
NK	Natural killer
NMR	Naked mole rat
NPC	Neuronal progenitor cells
NSC	Neural stem cell
p16sh	p16 shRNA
Pa	Pascal
PA	Polyacrylamide
PD	Population doubling
PGC-1	Proliferator-activated receptor gamma coactivator 1
pRb	Retinoblastoma protein
ROS	Reactive oxygen species
SAC	Stress activated channels
SAM	Senescence accelerated mouse
SASP	Senescence-associated secretory phenotype
SF	Stress fiber
SVZ	Sub-ventricular zone
TAM	Tyro/Axl/Mer
TAZ	Transcriptional co-activator with PDZ-binding motif
TDLU	Terminal duct lobular unit
TEAD	TEA domain family member
TEB	Terminal end bud
TKI	Tyrosin kinase inhibitor
tSNE	t-distributed stochastic neighbor embedding
VDCC	Vitamin K dependent carboxylase complex
VKORC1	Vitamin K 2,3-epoxide reductase complex subunit 1
y	Years old
YAP	Yes-associated protein

## Abstract

Aging is the critical risk factor for many forms of cancer. We used the mammary gland as a model system to study the impact of age on human epithelia in which age is the greatest risk factor for cancer. Dysfunctional progenitor and luminal cells with acquired basal cell properties accumulate during aging for reasons that are not understood. We evaluated the hypothesis that a novel effect of aging is a defective stem cell regulation by the microenvironment. We identified Axl as a previously unappreciated mammary stem cell marker involved in breast epithelial homeostasis and breast cancer progression. We showed that Axl is a marker of a subpopulation of cKit epithelial progenitors. These progenitors are tightly regulated by the microenvironment, specifically the mechanical properties of the niche. We observed that mechano-response mechanisms in cKit progenitors are altered with age. Thus, tissue-level phenotypes of aging in breast may arise in part due to alterations in the Hippo mechano-signal transduction pathway that lead to reduced efficiency of YAP/TAZ activation. Finally, using mass cytometry, we described the first high-dimensional phenotypic heterogeneity in normal human mammary epithelial cells. Computational analysis using unsupervised population partitioning identified clusters of a specific subset of luminal cells that acquired a more basal phenotype and accumulate with age. Moreover, distinct age-related phenotypic signatures were detectable in cKit-progenitor cells, considered the cell-of-origin for breast cancers. Here, we propose a model where reciprocal interactions between the microenvironment and breast epithelial progenitors are skewed during the aging process, leading to a decrease in breast tissue integrity, and increase in phenotypic divergence and susceptibility to tumorigenesis.

## List of Publications

**I-** Engelsen AST\*, Wnuk-Lipinska K\*, **Pélissier FA**, Tiron C, Bougnaud S, Haaland G, Miyano M, Aziz SM, Falk RS, Stampfer MR, Brekken RA, Straume O, Akslen LA, LaBarge MA\*, Lorens JB\*

*Multipotent mammary stem cell activity requires Axl receptor tyrosine kinase in mice and humans.* Submitted.\* Equal contribution

**II-** **Pélissier FA**, Garbe JC, Ananthanarayanan B, Miyano M, Lin CH, Jokela T, Kumar S, Stampfer MR, Lorens JB, LaBarge MA

*Age-related dysfunction in mechanotransduction impairs differentiation of human mammary epithelial progenitors.* Cell Reports 2014 Jun 26;7(6):1926-39

**III-** **Pélissier FA**, Schapiro D, Chang H, Borowsky AD, Parvin B, Bodenmiller B†, LaBarge MA†, and Lorens JB†

*High dimensional analysis of age-related phenotypic diversity in human mammary epithelial cells.* Manuscript.† Equal contribution

## Contributions

- Lin CH, **Pélissier FA**, Zhang H, Lakins J, Weaver VM, Park C and LaBarge MA. *Microenvironment rigidity modulates responses to the HER2 receptor tyrosine kinase inhibitor lapatinib via YAP and TAZ transcription factors.* Molecular Biology of the Cell, 2015
- Sputova K, Garbe JC, **Pélissier FA**, Chang E, Stampfer MR and LaBarge MA. *Aging phenotypes in cultured normal human mammary epithelial cells are correlated with decreased telomerase activity independent of telomere length.* Genome Integrity, 2013

The published paper is reprinted with permission from Elsevier. All rights reserved.

---

# Contents

Acknowledgments	4
Scientific Environment	6
Abbreviations	7
Abstract	9
List of Publications	10
<b>1 Introduction</b>	<b>13</b>
1.1 The use of animal models to identify the hallmarks of aging . . .	14
1.2 Stem cell and aging . . . . .	18
1.3 The stem cell niche . . . . .	23
1.4 Effect of aging on niche microenvironment and stem cells . . .	30
1.5 Human models to study aging . . . . .	33
1.6 Breast cancer as a model of aging disease . . . . .	35
1.6.1 Defining the mammary gland . . . . .	35
1.6.2 Axl may represent a breast stem cell marker . . . . .	39
1.6.3 Normal mammary gland changes with aging . . . . .	41
1.6.4 Post-menopausal breast cancer . . . . .	43
1.6.5 Treatments of post-menopausal breast cancer . . . . .	44
1.6.6 Understanding the breast aging process at the cellular level . . . . .	46
<b>2 Hypothesis and Aims</b>	<b>50</b>
<b>3 Summary of Results</b>	<b>52</b>

<b>4</b>	<b>Methodological Considerations</b>	<b>59</b>
4.1	Human mammary epithelial cells . . . . .	59
4.2	Cell segmentation with Matlab . . . . .	61
4.3	Immortalized cell lines . . . . .	63
4.4	Mouse models . . . . .	63
4.5	Ensemble-averaged measurements can mask information contained in heterogeneity . . . . .	65
4.6	Mass cytometry . . . . .	65
<b>5</b>	<b>Discussion</b>	<b>69</b>
5.1	The role of Axl in normal mammary gland . . . . .	69
5.2	Matrix stiffness exquisitely directs mammary progenitor differentiation . . . . .	72
5.3	Immortalization restores responsiveness to physiological stiffness in older HMEC . . . . .	73
5.4	The role of the Hippo pathway in age-related mechanoresponses	74
5.5	The paradox of mammographic density and breast cancer risk	75
5.6	The mammary gland exhibits an extensive range of heterogeneity	76
5.7	Luminal cells exhibit basal characteristics with age . . . . .	77
5.8	Evidence of age-dependent phenotypic divergence in HMEC progenitors . . . . .	79
5.9	Breast cancer susceptibility and prevention . . . . .	80
<b>6</b>	<b>Concluding Remarks</b>	<b>82</b>
<b>7</b>	<b>Future Perspectives</b>	<b>83</b>
<b>8</b>	<b>References</b>	<b>84</b>

# 1 Introduction

Aging is a universal trait that is observed across the evolutionary spectrum. Owing to increased lifespan and declining fertility, the world population aged over 60 is anticipated to reach 21.8% of the total population by 2050 (Lutz et al., 2008). Our species continues to live longer than seen in recorded history, but from a public health perspective, aging is also the critical risk factor for a range of human pathologies, including neuro-degenerative diseases, metabolic diseases and many forms of cancer (Holliday, 2004). Understanding the molecular processes that deteriorate with age and that are responsible for increased disease susceptibility is critical to reach the growing health care needs of aging human populations.

Age is the greatest risk factor for breast cancer, but the reasons underlying this association are unclear. Women over 55 years old account for 80% of new breast cancer diagnoses and 75% of breast cancer-related deaths. Importantly, the majority of these age-related breast cancers are of luminal subtype (Jenkins et al., 2014). While there is undeniably a genetic component to all cancers, the accumulation of mutations with age is insufficient to explain the age-dependent increase in breast cancer incidence (LaBarge et al., 2015; Stephens et al., 2012). However, there are a number of known changes in the breast microenvironment (endocrine profiles, breast density, stromal composition) that are unique to aging. Indeed, there are age-associated changes in normal human mammary stem and progenitor cells that correlate with an increased potential for malignant transformation.

A major barrier to study the aging process is a lack of available model systems. In this introduction, we evaluate the different common models developed with their strengths and limitations. We discuss the possibility of a novel theory of aging as a defect in stem cell regulation by the tissue microenvironment.

Finally, we apply these ideas to understand the role of aging on breast cancer susceptibility.

### **1.1 The use of animal models to identify the hallmarks of aging**

Aging is the result of an evolutionary trade-off. The antagonistic pleiotropy hypothesis was first introduced by George C. Williams in 1957 (Williams, 1957). Pleiotropy defines the phenomenon that a single gene controls more than one phenotype. Williams proposed that aging is caused by the combined effect of many pleiotropic genes that had a beneficial effect on the organism's fitness to increase reproduction in early life but also had an adverse effect in older age. Thus, an antagonistically pleiotropic gene can be selected for if it has advantageous effects in early life despite having negative effects in later life (Carter and Nguyen, 2011). It explains in part why organisms are never able to reach biological perfection (perfect adaptive fit) through natural selection as deleterious genes are still selected and propagated.

The modern history of the use of animal models began with the research of Clive McCay, a nutritionist in the 1930s. In the course of research on cancer, his group discovered that severe calorie restriction resulted in a significant increase in the lifespan of rats (McCay et al., 1935). Thirty years ago, a new era in aging research was initiated following the isolation of the first strains in *Caenorhabditis elegans* (*C. elegans*) with extended lifespan (Klass, 1983). A range of other non-mammalian systems have been used such as yeast, drosophila, ants, and fish (Conn, 2011). Domesticated species, such as dogs and cats, represent interesting aging model systems. Although the average

canine lifespan of 10-12 years discourages longevity studies, dogs spontaneously develop many age-related phenotypes (Fast et al., 2013). As in dogs, several age-associated phenotypes happen in felines. Lifespan studies in this species are likewise problematic (Taylor et al., 1995); however, their aging phenotype may make them attractive models.

We share more than 90% of our genome with the mouse (Mouse Genome Consortium Sequencing, 2002) and the ease with which its genome can be manipulated and analyzed, makes the mouse a convenient system to translate knowledge from lower organism models into mammalian species. Therefore, a number of mouse aging models have been generated. For instance, the senescence accelerated mouse (SAM) strains of mice showed different degree of loss of activity, hair loss and early death (Takeda, 1999). A mouse model of ataxia telangiectasia (AT) was created by disrupting the *Atm* gene. This AT phenotype is similar to the human AT phenotype which has a wide variety of clinical manifestations including premature aging (Barlow et al., 1996). In addition, other mutant models of mice have been reported to have a significant increase in lifespan (reviewed in (Liang et al., 2003)). The naked mole rat (NMR) is a non-genetically engineered model of murine aging and is the longest-living rodent known to man, with a maximum lifespan of approximately 30 years (Jarvis, 1981). NMRs aged over 24y do exhibit signs of aging consistent with human. However, rodents have been separated from humans for more than eighty million years with distinct evolutionary pressures. Many significant differences in processes implicated in aging and immortalization exist between human cells and cells derived from rodent model systems. For example, in contrast to human tissues, most mouse tissues have active telomerase which may explain the high frequency

of spontaneous immortalization in culture of mouse cells compared to human (Prowse and Greider, 1995). Moreover, the roles of the cyclin-dependent kinase inhibitors are drastically distinct in the two species:  $p16^{INK4a}$  takes center stage in senescence (described below) and tumor suppression in human cells, whereas alternate reading frame protein (ARF) assumes a more important role in mouse cells. In a comparable way, retinoblastoma protein (pRb) suppresses  $p16^{INK4a}$  expression in human but not mouse (Gil and Peters, 2006). Thus, the mouse model might not be an ideal aging model and a focus on longitudinal studies might be essential. Another species with close evolutionary affinity and similarity (compared to rodents) are the non-human primates. The human relevance of health diseases associated with aging in primates is unparalleled. Transgenic primate models have now been generated, and useful models for studying genetic pathways involved in aging could therefore be modulated (Yang et al., 2008). However, their long lives and complex social needs make primate aging research challenging and expensive. Currently, primate research is conducted in only a small number of laboratories.

As a model of aging, August Weismann suggested that multicellular organisms become more fragile with age due to a mechanism that limits the proliferative potential of the cells (Weismann, 1889). This cell condition has been described in human fibroblasts in culture and is known as senescence (Hayflick, 1965; Hayflick and Moorhead, 1961) which is the irreversible arrest of cell proliferation. Cells become senescent following the detection of DNA damage and the activation of persistent DNA damage response (DDR) (d'Adda di Fagagna, 2008) and oncogenic stimuli. Telomeres at the end of chromosomes shorten during mitosis, eventually become too short and are

recognized as DNA damage, causing cells to become senescent (d'Adda di Fagagna et al., 2003; Herbig et al., 2004). There is increasing evidence regarding the importance of cellular senescence as prevention against cancer (Serrano et al., 1997). This tumor suppressive mechanism contributes to aging by reducing the regenerative capacity of tissues and by degrading tissue structures, as senescent cells accumulate with age and secrete inflammatory cytokines and tissue remodeling enzymes. For instance, the pro-inflammatory cytokines interleukin (IL)-6 and IL-8 stimulate malignant phenotypes (Campisi and d'Adda di Fagagna, 2007). Do senescent cells reflect the aging process? Or do they contribute to the aging process and age-related diseases? There are no definitive answers to these questions.

Recent work on human mammary epithelial cells (HMEC) cultured *in vitro* revealed two distinct senescence barriers: stasis, resulting from chronic or acute stress, and telomere dysfunction due to telomere attrition (Garbe et al., 2009). Finite lifespan HMEC are also vulnerable to oncogene-induced senescence (OIS). Some HMEC may cease growth as a consequence of terminal differentiation. Thus, cellular senescence in culture might be attributed to cell culture conditions and stress rather than aging *per se*. Accumulated data support the notion that the loss of telomere repeats in cells contributes to human aging (reviewed in (Aubert and Lansdorp, 2008)). This notion is not widely accepted, primarily because the average telomere length varies a lot between species and individuals of the same age. Moreover, there were no associations between telomere length and age in HMEC (Sputova et al., 2013). The accumulation of senescent cells in tissues and organs with age might be attributed to an increased production of various stimuli that induce senescence (Garinis et al., 2008). Alternatively,

the elimination of senescent cells may decrease with age due to the alteration of the immune system with aging (reviewed in (van Deursen, 2014)).

Simple model organism to higher level mammalian species models in aging research permitted the recent categorization of nine hallmarks that contribute to the aging process (reviewed in ((López-Otín et al., 2013))). These hallmarks are: genomic instability, telomere attrition, epigenetic alterations, loss of proteostasis, deregulated nutrient sensing, mitochondrial dysfunction, cellular senescence, stem cell exhaustion, and altered intercellular communication (Figure 1). Because stem cells regenerate adult tissues and contribute to the development of cancer, age-related changes in stem cells likely contribute to age-related diseases. Evidence is emerging regarding hallmarks of aging at the stem cell level.

## 1.2 Stem cell and aging

In many tissues, homeostatic maintenance and regenerative responsiveness to injury depend on tissue-specific stem cells: long-lived cells with the capacity to both self-renew and differentiate to produce mature daughter cells. The ability of tissue stem cells to balance quiescence with proliferation appears to be critical for their survival and maintenance of appropriate physiological and regenerative responses (reviewed in (Cheung and Rando, 2013)). Stem cells in many tissues undergo profound changes with age, exhibiting dulled responsiveness to tissue injury, misregulation of proliferative activities and declining functional capacities (reviewed in (Signer and Morrison, 2013)). These changes result into reduced effectiveness of cell and tissue regeneration in aged organisms. In the quest for understanding their alteration with aging, analysis of stem cells in diverse tissues showed the presence of the nine

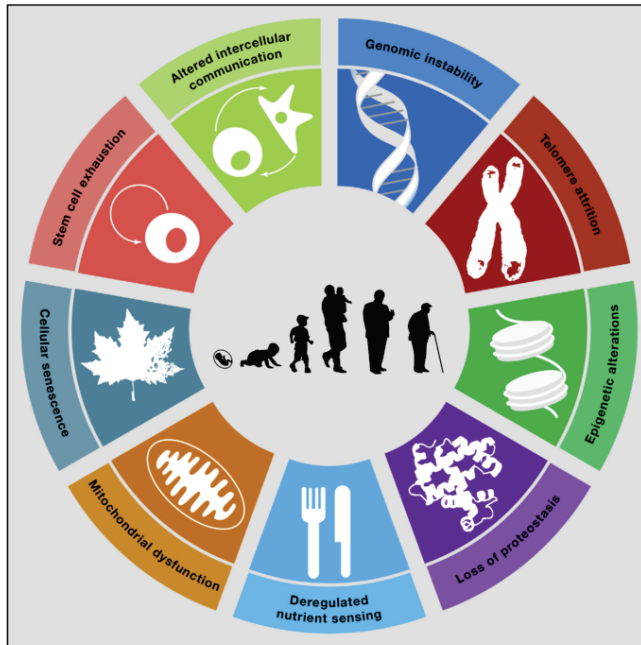


Figure 1: **The nine hallmarks of aging.** The scheme enumerates the nine hallmarks of aging: genomic instability, telomere attrition, epigenetic alterations, loss of proteostasis, deregulated nutrient sensing, mitochondrial dysfunction, cellular senescence, stem cell exhaustion, and altered intercellular communication. While these hallmarks are identified at the cellular level, a light is shed on the hallmarks of aging at the stem cell level. From (López-Otín et al., 2013).

hallmarks of aging (Figure 2). Pathways induced by reactive oxygen species (ROS) which "leak" during mitochondrial activity, appear to contribute to perturbed stem cell functions in the context of aging (Pervaiz et al., 2009; Takubo et al., 2013; Yu et al., 2013). In addition, DDR pathway showed

reduced activity in stem cells with age (Moskalev et al., 2013). Thus, the accumulation of damage in the cells eventually reaches a threshold, resulting in altered stem cell function in aged animals. Proteostasis (protein homeostasis) has been implicated as an important factor of stem cell maintenance through studies in hematopoietic stem cells (HSCs). Autophagy is a lysosomal degradation pathway which prevents cellular damage. *Autophagy-related gene 7 (Atg7)* is an essential autophagy gene and deletion of *Atg7* leads to an increase in ROS levels and reduces HSCs function, although the overall Lin-Sca-1+cKit+ (LSK) compartment was expanded (Mortensen et al., 2011). Moreover, autophagy induction by FoxO3A is an essential mechanism that protects HSCs from metabolic stress during aging (Warr et al., 2013). Another hallmark of aging implicates mitochondria function in stem cells. Over-expression of peroxisome proliferator-activated receptor gamma coactivator 1 (PGC-1) stimulates mitochondrial activity. PGC-1 delays the age-dependent decline in intestinal stem cells in drosophila and extends longevity in old flies (Rera et al., 2011), although its role in mammalian stem cells needs further investigation.

Epigenetic regulation is important in determining stem cell function. Alterations in the epigenome that occur with age can disturb cellular functions in aged stem cells. Epigenetics include modifications of histone proteins, RNA and DNA methylation. The most common form of DNA methylation is the addition of a methyl group to the 5' cytosine of C-G dinucleotides, denoted CpGs. Epigenetic clock defines DNA methylation levels at specific sites in the genome that are correlated with age (Horvath et al., 2012). Epigenetic clock sites show a relationship between age and DNA methylation that is consistent between individuals (Hannum et al., 2013). For instance, aging HSCs show increases in DNA methylation in the

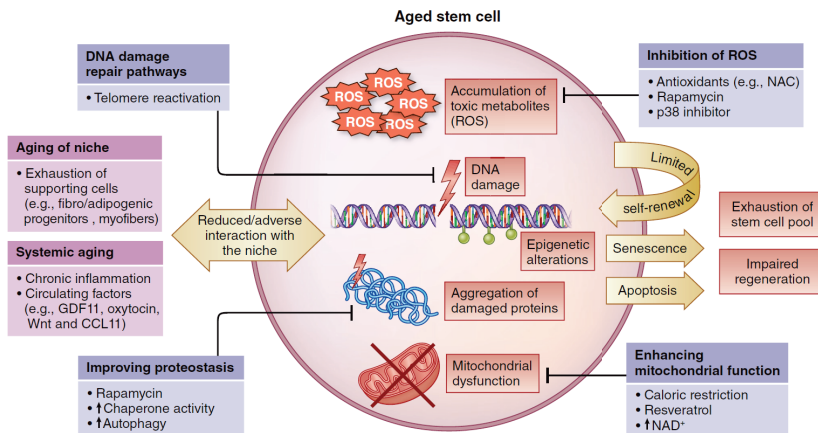


Figure 2: **The aged stem cell.** The cartoon shows the common pathways contributing to stem cell loss and dysfunction in the aging process. The nine hallmarks of aging have been identified at the stem cell level. From (Oh et al., 2014).

regions of the genome important for lineage-specific gene expression (Beerman et al., 2013). Cellular senescence is another hallmark of stem cell aging as HSCs from older donors exhibit increased senescence (Stenderup, 2003). Moreover, depletion of  $p16^{INK4a}$  expressing cells in mice extended their life-span and attenuated age-related diseases (Baker et al., 2016). Thus, in some cases these aging-associated phenotypes can be reversed to restore the regenerative function of stem cells (reviewed in (Oh et al., 2014)). As one of the hallmarks of aging, stem cell exhaustion may also be driven by an imbalance of stem cell quiescence and proliferation. It is crucial to maintain this balance to preserve the stem cell pool through multiple rounds of tissue regeneration (Mansilla et al., 2011).

Conversely, a functional decline is not necessarily caused by a loss of the ability to self-renew but may also reflect an inability of stem cell progeny to properly differentiate, resulting in the accumulation of non-fully differentiated cells and an increased potential for oncogenic transformation. Elevated Jun N-terminal kinase (JNK) activity in intestinal stem cells causes a misregulation of cell differentiation leading to a stem cell pool accumulation (Biteau et al., 2008). In addition, cells from the gastrointestinal tract from older mice exhibit reduced regenerative potential despite an increase in the number of crypt cells (Martin et al., 1998). In addition, high levels of the inflammatory cytokine Rantes are found in the aging stem cell milieu, resulting in a decrease in T-cell progeny concomitant with an increase in myeloid progenitors (Ergen et al., 2012). As a comparison, the number of HSCs in the bone marrow increases with age (Beerman et al., 2010, 2013; Challen et al., 2010) with no difference in cycling activity and aging skews differentiation potential toward myeloid lineages (Geiger et al., 2013). Astroglial neural stem cells (NSCs) in the sub-ventricular zone (SVZ) give rise to transit-amplifying progenitors. A progressive age-related cognitive impairment has been observed in different species. This is correlated with decay in the number of NSCs and accumulation of transit-amplifying progenitors (Encinas et al., 2011; Lugert et al., 2010). These changes correlate with a discrepancy to produce newborn neurons in the aged brain.

Intuitively, increased stem cells may seem beneficial. However, this accumulating pool of stem cells is functionally impaired and may be more susceptible to oncogenic events. In conclusions, tissue stem cells progressively

experience cell-intrinsic alterations that profoundly affect their regenerative function with aging. In addition, extrinsic age-related alterations in the microenvironment are attributed to tissue homeostasis disruption. Stem cells reside in specialized microenvironments, called niches that promote their maintenance and regulate their functions. Aging of niche cells and age-dependent alterations in the components of stem cell niches can cause damaging changes in stem cell function.

### **1.3 The stem cell niche**

Stem cells reside in a specific location within the tissue (for review see (Fuchs et al., 2004)). To mention but a few examples, bone marrow serves as the pioneer system for studying stem cells. Homing experiments pointed the HSC niche to the endosteal surface of the bone marrow (Nilsson et al., 2001). In the skin, the epithelial stem cell niche is located in the bulge area of the hair follicle (Cotsarelis et al., 1990; Niemann and Watt, 2002). The intestinal stem cells are proposed to be located at the fourth or fifth position from the crypt bottom, above the Paneth cells (Barker et al., 2007). Neural stem cells reside in the SVZ of the adult mammalian brain (Qian et al., 1998). In the muscle, skeletal satellite cells are positioned between the basal lamina and the plasma membrane of muscle fibers (Muir et al., 1965). In mice, the location of mammary gland stem cells is not well defined, but was narrowed down to the peripheral cap cells of the terminal end buds (reviewed in (Woodward et al., 2005)). However, a human breast epithelial stem cell zone *in vivo* and a progenitor hierarchy both inside and outside this zone have been identified (Villadsen et al., 2007).

A microenvironment is defined by the sum of cell-cell, extracellular matrix (ECM), and cell-soluble factor interactions, in addition to its architecture and physical constraints that are experienced by a cell. There is increasing evidence that the microenvironment regulates stem cell and progenitor fate. For instance, progenitors in skin and skeletal muscle can exhibit homing to vacated stem cell niches and reacquire stem cell traits (Collins et al., 2005; Nishimura et al., 2002; Sacco et al., 2008). Mimetic combinatorial microenvironments reveal a quantification of adult stem and progenitor cell fate decisions (LaBarge et al., 2009; Soen et al., 2006). Moreover, previous work showed that stem cell niche microenvironments regulate stem cell functions (LaBarge et al., 2007). The ECM provides support to the tissue in addition to regulate its homeostasis via different mechanisms (Figure 3). Anchorage to the basement membrane is essential for diverse biological processes, including asymmetric cell division, quiescence and maintenance of tissue polarity. Certain ECM components can selectively bind to different growth factors and function as a signal co-receptor and modulate the direction of cell-cell communication (Lu et al., 2011). The ECM also modulates signals to the cell by using its fragment processed by proteases, such as matrix metalloproteinases (MMPs). Finally, cells sense the biomechanical properties of the ECM, including its stiffness via cell mechanics, and change a wide variety of mechanoresponses accordingly. Therefore, stem cell fate and homeostasis are modulated by a combination of different microenvironment cues.

In order to understand this process, a deconstruction of each component of the niche is crucial to recapitulate their specific role. Specifically, increasing evidence support the role of ECM stiffness as a rheostat for stem cell and

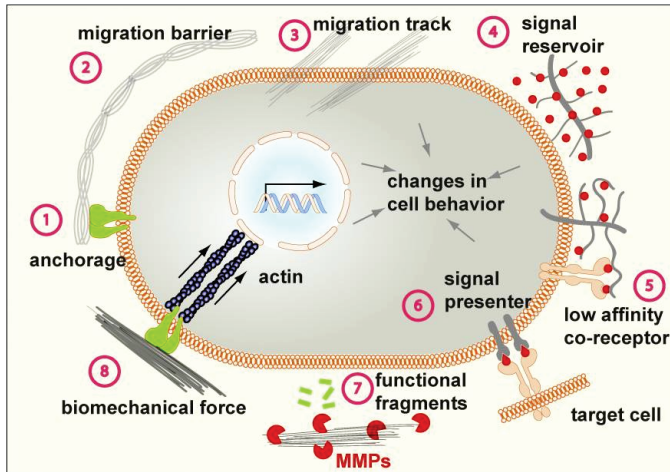


Figure 3: **Mechanisms of ECM function.** The various functions of the ECM are: 1) anchorage to the basement membrane, 2 and 3) regulation of cell migration, 4) sink of growth factor signaling molecules, 5) signal co-receptor or 6) presenter, 7) regulation of functional fragments via matrix metalloproteinases (MMP), and 8) mechanosignaling. From (Lu et al., 2012).

tissue homeostasis. The stiffness or elastic modulus measures an object or substance's resistance to being deformed elastically when a force is applied to it. Each organ has a distinct rigidity pattern, governed by the ECM stiffness and the three-dimensional architecture of the tissue. The stiffness of a mammary gland is around 160 Pascal (Pa), while muscle stiffness is 10kPa and collagenous bone stiffness is 100kPa (Reviewed in (Levental et al., 2007)). As a comparison, regular tissue culture dish stiffness is between 2 and 4GPa (Callister and Rethwisch, 2000). Studies of mesenchymal stem cell (MSC) differentiation highlighted the importance of how cells respond to different stiffness. MSC differentiate into osteoblasts when cultured on stiff

substrata, into myoblasts when grown on intermediate stiffness substrata or into neurons and adipocytes when cultured on a soft ECM (Figure 4) (Engler et al., 2006).

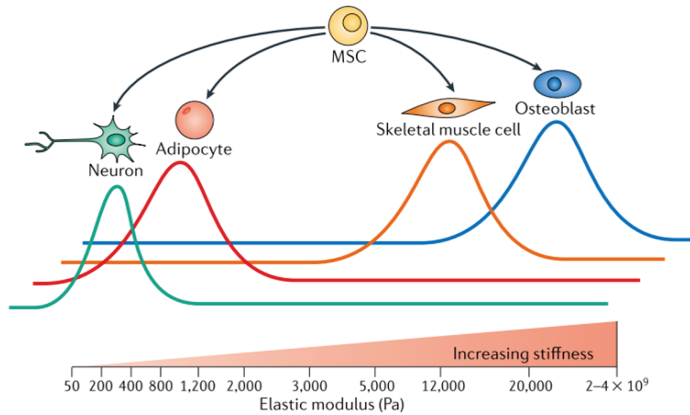


Figure 4: **Influence of mechanical and physical properties of the ECM on cell behavior.** By recapitulating different ECM elasticities *in vitro*, it was found that MSC differentiate optimally into neurons, adipocytes, skeletal muscle cells or osteoblasts at elasticities that match the physiological ECM stiffness of their corresponding natural niche. From (Halder et al., 2012).

Cell mechanics involves three steps (Figure 5). **Mechanosensing** at the molecular scale requires the ability to pull against the matrix. Sensing matrix elasticity occurs through cell-cell and ECM interactions mediated by adherens, integrins, vinculin, focal adhesion kinase (FAK), and others (Beningo et al., 2001; Bershadsky et al., 2003; Tamada et al., 2004). The actinomyosin network includes RhoA, which regulates the actin cytoskeleton in the formation of stress fibers (SF) and focal adhesions (FA). Activation of

ROCK1/ROCK2 causes increased activity of the motor protein myosin II by phosphorylation of the myosin light chain (MLC) and inactivation of the MLC phosphatase (Ishizaki et al., 1997; Kimura et al., 1996). Vinculin and talin are part of a FA complex-based mechanosensing mechanism and are capable of unfolding under physiological force. Talin binds to integrins and actin, upon unfolding, expose domains for vinculin which has itself a force-dependent activation (Golji et al., 2011). Mechanosensing through stretch activated channels (SAC) are reviewed in (Holle and Engler, 2011). In addition, the contractile forces exerted by filamentous actin (F-actin) cables and their associated myosin motors are responsible for generating tension in cells (Schwartz, 2010; Vogel and Sheetz, 2006). Next,

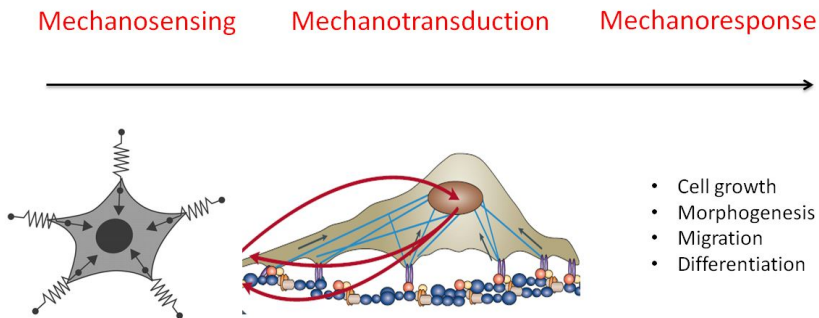


Figure 5: **Cell mechanics.** Cell Mechanics involves three steps: mechanosensing, mechanotransduction and mechanoresponse. Adapted from (Bischofs and Schwarz, 2003; Vogel and Sheetz, 2006).

**mechanotransduction** signals relay the sensing cues to the nucleus. The Hippo pathway was originally identified as the signaling that control organ size in drosophila. The pathway takes its name from the main signaling components Hippo (Hpo). Mutations in this gene lead to tissue overgrowth,

or a “hippopotamus”-like phenotype (Wu et al., 2003). The transcription co-activators Yes-associated protein (YAP) and transcriptional co-activator with PDZ-binding motif (TAZ also known as WWTR1) belong to the Hippo pathway, and recently emerged as key mediators of mechanotransduction. Upon activation of the Hippo pathway, mammalian Ste20-like kinases (MST1 and MST2) phosphorylate and activate large tumor suppressor kinases (LATS1 and LATS2) which in turn phosphorylate YAP and TAZ (Kanaï et al., 2000; Sudol, 1994). Phosphorylated YAP and TAZ are excluded from the nucleus and accumulate in the cytoplasm where they are degraded by the proteasome. When the Hippo pathway is inactivated, YAP and TAZ are dephosphorylated, translocate into the nucleus and regulate gene transcription when associated with DNA-binding transcription factors such as TEA domain family members (TEAD) (Figure 6) (Pobbati and Hong, 2013; Zhang et al., 2009; Zhao et al., 2008). In addition, angiomin (AMOT) family proteins interact with YAP and TAZ at the tight junctions to promote their phosphorylation by the Hippo pathway (Zhao et al., 2011). YAP and TAZ are tightly linked to the actomyosin cytoskeleton, thus they not only respond to mechanical cues, but are also mediators of mechanical signals (reviewed in (Halder et al., 2012)). YAP and TAZ are the main triggers of various cell- and context- dependent **mechanoresponses**. Paired with TEADs, they upregulate the expression of several growth promoting factors. The direct targets are connective tissue growth factor (CTGF), ankryn repeat domain 1 (ANKRD1) and cystein-rich angiogenic inducer 61 (Cyr61) (Zhao et al., 2008), in addition to Ki67, Axl (Kim et al., 2013; Xu et al., 2011), c-Myc and survivin (Dong et al., 2007). CTGF has been shown to induce collagen I expression in human fibroblasts (Lin et al., 2013) which is an important ECM component. The Hippo pathway is involved in tissue

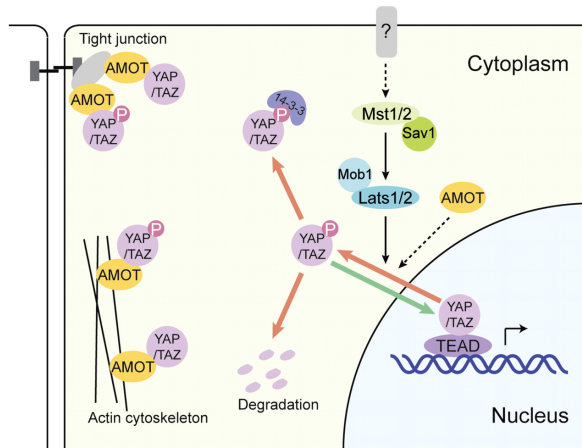


Figure 6: **A model of Hippo pathway regulation.** Phosphorylated MST1/2 phosphorylate LATS1/2 which in turn phosphorylate YAP/TAZ which are excluded from the nucleus. Nuclear YAP/TAZ associate with TEADs to activate target gene transcription. AMOT regulates YAP/TAZ localization via physical interaction and promoting YAP/TAZ phosphorylation by the Hippo pathway. From (Zhao et al., 2011).

specific stem cells, tissue homeostasis (reviewed in (Kodaka and Hata, 2015)), tissue growth control (Zhao et al., 2007) and cancer (reviewed in (Harvey et al., 2013)).

In conclusion, the stem cell niche has a specific location within a tissue and is defined by its physical constituents in addition to its molecular components and architecture. Thus, niche alteration is of critical concern. Cancer may result from errant stem or progenitor cells that were misguided by their microenvironment (Bissell and Labarge, 2005). Given the relationship between reduced stem cell activity, loss of tissue homeostasis, and aging, questions emerge. Is loss of tissue homeostasis due to an inability

of stem cells to respond appropriately to signals from the niche or reduced signaling from the niche?

#### **1.4 Effect of aging on niche microenvironment and stem cells**

Aging of the niche and its components can cause alteration in stem cell function. The number of cap cells in the testes and hub cells in the ovaries, which serve as support for germline stem cells (GSCs), decreases with age in *Drosophila*. This causes an alteration of the bone morphogenetic protein (BMP) signaling from the niche that is necessary for GSC maintenance (Boyle et al., 2007; Pan et al., 2007). Similarly, expression of glial cell-derived neurotrophic factor, which is required for normal regulation of spermatogonial stem cell self-renewal and differentiation, is reduced with age in Sertoli cells, the nurse cells of the testes (Ryu et al., 2006). Both systemic and local factors contribute to lineage skewedness of HSCs. Rante/Ccl5 cytokine has been shown to increase myeloid progenitor proliferation, and is highly expressed in the aged stem cell milieu (Ergen et al., 2012). Muscle fibers are an important source of ECM signals to regulate stem cell function. Increased levels of FGF signaling in the aged satellite cell niche lead to the loss of quiescence and depletion of the resident stem cell population, which eventually diminishes muscle regenerative capacity (Chakkalakal et al., 2012). A loss of Notch signaling induces a decline in skeletal muscle stem cell activity resulting in impaired regeneration of aged muscle (Conboy et al., 2003; Conboy and Rando, 2002). In addition to local signals, aging also causes changes in systemic factors that can impact tissue stem cells. This is the last hallmark of aging listed above. The exposure of satellite cells from old mice to young serum increased Notch activation and restored the

proliferation and regenerative capacity of aged satellite cells (Conboy et al., 2005), illustrating the role of systemic environment on stem cell function. In addition, whole-muscle transplantation between old and young rats resulted in a significant muscle regeneration only in young hosts (Carlson and Faulkner, 1989). Another group rejuvenated muscle stem cells by culturing them on hydrogels restoring strength to injured muscles from aged mice (Cosgrove et al., 2014), illustrating the predominant role of microenvironment stiffness.

The status of the ECM affects mechanotransduction, which regulates mechanical stress, cell shape, architecture and signaling. With aging, a persistent inflammatory response increases fibrosis, leading to altered composition of the tissue and increased rigidity. In the muscle, the normally laminin-rich myofiber niche shifts toward a composition enhanced in collagen IV (Kovanen et al., 1988). Moreover, old wild-type myoblasts continue to produce collagen III but cease to synthesize collagen I (Alexakis et al., 2007). Both cellular fibroblast aging and defective mechanical stimulation in the aged tissue contribute to reduced collagen synthesis (Qin et al., 2014; Shuster et al., 1975; Varani et al., 2006). On another hand, enhanced collagen cross-linking, mediated by lysyl oxidase, promotes growth and invasion by pre-malignant human mammary epithelial cells. In addition, interactions between adhesion molecules such as filamin A and b1 integrin can alter the cells' response to collagen tension (Gehler et al., 2009; Levental et al., 2009). Increased stiffness also can induce adipocyte progenitors to differentiate into fibroblasts, which can positively feedback to further increase tissue stiffness (Chandler et al., 2012). YAP/TAZ produce Laminin511 via a feedback loop involving activation of integrins which feedback on YAP/TAZ to contribute

to breast cancer progression (Chang et al., 2015). This correlates well with previous work showing that YAP/TAZ activity is increased in aggressive human mammary tumors in regions of higher collagen cross-linking (Acerbi et al., 2015). This might have implications for tumor treatment, since ECM stiffness promotes, through YAP/TAZ, the resistance of HER2-amplified breast cancer cells to HER2-targeted kinase inhibitor lapatinib. Down-regulation of YAP/TAZ eliminated modulus-dependent lapatinib resistance (Lin et al., 2015).

Little is known about whether YAP/TAZ play a role in phenotypes of aging. Deficiency in *C. elegans* YAP resulted in overall healthier aging relative to controls (Iwasa et al., 2013). TAZ functions as a rheostat that modulates MSC differentiation by promoting osteoblast while simultaneously preventing adipocyte differentiation (Hong et al., 2005). During aging, the progressive loss of bone mass occurs with a gradual replacement of the bone marrow with fat (Moerman et al., 2004). Both of these phenomena could be explained by a reduction in TAZ-driven gene expression with age. Thus, mechanical regulation of stem cell homeostasis via the Hippo pathway maintains an equilibrium between altered differentiation and proliferation.

Altogether, emerging evidence suggests the presence of the nine hallmarks of aging at the stem cell level and that dysregulation of stem cell activity is an important determinant of aging phenotypes. In addition to its molecular constituents, the physical constraints of the niche tightly regulate stem cell homeostasis. The stem cell intrinsic- and extrinsic- alterations are the main causes of aging. Thus, we define the microenvironment alteration of stem cell regulation as a previously unappreciated hallmark of aging. To understand the aging process in human, each component of the niche is required to be

identified in order to characterize specific microenvironment functions in stem cell regulation in the context of aging. Although an extensive range of animal models have been developed to study aging, these models do not entirely recapitulate the human model.

## 1.5 Human models to study aging

The laws, morals, and ethics of modern society ensures the protection of human subjects. Thus, no research as extended as experiments performed on rodent models can be conducted on humans. Longitudinal studies follow individuals throughout their lives while cross-sectional studies compare young and old individuals at distinct time points (Cevenini et al., 2015). Both types of studies are observational, not mechanistic. However in order to study aging at the cellular level, human tissue can be obtained. Fluids and blood are easily collected (Lifshitz and Kramer, 2000; Navasesh, 1993; Tuck et al., 2009), in addition to tissue from patient's tumor (Mitra et al., 2013), biopsies, organ donation (Millar et al., 2007), and surgery. The human blood has been extensively studied in patients of all age-groups. With age, there is evidence of a gradual decline in all of the hematopoietic system functions (Carmel, 2001; Gomez et al., 2005). Cell lines are grown from tumors and biopsies, and are used in experimental investigation of cancer but genomic differences between cancer cell lines and tissue samples have been pointed out (Ertel et al., 2006; Gillet et al., 2011; Stein et al., 2004). An illustrating example is the MDA-MB-435 strain, derived from a metastatic breast tumor. It is debated whether the cell line has a breast or a melanoma cell line identity (Ellison et al., 2002; Lacroix, 2009). Nevertheless, important work with primary tumors in the context of aging revealed that breast tumors

have age-specific gene expression signatures (Yau et al., 2007).

Moreover, age-related changes in epigenetic modifications, such as DNA methylation, have been reported in a number of different tumors (Issa et al., 1994). Aging has also been studied on various sources of human tissue. To cite but a few: epithelial skin tissue (Swindell et al., 2012; Varani et al., 2006), epidermal keratinocytes (Berdyeva et al., 2005), breast tissue (Garbe et al., 2012; Stampfer et al., 2013), sub-cutaneous adipose tissue (Bolinder et al., 1983), kidney (Melk et al., 2005), *ex vivo* lungs (Thurlbeck, 1975). However, cell lines derived from organs are mainly cultured on tissue culture dishes, with formulated media that does not resemble their natural habitat. Efforts have been made to develop organ culture as an advancement of tissue culture methods of research. For example, scientists reported a successful trial of bladders grown *in vitro* and given to humans (Atala et al., 2006). A jawbone has been grown from stem cells (Grayson et al., 2010), a lung has been engineered (Petersen et al., 2010) and renal tubules have been cultured (Tumlin et al., 2008). Silk cut from silkworm cocoons has been successfully used as growth scaffolding for heart tissue production (Patra et al., 2012). However, organ cultures suffer from important limitations: results from organ cultures are often not comparable to those from whole animal studies. For each study, fresh organ cultures have to be initiated, which makes them labor-intensive and they can be maintained only for a few months.

Samples and tissue can be obtained from human, and efforts have been made to retain the *in vivo* characteristics of these tissues *in vitro*. Human models can be successfully used to study normal aging and age-related pathologies. As cancer is the main age-related disease and more than 80% of women diagnosed with breast cancer are over 50 years old, we review in this final

chapter the use of human mammary epithelial cells as a model to study aging and the susceptibility to breast cancer.

## **1.6 Breast cancer as a model of aging disease**

Mammary cells present a convenient model system because large quantities of normal and abnormal tissues are available due to the frequency of reduction mammoplasty and mastectomy surgeries. Aging is the greatest risk factor for breast cancer. Aging has been attributed to degenerative changes in mammary stem cells and microenvironment that regulates stem cell activity. In order to understand the microenvironment regulation of mammary stem cells and its alteration with age, it is crucial to deconstruct each property of the niche and assess its role in mammary stem cell quiescence and fate as a function of age. First, we outline the human mammary gland hierarchy and aging biology. We observe that the luminal lineage is the principal subtype of post-menopausal breast cancer. Then, we describe the principal breast cancer treatments undergone by older women in order to emphasize the necessity to find preventive cures. Finally, we report the recent advances in understanding the microenvironment regulation of mammary progenitors and its alteration with age.

### **1.6.1 Defining the mammary gland**

Each breast is composed of up to 20 compartments called lobes. Each lobe is made up of smaller lobules, where milk is produced. Lobes and lobules are connected by a system of ducts that carry milk to the nipple (Figure 7). The mammary gland is a hormone sensitive, branching, and bilayered tissue consisting of an inner secretory luminal epithelial (LEP) layer, and an outer contractile myoepithelial (MEP) layer surrounded by a basement membrane

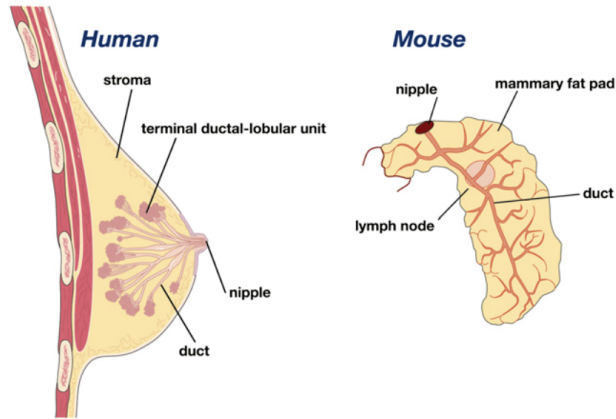


Figure 7: **Schematic representations of the human and mouse mammary glands.** Muscles lie under each breast and cover the ribs. Each lobe is composed of lobules which produce the milk carried through the ducts and ultimately to the nipple. The mammary gland is surrounded by adipose and connective tissue. In contrast, the mouse mammary epithelial tree does not possess TDLUs, but comprises alveolar buds that are formed during each estrous cycle. From (Visvader, 2009).

in a stromal connective tissue (Figure 8). The arbor-like gland is organized into lobular acini that are interconnected by a system of ducts; the basic functional units of the breast are termed terminal ductal lobular units (TDLUs), which are derived from stem cells that reside in the ducts. TDLUs are composed of an inner layer of cytokeratin (K)8-, K7- and K19-expressing luminal epithelial cells (LEP; K14<sup>-</sup>/K5/6<sup>-</sup>/K19<sup>+</sup>/K8<sup>+</sup>/K7<sup>+</sup>) and an outer layer of K14<sup>-</sup> and K5/6<sup>-</sup> expressing myoepithelial cells (MEP; K14<sup>+</sup>/K5/6<sup>+</sup>/K19<sup>-</sup>/K8<sup>-</sup>/K7<sup>-</sup> (Figure 9)). Mammary progenitor cells express K14 and K19 (Villadsen et al., 2007). Additionally, the receptor tyrosine

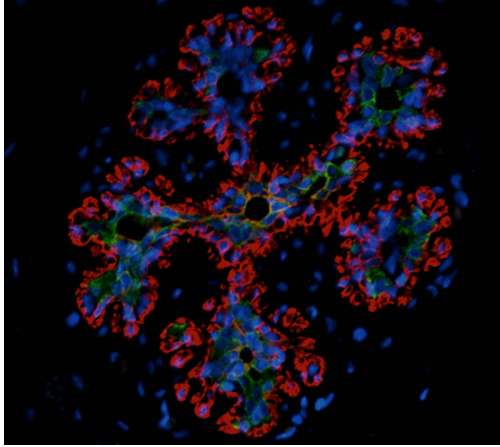


Figure 8: **The terminal duct lobular unit.** A tissue section from a normal mammary gland immunostained to show expression of the MEP and LEP markers K14 (red) and K19 (green), respectively. A co-expression of K14 and K19 in the central duct indicates the presence of progenitors. From Mark LaBarge.

kinase cKit (CD117) was postulated to be a marker of luminal progenitors in human (Lim et al., 2009; Regan et al., 2012). Previous work showed that they were capable of multilineage differentiation (Garbe et al., 2012).

The Hippo pathway acts as a differentiation rheostat in the normal breast. YAP expression is higher in the myoepithelium and myoepithelial cells have a stronger nuclear YAP localization pattern (Jaramillo-Rodríguez et al., 2014; Vlug et al., 2013). In addition, TAZ associates with SWI/SNF chromatin-remodeling complexes to both repress the expression of luminal specific genes and activate basal differentiation genes (Skibinski et al., 2014).

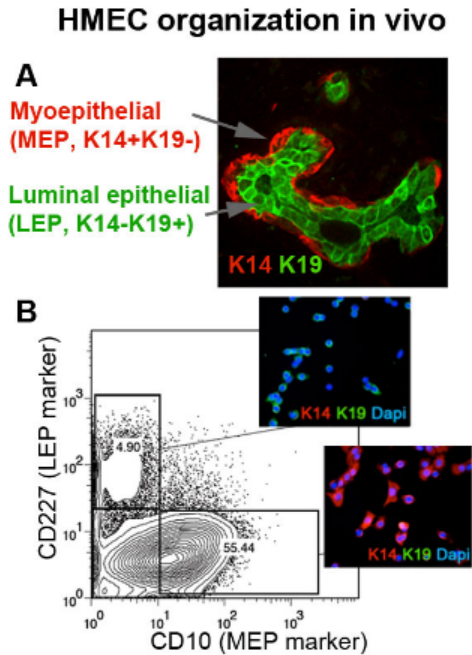


Figure 9: **Luminal and myoepithelial populations express lineage-specific markers.** (A) A tissue section from a normal mammary gland immunostained to show expression of the MEP and LEP markers K14 (red) and K19 (green), respectively. (B) Flow cytometry analysis of a HMEC strain: MEP, is defined here as CD227-/CD10+, and LEP, is defined as CD227+/CD10-. Immunofluorescence of sorted cells for MEP and LEP markers K14 (red) and K19 (green), respectively, verified that CD227+ LEP were K14-/K19+, and CD10+ MEP were K14+/K19-. From (Chanson et al., 2011).

### 1.6.2 Axl may represent a breast stem cell marker

Axl is a member of the TAM (Tyro/Axl/Mer) receptor tyrosine kinase family, united by a common protein ligand, Gas6, and extracellular domain similarity to cell adhesion proteins (Linger et al., 2008) (Figure 10).

The Axl receptor tyrosine kinase has been closely associated with a wide variety of advanced solid and myeloid cancers, and correlated with metastasis and poor overall survival (Gjerdrum et al., 2010; Linger et al., 2008). Axl is expressed by aggressive basal breast cancer subtypes that exhibit mesenchymal and stem cell gene expression profiles (Blick et al., 2010; Neve et al., 2006). Axl expression is induced by Epithelial to Mesenchymal transition (EMT) transcription factors and Axl signaling is essential for breast cancer metastasis in experimental systems (Gjerdrum et al., 2010). Notably, Axl is distinguished from other EMT-related genes as its expression is enhanced in matched breast cancer patient metastases relative to the primary tumor (Gjerdrum et al., 2010). These results indicate that Axl expression may be associated with epithelial plasticity that drives both malignant progression and metastatic colonization.

Axl is a common effector of the EMT and regulates the expression of EMT markers, such as E- and N-cadherin, Snail and Slug (Asiedu et al., 2014). Recent evidence highlights a role for Axl signaling in the maintenance of progenitor cell types. Axl was detected in neuronal progenitor cells (NPC) in the subventricular zone of the brain; and inhibition of Axl or Gas6 in NPC induced neuronal differentiation consistent with a role for Gas6-Axl signaling in neuronal progenitor maintenance (Gely-Pernot et al., 2012; Wang et al., 2011). Axl was reported to be expressed by CD34+ hematopoietic precursors and Axl inhibition was associated with impaired natural killer (NK) cell

differentiation due to reduced precursor cell pools (Caraux et al., 2006). Indeed, Axl activation was necessary for cKit activity in NK precursors (Park et al., 2009). Remarkably, recent studies show that Axl transcripts are associated with a gene signature derived from pluripotent human embryonic germ cells that includes SOX9 and that the inhibition of Axl kinase activity facilitates induced-pluripotent stem cell (iPSC) generation by suppressing EMT (Pashai et al., 2012; Son et al., 2013). Hence, it is plausible that Axl signaling may contribute to stem/progenitor plasticity in other tissues.

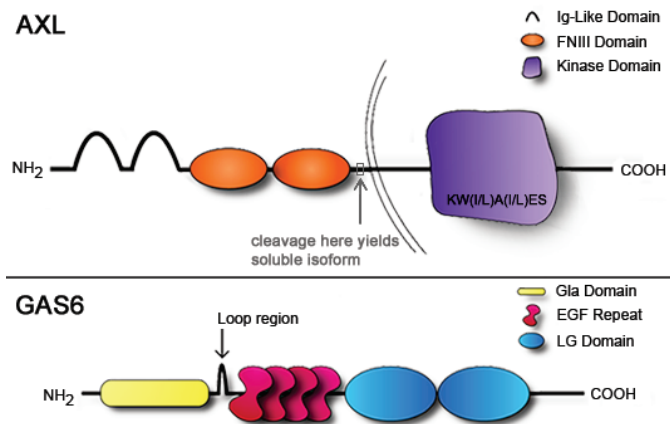


Figure 10: **Axl and Gas6 structure.** The intracellular kinase domain includes the seven-residue sequence conserved among TAM family receptor tyrosine kinases. Proteolytic cleavage of residues between the transmembrane and closest FNIII domains renders a soluble isoform of Axl, which contains its fully functioning extracellular domains. Gas6 is activated by vitamin K-dependent carboxylation of the Gla domain. From Atlas of Genetics and Cytogenetics in Oncology and Haematology website.

Gas6 requires  $\gamma$ -carboxylation of the N-terminal  $\gamma$ -carboxyglutamic acid (Gla) domain to activate Axl (Hasanbasic et al., 2005; Nakano et al., 1997; Tanabe et al., 1997). This is carried out in the endoplasmic reticulum (ER) by the vitamin K dependent carboxylase complex (VDCC). The carboxylation reaction is strongly dependent vitamin K levels, which are determined by the vitamin K recycling enzyme complex. Vitamin K 2,3-epoxide reductase complex subunit 1 (VKORC1) is the target of warfarin. Decarboxylated Gas6 is suspected to be an Axl antagonist. Gas6 has very high affinity for Axl (0.4nM); and decarboxylated Gas6 is reported to have a binding affinity of 4nM (Nakano et al., 1997). Hence regulation of  $\gamma$ -carboxylation activity will toggle Gas6 between activator and inhibitor states. Mammary luminal epithelial cells express Gas6 and the ER carboxylase complex, and secrete Gas6 (Ji et al., 2011). Hence when luminal cells secrete carboxylated Gas6, they will activate Axl and maintain the juxtaposed suprabasal progenitors in the multipotent state. If the luminal cells inactivate the  $\gamma$ -carboxylase activity, they would secrete an Axl inhibiting decarboxylated Gas6. This would block Axl signaling and drive the progenitors into luminal commitment. This hypothetical mechanism would contribute to the maintenance of luminal epithelial homeostasis.

### **1.6.3 Normal mammary gland changes with aging**

Normal breast tissue aging is associated with involution of the breast and a loss of mammographic density (Figure 11) (Hutson et al., 1985; Maskarinec et al., 2006). Mammographic density is a major risk factor for a breast cancer subtype (Bertrand et al., 2013; Maskarinec et al., 2006) (Figure 11); however, the significance of that tissue density has been poorly understood.

Matrix stiffness is mechanistically important in breast cancer progression; rigid breast tissue correlates with high breast cancer risk and drives malignant phenotypes in breast cancer cell lines (Paszek et al., 2005; Yu et al., 2011). However, radiographic density of breast tissue decreases with age, suggesting that the mechanical environment is also altered (Benz, 2008). Over time, the collagenous stroma and glandular elements are replaced by fatty tissue. The decline of mammographic density with age parallels that of the rate of breast tissue aging in a model proposed by Pike (Boyd et al., 2005; McCormack et al., 2010). Although the mammographic density decreases, we do not know whether the mammary gland itself may become tenser with age.

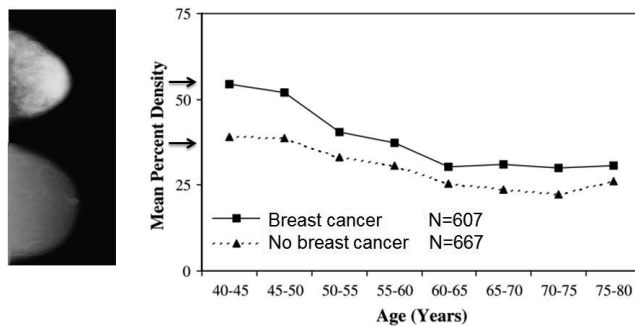


Figure 11: **Albeit mammographic density is a breast cancer risk, it decreases with age.** Left, the fibroglandular tissue has a higher X-ray attenuation coefficient than the fat tissue, and therefore appear brighter on the radiograph. The upper breast has a higher mammographic density than the lower breast. Right, unadjusted mean percent mammographic density as a function of age group and case status. Adapted from (Maskarinec et al., 2006).

Changes in endocrine regulation and in the cellular and molecular composition of breast microenvironment are the most important factors that a majority of women aged over 50y have in common. Estrogen and progesterone can directly impact the epithelium by causing fluctuations in the stem cell pool (Asselin-Labat et al., 2010; Hilton et al., 2014). The effects of cyclic and prolonged exposures of the normal epithelium to sex hormones over a lifespan are not well defined, although it is known that an increase in sex hormones are associated with a higher breast cancer risk (Endogenous Hormones Breast Cancer Collaborative Group, 2003). Aging is also associated with changes in protease expression (Well et al., 2007), that could be related to age-related discontinuities in laminin-111 of the basement membrane (Howeedy et al., 1990), which could impact tissue polarity (Gudjonsson et al., 2002). These changes occur gradually, thus slowly evolving the molecular constituency of the breast microenvironment.

#### **1.6.4 Post-menopausal breast cancer**

Despite the fact that breast cancer incidence increases with the age of the patient, it is generally stated that old women develop cancer with a relatively slower growth (Clark, 1992; Eppenberger-Castori et al., 2002; Peer et al., 1993; Schaefer et al., 1984) and that their prognosis is therefore better than the one of the general population (Bonnier et al., 1995; Schaefer et al., 1984). Advanced age is associated with favorable biological features, including a higher proportion of estrogen receptor (ER)-positive cases (Anderson et al., 2001; Clark et al., 1993; Diab et al., 2000). Gene expression is used to classify invasive breast cancers into biologically and clinically distinct subtypes that are known as Luminal A, Luminal B, HER2-Enriched

(HER2-E) and Basal-like (Prat and Perou, 2011; Sørlie et al., 2001). The incidence of luminal tumors (luminal A and luminal B combined) increases with age, whereas the incidence of basal-like tumors decreases (Jenkins et al., 2014). The luminal A subtype has a better outcome than the other subtypes. Nevertheless, a significant proportion of patients older than 70y and of the 40–50y subgroups will develop large, highly proliferating, high histological grade, ER-positive luminal B tumors that are associated with positive nodal invasion (Durbecq et al., 2008). Moreover, even if the age-related hormone positive breast cancers are less aggressive, they are more insidious and the risk of recurrence in age-related breast cancers is protracted (Esserman et al., 2011).

Age-related changes in epigenetic modifications, such as DNA methylation, have been reported in a number of different tumors (Issa et al., 1994; Waki et al., 2003). An age-dependent, estrogen receptor-independent gene expression signature identified in type-matched breast tumors (Yau et al., 2007), also suggests epigenetic changes are involved in the pathogenesis of age-related breast cancers. Thus, the biology of post-menopausal breast cancer may differ substantially from that of younger women, suggesting the role of aging in its susceptibility. In addition, older women, may be offered different or no treatments for breast cancer leading to higher mortality.

### **1.6.5 Treatments of post-menopausal breast cancer**

Older women with breast cancer are less likely to be offered or receive standard treatments and that such under-treatment may impact on disease-specific mortality (Bouchardy et al., 2007; Lavelle et al., 2007). Better understanding treatment decisions of older women is important

because less-aggressive treatment has been associated with greater breast cancer mortality (Schonberg et al., 2010). Available treatments for post-menopausal breast cancer patients and their associated risks are listed in Table 2.

In conclusion, older patients should be treated according to tumor biology

Treatment	Age-associated co-morbidity	References
Surgery (Mastectomy)	Morbidity and mortality in anesthesia	(Turrentine et al., 2006; Wyld and Reed, 2007)
Adjuvant radiotherapy	Heart disease and lung cancer	(Early Breast Cancer Trialists' Collaborative Group, 2005)
Endocrine therapy	Decline in bone mineral density	(Mustacchi et al., 2007; Reid et al., 2008)
Chemotherapy	Toxicity and cardiac failure	(Muss et al., 2005; Pinder et al., 2007)
Trastuzumab	Cardiac dysfunction	(Chavez-MacGregor et al., 2013; Tsai et al., 2014)

Table 2: This table summarizes the available treatments offered to women with post-menopausal breast cancer. The age-associated co-morbidities impact the treatment decision.

as for younger patients, except when co-morbidities or frailty are likely to affect the benefits of treatment to a certain extend.

While breast cancer treatments exist for older women, the best solution would be ultimately to find non-invasive means to prevent breast cancer. In order to prevent age-related breast cancer, we need to understand the risks associated with normal aging. Understanding what is an abnormal biological

process, assumes knowledge of what is normal, for comparison. Understanding the mechanisms by which a normal human epithelial cell transforms to malignancy requires knowing the state of the starting point, the normal human epithelial cell.

### 1.6.6 Understanding the breast aging process at the cellular level

Early passage HMEC cultures may be provided from an existing bank of specimens ([hmec.lbl.gov](http://hmec.lbl.gov)) (see Methodological Considerations).

Analysis of HMEC with age revealed that proportion of LEP increases while proportion of MEP decreases with age. In addition, cKit progenitors which are luminal progenitors and main suspect in the breast tumorigenesis are also increasing in proportion with age (Figure 12) (Garbe et al., 2012). These luminal cells express K14 and integrin $\alpha$ 6 which are almost exclusively

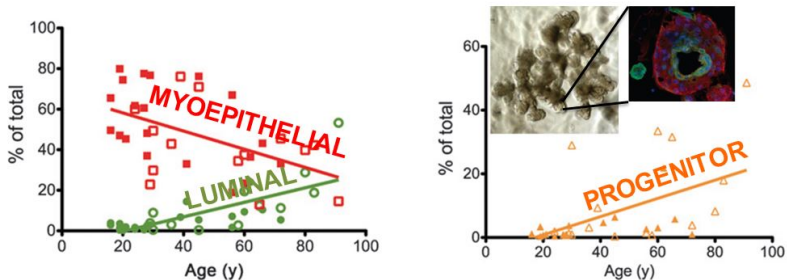


Figure 12: **Epithelial lineages change as a function of age.** The proportion of LEP and cKit progenitors increases while proportion of tumor-suppressive MEP decreases with age. Adapted from (Garbe et al., 2012).

expressed in young myoepithelial cells. Thus, with age, cKit progenitors

accumulate and give rise to incompletely differentiated luminal cells that together appear to increase the potential for malignant transformation. Accumulating evidence has provided support for the cancer initiating cell hypothesis. A mechanistic insight can be drawn from breast cancer 1 (BRCA1) basal-like breast cancer. Heterozygous germ-line mutations in the BRCA1 gene predispose women to breast and ovarian cancer with a lifetime risk of breast cancer of up to 85% (Narod and Foulkes, 2004). Loss of BRCA1 function results in blocked epithelial differentiation with expansion of the undifferentiated stem/progenitor cell compartment (Liu et al., 2008). In BRCA1-associated preneoplastic tissue and tumors, cKit was more highly expressed (Lim et al., 2009). In addition, cKit over-expression prevents normal differentiation (Regan et al., 2012) suggesting a role for cKit in the BRCA1 mutated tumorigenesis. Instead of mutation, other mechanisms lead to decreased BRCA1 expression (Turner et al., 2007) and increased methylation (Esteller et al., 2000). Recent work demonstrated that in both mice and humans, aging results in an increased incidence of double-stranded breaks (DSB) in oocytes and a concomitant decrease in expression of DNA repair genes involved in DSB repair, including BRCA1 (Titus et al., 2013). Thus, applying the idea of the BRCA1-mediated expansion of progenitor model, we hypothesized that during the normal aging process, cKit progenitors become less responsive to their surrounding microenvironment leading to their accumulation, dysfunction and susceptibility to tumorigenesis.

The significant age-dependent changes to the mammary epithelium that we observed could make older women more vulnerable to malignant progression and underlay the increased luminal breast cancer incidence in women >55

years. Myoepithelial cells are thought to be tumor-suppressive (Gudjonsson et al., 2002) and progenitors are putative etiologic roots of some breast cancers. Thus, during the aging process, the potential target cell population may increase, while there is a simultaneous decrease in the cells thought to suppress tumorigenic activity.

While there is undeniably a genetic component to all cancers, the accumulation of mutations with age is insufficient to explain the age-dependent increase in breast cancer incidence (LaBarge et al., 2015; Stephens et al., 2012). In opposition to this conventional view, the age-related susceptibility to breast cancer might follow the adaptive oncogenesis model, where the reciprocal dynamic between the microenvironment and the progenitor is skewed, leading to a decrease in breast tissue fitness and an increase in susceptibility to tumorigenesis (Figure 13) (Henry et al., 2011). We hypothesize that age-associated responses to microenvironment changes arise due to fundamental changes in signal transduction pathways in stem/progenitor cells, which promotes susceptibility to malignant transformation.

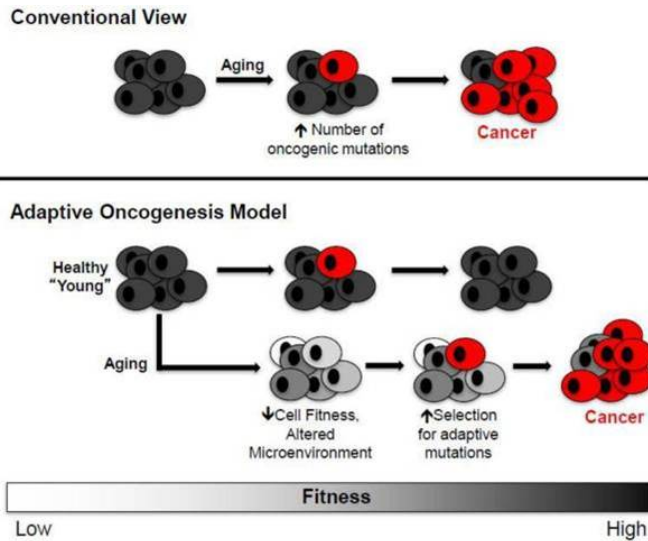


Figure 13: **Conventional and adaptive oncogenesis models for tumorigenesis.** Conventional View: Aging primarily contributes to increased cancers by facilitating the accumulation of oncogenic mutations (red cells). Adaptive Oncogenesis Model: The ability of an oncogene to induce cancer is context specific. If cellular fitness decreases as a result of aging, the acquisition of an oncogenic mutation could be adaptive. In this context, these cells would be selected for leading to carcinogenesis. From (Henry et al., 2011).

## 2 Hypothesis and Aims

The central hypothesis of this dissertation is that a novel effect of aging is a defective stem cell regulation by the microenvironment. The main objectives of the presented work were to identify age-related changes in mammary stem and progenitor cell responses to the microenvironment, and define breast epithelial cell subpopulations that change with age. Thus, the following aims are outlined:

### **A- Determine the role of Axl signal transduction in human mammary stem and progenitor cell differentiation**

Previous results indicate that Axl expression may be associated with epithelial plasticity that drives both malignant progression and metastatic colonization. As the EMT gene program has been associated with mammary epithelial stem cell activity and embryonic stem cells, we hypothesized that Axl is a regulator of stem cell functions in normal breast epithelial cells. We reasoned that genes associated with breast carcinoma plasticity might serve roles in normal breast epithelial homeostasis. Samples from the LBNL HMEC Resource are analyzed to evaluate the possibility that Axl could be present in rare human mammary epithelial cells that are enriched for multipotent progenitor activity.

### **B- Determine the effect of microenvironmental changes on human mammary progenitor cell differentiation**

In light of the findings that differentiation-defective cKit-expressing multipotent progenitors accumulate with age, and proportions of daughter myoepithelial and luminal epithelial cells shift with age (Garbe et al., 2012), we hypothesized that these age-associated changes render aged breast tissue

susceptible to malignant progression. Matrix stiffness is mechanistically important in breast cancer progression and the physiological range of elastic modulus in breast plays an instructive role in the differentiation of normal mammary progenitors. We propose that perturbing matrix stiffness may reveal aging phenotypes due to altered cell mechanics pathways. We aimed to determine if the three steps of cell mechanics (mechanosensing, mechanotransduction and mechanoresponse) are altered with age using samples from the LBNL HMEC Resource.

### **C- Characterize the age-related cell subsets at high-resolution**

We previously demonstrated that post-menopausal LEP frequently express some K14, as well as other markers typically associated with myoepithelial cells. Moreover, age-dependent changes in the efficiency of YAP/TAZ-mediated mechanotransduction may help drive that phenotype of aging. More YAP has been observed in the nucleus of older LEP *in vivo* (Pelissier et al., 2014) which homolog TAZ is associated with basal differentiation transcription program (Skibinski et al., 2014). However, a quantitative understanding of the phenotypic and functional heterogeneity within aged tissues is lacking, which would allow us to pinpoint subpopulations of cells that are changing during the aging process and that may be missed in population-average experiments. We hypothesized that human mammary epithelial cells exhibit age-related phenotypic heterogeneity that may be implicated in breast cancer susceptibility. Thus, phenotypical identification of cells in heterogeneous populations requires simultaneous multiparametric measurement of distinguishing markers at the single cell level. We aimed to analyze LBNL HMEC samples at high resolution using mass cytometry.

### 3 Summary of Results

#### Paper I

*Multipotent mammary stem cell activity requires Axl receptor tyrosine kinase in mice and humans.* Engelsen, Wnuk-Lipinska, Pelissier, *etal.*, Submitted.

We evaluated the hypothesis that Axl is a regulator of stem cell functions in normal breast epithelial cells; serving an unappreciated role in the maintenance of the normal mammary epithelial hierarchy and conferring stem cell traits to breast cancer cells. This study aimed to analyze dissociated primary HMEC from the Aging Resource to determine the potency of Axl-enriched population and to modulate Axl signal transduction to understand its role in normal mammary epithelia.

#### **Main methods:**

HMEC populations comprising differentiated LEP, MEP and mammary stem/progenitor epithelial cell populations were resolved by staining for established surface marker combinations. TDLU-forming assays were performed to determine the potency of Axl-enriched population by culturing in 3D Matrigel for 10-20 days at which time morphology is assessed by phase microscopy and stained with a number of intracellular markers (e.g. keratin) and evaluated by laser scanning confocal microscopy to determine the presence of cells representative of the two main mammary cell lineages, LEP and MEP. Axl signal transduction was modulated using a selective Axl kinase inhibitor (BGB324, BerGenBio AS), function-blocking monoclonal

antibody (MAB 10C9, (Kirane et al., 2015)) and warfarin (ligand binding inhibitor, (Kirane et al., 2015)). Next, we hypothesized that a juxtacrine Gas6-Axl signaling axis regulates adult regenerative homeostasis between Gas6-producing LEP and adjacent Axl-expressing suprabasal stem cells. To test this, we treated 3 week old mice with warfarin (1mg/ml in drinking water) for 4 weeks to block vitamin K-dependent glutamic acid  $\gamma$ -carboxylation of Gas6 that is required for Axl receptor activation.

**Results:**

Axl-expressing HMEC represented 1-6% of the total HMEC population from different patients, residing mainly within the EpCAM+/CD49f+ subpopulation. Moreover, all Axl+ HMEC co-expressed cKit, with cKit+Axl+ HMEC representing 16% of the total cKit+ progenitor cells. We isolated cKit+ HMEC progenitors and performed in vitro serial mammosphere transfers and clonal formation of multi-lineage acini in 3D laminin-rich ECM (lrECM) in the presence of Axl tyrosine kinase inhibitors (TKIs). Secondary mammosphere formation was significantly reduced by treatment with BGB324. cKit+ HMEC embedded at clonal density in lrECM displayed multipotent progenitor activity, forming LEP-MEP bilayered acini. These results indicate that cKit+/Axl+ mammary epithelial cells exhibited self-maintenance and multipotent activity that required Axl kinase activity.

Next, we assessed the differentiation profile of Axl-inhibited HMEC using BGB324. As observed before, LEP proportion decreases with culture passage (Garbe et al., 2012). However, addition of Axl TKI to HMEC cultures slowed loss of LEP.

Finally, we sought to determine if Axl contributes to the maintenance of

mouse multipotent progenitors in the mammary gland. Warfarin treatment resulted in a significant decrease in the number of terminal end bud (TEB) structures, where mouse mammary multipotent/stem epithelial cells are thought to reside.

**Conclusions:**

Collectively, this study identifies Axl signaling as a novel regulator of the regenerative stem cell state that is conserved in human and mouse mammary epithelia. Our results suggest a unique mode of adult luminal cell homeostasis governed by a Gas6-Axl signaling axis where adjacent differentiated cells determine stem cell maintenance and luminal potency. We establish for the first time that Axl signal transduction is required for the multipotent activity of Axl-expressing human mammary epithelial progenitor cells. These findings provide a novel mechanistic rationale whereby Axl signaling contributes to sustain the phenotypic plasticity characteristic of normal breast stem/progenitor and malignant carcinoma cells.

**Paper II**

*Age-related dysfunction in mechanotransduction impairs differentiation of human mammary epithelial progenitors.* Pelissier, *etal.*, Cell Reports, Jun 26;7(6):1926-39 2014.

We hypothesized that perturbing matrix stiffness reveals aging phenotype due to altered cell mechanics pathways. We aimed to determine if the three steps of cell mechanics are altered with age in mammary progenitors using samples from the LBNL HMEC Resource. Since all Axl+ HMEC co-express cKit and represent a really scarce population of cells we focused our work on

cKit+ progenitors.

**Main methods:**

Polyacrylamide (PA) gel concentration was tuned to mimic soft physiological stiffness range (200Pa to 2350Pa) (Tse and Engler, 2010). Multipotent progenitor population from women under 30 years old (y) and women over 55y were fluorescence-activated cell sorting (FACS)-enriched using the cKit marker and cultured for 48h onto PA gels or glass (>3GPa) control. LEP and MEP population proportions and proliferation were quantified using immunofluorescence and are the output of the mechanoresponse. Mechanosensing was measured using stress fibers and focal adhesions formation. YAP and TAZ are transcription co-activators and belong to the Hippo pathway, they shuttle to the nucleus with increasing stiffness and activate target gene expression responsible for the various mechanoresponses. Mechanotransduction was quantified via YAP and TAZ translocation to the nucleus.

**Results:**

With increasing stiffness, multipotent (MPP) progenitors gave rise to more MEP and less LEP. This is a protective mechanism, as the matrix was tensed to approach a malignant tissue stiffness, the progenitors differentiate toward tumor-suppressive MEP. This phenotype was observed only in younger women. While mechanosensing was working equally in the two age groups, YAP and TAZ translocated into the nucleus of younger women cultured onto substrata with increased stiffness and only into the nucleus of older women plated onto >3GPa condition. On this extraphysiological condition, older MPP differentiated toward more LEP. Older multipotent progenitors need to

be stressed with extraphysiologically stiff substrata to reveal their YAP/TAZ-dependent bias toward LEP. This result was consistent with our observation *in vivo* that YAP tended to be located in LEP with increased age.

We made some genetic modifications in the normal progenitors to make them immortal, which is a rate-limiting step in cancer progression. This act of transformation rejuvenated the older cells' ability to respond to physiological changes stiffness, but the immortal older cells still exhibited the same tendency to make weird luminal-like progeny on stiffer matrices, whereas the immortal younger cells still made basal-like cells.

### **Conclusions:**

Matrix rigidity is a determinant of mammary epithelial progenitor differentiation. Exposure of progenitors to mechanically tuned culture substrata revealed two fundamental changes that arise in MPP with age: (1) the mechanical trigger point for activation of YAP/TAZ increases, and (2) the YAP/TAZ-dependent differentiation programs become distinct. Our experimental approach took advantage of tuned mechanical perturbations of matrix to functionally probe the HMEC, but more broadly these results revealed that aging fundamentally alters Hippo pathway regulation. Accumulation of MPP with age may be attributed to inefficient transduction of differentiation cues through the Hippo pathway.

### **Paper III**

*High dimensional analysis of age-related phenotypic diversity in human mammary epithelial cells.* Pelissier, *etal.* Manuscript.

The dynamic reciprocity between HMEC progenitors and the microenvironment regulation is altered with age. This alteration results in accumulation of progenitors with a basal differentiation bias toward LEP. These luminal cells acquire basal traits and thus exhibit a phenotypic divergence. The phenotypic heterogeneity within a tissue reflects the phenotypic divergence between different cell states. Hence quantifying age-dependent phenotypic heterogeneity may reveal specific subpopulations of cells that accumulate with age.

**Main methods:**

Standard immunofluorescence and flow cytometry methods are limited to relatively few parameters. Mass cytometry is a recent technology that allows high-content multiparametric analysis of single cells in complex heterogeneous biological system (Bandura et al., 2009). A test-set of HMEC samples from forty-four women from 16 to 91y was analyzed at once using a multiplexing approach called mass-tag cellular barcoding (MCB). We selected 10 highly informative surface markers that captured the lineage-heterogeneity in HMEC. We added 12 antibody probes against intracellular phosphorylation, 4 antibody probes against the Hippo pathway and 3 antibody probes against cell cycle and apoptosis pathway, thus allowing simultaneous measurement of surface phenotype and signaling behavior in single cell. The data is analyzed using t-distributed stochastic neighbor embedding (tSNE), PhenoGraph, and Citrus for the identification of stratifying subpopulations changing with age.

**Results:**

We demonstrated in high definition that luminal and myoepithelial

populations had lineage-specific phenotypic divergence and high intra-lineage heterogeneity. Unsupervised population partitioning revealed age-dependent clusters, only in the luminal compartment, that were more abundant with age. These seven clusters had specific marker expression signature and were characterized as:  $K14^{high}/K19^{low}$ , Proliferative LEP, Basal LEP,  $Keratin^{low}$ , pS6 luminal,  $Keratin^{low}$ -S and  $Axl^{high}$ . The aged luminal cells manifested a marker expression signature that correlated with an enhanced basal phenotype. Using this data set we built an unsupervised classification model that correctly assigned more than 80% of the samples into their correct age-group. Further, we found age-related changes in luminal progenitor cells, supporting the notion of accumulated age-altered stem/progenitor cell populations during aging. Hence, high-dimensional analysis of normal human mammary epithelial cells revealed a remarkable age-related phenotypic divergence in the luminal and luminal progenitor cells.

**Conclusions:**

We describe the first multiparametric analysis of complex heterogeneous HMEC populations. Taken together, high-dimensional analysis of normal human mammary epithelial cells revealed an age-related divergence in the luminal and progenitor populations. This study presents a unique in-depth perspective of age-related phenotypic diversity of human mammary epithelial cells and pinpoints a specific progenitor and luminal subpopulation that may be an origin of age-related breast cancer.

## 4 Methodological Considerations

### 4.1 Human mammary epithelial cells

It is important to be able to empirically examine the cell and molecular consequences of aging in normal human epithelia because most carcinomas are age-related. Wild-type mice are typically resistant to cancers, murine models of breast cancer do not completely model the steps of cancer progression in HMEC (Stampfer et al., 2013), and most inbred strains exhibit tumor incidence curves consistent with sporadic tumor genesis. In addition, it is notable that there are morphological differences between mouse and human mammary parenchyma (Figure 7). Thus, mice may not be an optimal model for studying the genesis of age-related breast cancers.

Normal human mammary cells can be obtained directly from surgical tissues (reduction mammoplasties, mastectomies, normal biopsies) and milk fluids. Early passage HMEC cultures are provided from an existing bank of specimens ([hmec.lbl.gov](http://hmec.lbl.gov)). These pre-stasis HMEC cultures established from organoids are uniquely well- characterized, multi-lineage strains with normal finite-lifespan. Early passage populations from reduction mammoplasty contain a mixture of cells with marker of myoepithelial, luminal and progenitor lineages (Figure 14). Both luminal and myoepithelial populations develop from progenitor cells, a small fraction of the cells in the gland that retain the ability to divide. The HMEC resource is a unique system to understand normal breast aging and its correlated risk to breast cancer. A recent M87A media support long-term pre-stasis growth of 60 population doubling (PD). However, the luminal cells do not maintain active growth with long-term passage (Garbe et al., 2009). The Aging Resource makes large standardized HMEC batches from individual specimen donors at

passages 2–5. These uniform batches permit reproducible large-scale and high-throughput experimentation with normal HMEC from multiple individuals of different ages. Currently, cultures from 50 individuals of women ranging in age from 14 to 91 have been initiated (Stampfer et al., 2013).

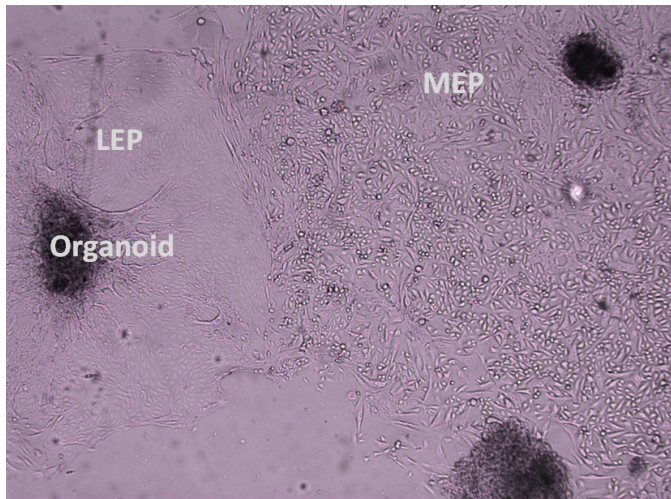


Figure 14: **HMEC cells in culture.** Morphologically, the border of MEP is more delineated, and they have an ellipsoid shape. LEP are more compact than MEP. An organoid is shown. Image from Mark LaBarge.

It is important to note that all the HMEC strains from the American Type Culture Collection (ATCC) are post-stasis: they have bypassed at least two major barriers to malignancy and thus are not normal. In addition, the MCF10a cell line has been widely used and considered as normal. However, it is immortalized and thus not normal (Soule et al., 1990). This explains why research on these cell lines cannot be fully translated. In our study, we

used MCF10a to induce EMT using Slug over-expression due to the ease of transformation of this cell line as compared to normal HMEC.

## 4.2 Cell segmentation with Matlab

The identification of LEP (K19+/K14-) and MEP (K19-/K14+) at the single cell level in immunofluorescence staining images requires the absolute quantification of each marker intensity for each cell. In our immunofluorescence settings, K19 and K14 are visualized in the green and red channel respectively. The lineage determination is obtained using a ratio:  $R = \log_2 \frac{\text{Mean red intensity}}{\text{Mean green intensity}}$ . This ratio is negative for green cells, positive for red cells and zero for yellow cells (co-expression). A manual quantification of each cell using an image analysis program like ImageJ is time-consuming and is prone to bias. Thus, we developed an image segmentation method using Matlab. The program analyzes each image (Figure 15A) and applies a threshold to segregate the cells from the background (Figure 15B). Next, it finds cell nuclei using the DAPI channel (Figure 15C). The nuclei and the background are marked as "valleys" and the cells as "mountains" (Figure 15D). Then, a marker-controlled watershed segmentation is applied to dissociate "valleys" from "mountains" by filling "water" in between. Each cell is segmented and labeled and quantification of each fluorescence channel is obtained (Figure 15E). This program has been used additionally in (Sputova et al., 2013) and (Garbe et al., 2012) and has been modulated to measure cell feature and YAP/TAZ nucleus and cytoplasmic level and has been also used in (Lin et al., 2015). The description of the code is found in the Supplemental Information of Paper II.

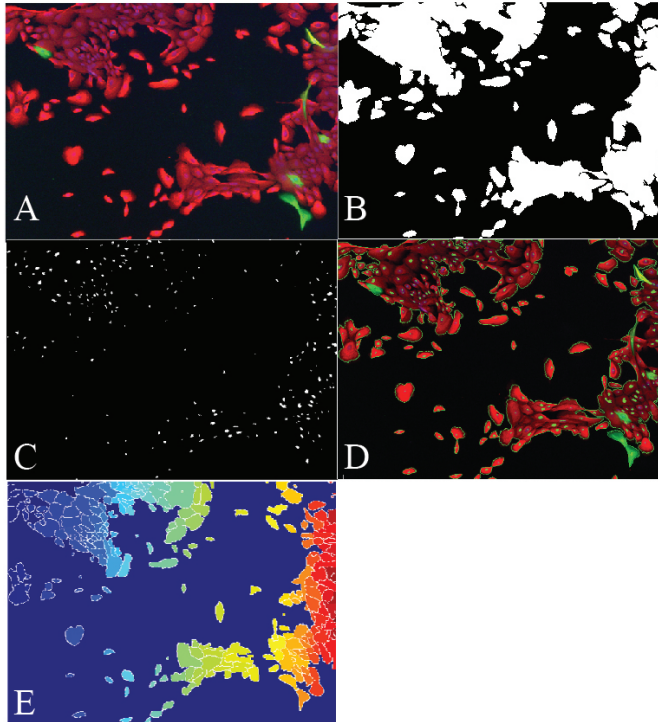


Figure 15: **Marker-controlled watershed cell segmentation with Matlab.** (A) Immunofluorescence of HMEC in culture using the MEP and LEP markers K14 (red) and K19 (green) respectively. The nuclei are stained with DAPI (blue). (B) Background segregation. (C) Nuclei segmentation. (D) A mask of the nuclei and the cell contour are overlaid on top of the image to represent the "valley" and the cells the "mountains". (E) Segmented labeled image. Each color indicates an unique segmented object with unique properties (e.g. channel fluorescence, shape, area etc.). See also Supplemental Information of Paper II.

### 4.3 Immortalized cell lines

In cancer research, the majority of immortal cell lines used are either expanded from tumors or become genetically unstable, making it impossible to understand the process of a cell's malignant transformation and its underlying causes.

Efficient non-clonal immortalization of normal HMEC can be achieved by directly targeting the two main senescence barriers encountered by cultured HMEC. The stress-associated stasis barrier is bypassed using shRNA to  $p16^{INK4}$ ; replicative senescence due to critically shortened telomeres was bypassed in post-stasis HMEC by c-Myc transduction (Garbe et al., 2014). The resultant non-clonal immortalized lines have normal karyotypes and lack the confounding gross genomic changes commonly seen in tumors, tumor-derived cell lines, and clonally derived in vitro immortalized lines.

Pre-stasis HMEC strains 184D, 240L, 122L, and 805P were transduced with retroviruses that expressed either p16 shRNA (p16sh) or cyclinD1/CDK2 (D1), or with a control empty vector. These gave rise to the post-stasis cultures which were transduced either with an empty vector control, or a c-Myc expressing retrovirus in order to transactivate telomerase, giving rise to the non-clonal immortal lines 184Dp16sMY, 240Lp16sMY, 240LD1MY, 122Lp16sMY, 122LD1MY, and 805Pp16sMY (Lee et al., 2015).

### 4.4 Mouse models

#### **Ethics statement**

All mouse experiments were approved under the surveillance of the Norwegian Animal Research Authority. The participants and the candidate, who worked with live vertebrate animals for scientific purposes, were trained

and certified by the Federation of European Laboratory Animal Science Associations.

*In vitro* analysis do not entirely recapitulate physiological context. Although mice are not an optimal model for studying age-related breast cancer, *in vivo* model systems are necessary to validate *in vitro* findings. Mouse models are widely used in translational cancer research due to short gestation period, low maintenance cost and ease of genetic manipulations (Cheon and Orsulic, 2011). In our studies we have used different types of animals, such as athymic nude mice. These hairless mice due to the *Foxn1* gene mutation, were used to easily engraft xenogeneic cell lines. Balb/c mice have a normal immune system and are also reported as having a low mammary tumor incidence. These mice were used to study normal mouse mammary gland development and its perturbation using tyrosine kinase inhibitors targeting Axl. Genetically engineered mouse strain of *B6.129P2 - Axl<sup>tm1Dgen</sup>* carries a targeted LacZ gene knock-in mutation that disrupts Axl protein expression. As a genetic background, strain C57BL/6 was used due to the ease of propagation, availability of congenic strains and their robustness which make them the most commonly used rodent model in research (Brayton et al., 2012).

We hypothesized that a juxtacrine Gas6-Axl signaling axis regulates adult regenerative homeostasis between Gas6-producing LEP and adjacent Axl-expressing suprabasal stem cells. To test this hypothesis, we treated 3 week old Balb/c with warfarin (1mg/L in drinking water) to block vitamin K-dependent glutamic acid  $\gamma$ -carboxylation of Gas6 that is required for Axl receptor activation. After 4 weeks of treatment, mammary glands from the

pubescent mice were analyzed.

## **4.5 Ensemble-averaged measurements can mask information contained in heterogeneity**

Phenotypic differences among cells are always present at a high resolution of inspection. Population-averaged assays are powerful tools in biology, enabling the identification of components and interactions within complex metabolic, signaling, and transcriptional networks. The problem occurs when the ensemble-averaged measurement poorly reflects the states of the majority of the cells, subpopulations of cells, or even single cells (Figure 16). This can occur, for example, when the population contains several dominant, yet phenotypically distinct subpopulations. In order to measure tissue heterogeneity, the number of parameters analyzed should be augmented. Standard immunofluorescence and FACS technique are unfortunately limited to relatively few parameters.

## **4.6 Mass cytometry**

Mass cytometry is a recent technology that allows high-content multiparametric analysis of single cells in complex heterogeneous biological system. Mass cytometry increases the number of parameters that can be measured, reduces overlap between channels and eliminates background fluorescence (Bandura et al., 2009; Ornatsky et al., 2010). The approach is based on attaching specially designed multiatom elemental tags to antibodies, in place of fluorescent labels, and takes advantage of the high resolution, sensitivity, and speed of analysis of inductively coupled plasma

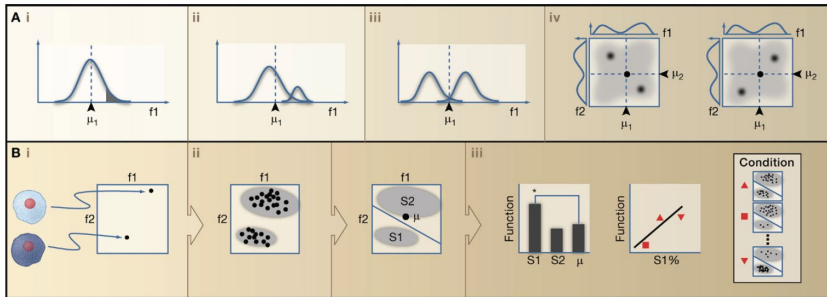


Figure 16: **Ensemble-averaged measurements can mask information contained in heterogeneity.** (A) A population mean ( $\mu$ ) may poorly represent the majority of cells. (B) Heterogeneity and function: single-cell measurements allow cells to be represented as points in a high-dimensional space. Cell populations can be partitioned into distinct regions of feature space. Illustrated is a decomposition into two subpopulations, S1 and S2. From (Altschuler and Wu, 2010)

time-of-flight mass spectrometry (ICP-TOF-MS). The CyTOF system (Fluidigm, formerly DVS Sciences) measures the abundance of metal isotopes tagged to antibodies (Lou et al., 2007). Signaling pathways, cell cycle state, cell viability, using platinum-based viability reagent (Fienberg et al., 2012) and many other cellular pathways can be simultaneously interrogated (Bendall et al., 2011). In order to avoid staining over multiple samples leading to staining heterogeneity and high cost, MCB is adapted (Bodenmiller et al., 2012) (Figure 17A).

However, it is difficult to visualize such high numbers of dimensions in a meaningful manner. Single-cell data are often examined in two dimensions at a time in the form of a scatter plot. Yet, as the number of parameters

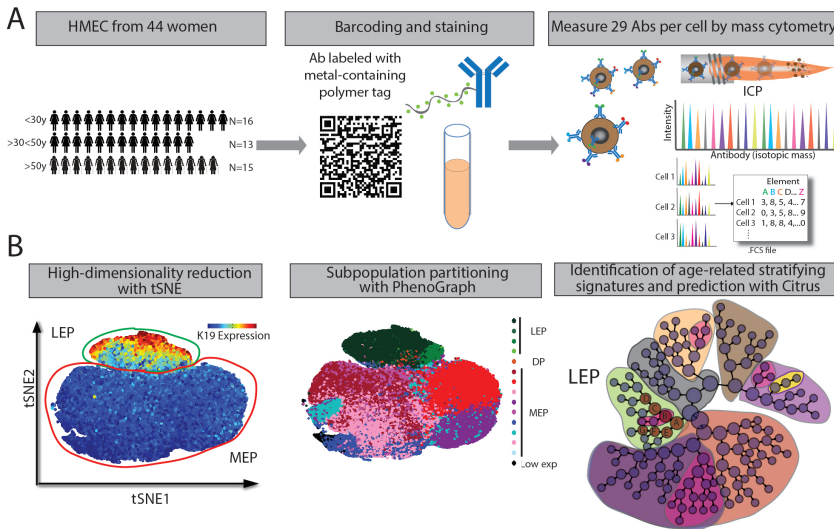


Figure 17: **Summary of experimental design.** (A) Samples of HMEC from 44 women are analyzed at once using MCB, stained using antibodies labeled with isotopes and analyzed using mass cytometry. (B) Strategy to cluster high-dimensional single-cell data and identify age-related phenotypic divergence.

increases, the number of pairs becomes overwhelming. Dimensionality reduction techniques such as tSNE help visualize the data (Figure 17B). Using tSNE, each cell is represented as a point in high-dimensional space. Each dimension is one parameter (that is, the expression level of one protein). An optimization algorithm searches for a projection of the points from the high-dimensional space into two dimensions such that pairwise distances between the points are best conserved between the high- and low-dimensional spaces (Amir et al., 2013). In addition, the PhenoGraph algorithm robustly partitions high-parameter single-cell data into

phenotypically distinct subpopulations (Levine et al., 2015). Finally, Citrus (cluster identification, characterization and regression) is a data-driven approach for the identification of stratifying subpopulations in multidimensional cytometry data-sets (Bruggner et al., 2014). Citrus applies hierarchical clustering to identify clusters of cells within the dataset, calculating descriptive features of each cluster, and then applying regularized regression model to determine which cell subsets' behavior are correlated with aging. Shortly, the Citrus algorithm combines all samples into one aggregate dataset before identifying cell populations by hierarchical clustering of phenotypically similar cells. Next, cells are assigned back to the individual samples and cluster abundance or marker median is calculated.

## 5 Discussion

Our functional characterization of Axl in Paper I supports a model where Axl contributes to the maintenance of progenitor and stem cell traits in normal mammary epithelial cells. Axl is expressed by 16% of the cKit+ epithelial progenitor population and all Axl+ HMEC co-expressed cKit, thus Axl represents a marker of stem cell higher in the progenitor hierarchy and basally located. These cKit+ progenitors are tightly regulated by the microenvironment and more precisely by substrate stiffness. Their accumulation with age may be attributed to the inefficient transduction of differentiation cues through the Hippo pathway as described in Paper II. Finally, clusters of cells accumulating with age with a basal phenotype, were identified in high definition in Paper III and were found only in the luminal and progenitor compartments.

### 5.1 The role of Axl in normal mammary gland

We identified Axl signaling as a novel regulator of the regenerative stem cell state that is conserved in human and mouse mammary epithelia. Our results suggest a unique mode of adult luminal cell homeostasis governed by a Gas6-Axl signaling axis where adjacent differentiated cells determine stem cell maintenance and luminal potency.

We showed that Axl-expressing multipotent epithelial progenitor cells co-express cKit and cluster independently by gene expression and immunophenotyping. Gas6 secretion by LEP represents a local source of ligand within the ductal bilayer (Ji et al., 2011). Hence, Gas6 production by LEP could conceivably regulate epithelial lineage commitment by

juxtapositioned Axl-expressing progenitors.

Using mass cytometry we identified an Axl<sup>+</sup> cluster of cells in the cKit<sup>+</sup> progenitors, as previously observed. On another hand, Axl has been previously identified as a YAP downstream target (Xu et al., 2011). We have shown that Axl expression correlates with YAP in MEP. This phenotype also validates the hypothesis of a luminal regulation of Axl commitment. However, we did not observe Axl expression in MEP *in vivo*, this phenotype might be the results of a culture adaptation as MEP cultured on an extraphysiological substrata (tissue culture dish) would activate YAP and thus Axl. On another hand, HMEC were permeabilized before analyzed with mass cytometry, thus the observed Axl expression may be intracellular, although we did not observe Axl mRNA in MEP using RNAscope. In our hands, HMEC from a young woman (19y) treated with Verteporfin, a YAP/TEAD interaction inhibitor, exhibited a decrease in Axl and K14 and an increase in K19 expression in both LEP and MEP (Figure 18). These results need further investigation.

Our results show that Axl is expressed by rare stem/progenitor cells and regulates multipotent progenitor activity, supporting the concept that Axl signaling contributes to the maintenance of the stem-progenitor cell state within the normal breast epithelial hierarchy. Hence Axl expression during breast cancer development can be viewed as a consequence of the reactivation of stem/progenitor-related gene programs in tumor cells.

Our following work was mostly focused on cKit<sup>+</sup> progenitor population which contains Axl<sup>+</sup> stem cells. Axl<sup>+</sup> stem cells reside in specialized niche in a more basal location and cKit<sup>+</sup> progenitors are more committed progenitors residing outside of a niche. This may explain why the Axl<sup>+</sup> stem cell population is lost after passaging HMEC *in vitro*, while cKit<sup>+</sup> progenitors

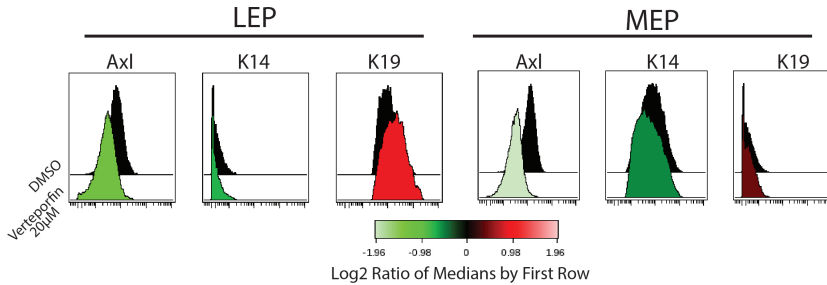


Figure 18: **YAP/TEAD inhibition with Verteporfin.** Histograms of Axl, K14 and K19 expression in HMEC treated with DMSO or 20µM Verteporfin for 15min measured with mass cytometry. LEP and MEP were manually gated.

still give rise to both LEP and MEP daughter cells. In addition, the age-related increase in cKit<sup>+</sup> progenitors was not observed in cKit<sup>+</sup>/Axl<sup>+</sup> stem cells (Figure 19) which supports the hypothesis that Axl<sup>+</sup> stem cells reside in a niche that is more protected from microenvironment changes.

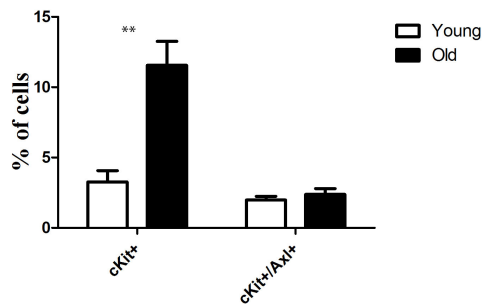


Figure 19: **Proportion of cKit<sup>+</sup> and cKit<sup>+</sup>/Axl<sup>+</sup> as a function of age.** N=5, \*\* p=0.0021.

## 5.2 Matrix stiffness exquisitely directs mammary progenitor differentiation

Changes to the mechanical microenvironment likely have pleiotropic effects on multiple breast cell types. High breast stiffness and density are correlated with increased risk and cancer progression (Yu et al., 2011). Increased stiffness also can induce adipocyte progenitors to differentiate into fibroblasts, which can positively feedback to further increase tissue stiffness (Chandler et al., 2012). Our results document the role of YAP/TAZ transcription factors as drivers of modulus- dependent differentiation in human mammary epithelial progenitors and suggest that YAP/TAZ activity favors differentiation into MEP and other basal cell types. A previous report showed the role of mechanical environment in the differentiation of mammary progenitors (Lui et al., 2012), however the authors used an immortalized cell line, MCF10a which is already transformed, thus not considered as normal.

Studies have shown that normal breast tissue is much more compliant than tumor tissue and it turns out that stiffer tissue enhances malignant behavior of cancer cells (Paszek et al., 2005). Normal progenitors from younger women would differentiate into myoepithelial/basal cells as the matrix was tensed to approach a physiological, albeit malignant, tissue stiffness. This is a protective mechanism because myoepithelial cells are tumor suppressors (Gudjonsson et al., 2002). Thus, when the breast stiffness increases and reaches a malignant stiffness, cKit progenitors differentiate toward MEP, leading to their decrease in proportion. We may hypothesize that this protective mechanism is altered in older progenitors leading to their accumulation (Figure 20).

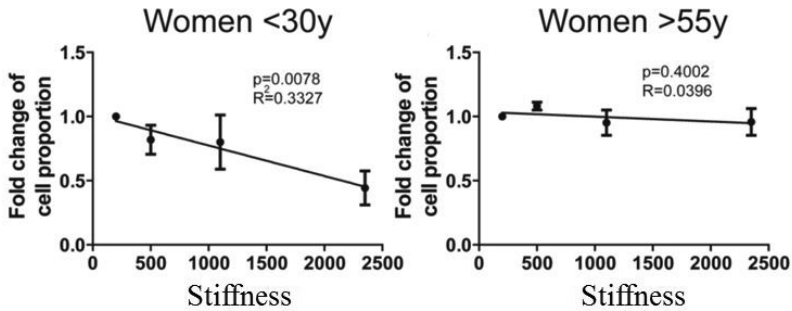


Figure 20: **Linear regression plots of MPP proportion as a function of modulus and age.** The accumulation of progenitors with age may be explained by the altered response of progenitors to mechanical cues. Adapted from (Pelissier et al., 2014).

### 5.3 Immortalization restores responsiveness to physiological stiffness in older HMEC

When older cKit progenitors were exposed to extraphysiological stiff substrata, they exhibited LEP-biased differentiation, the exact opposite of the younger progenitors. Age-dependent differentiation patterns were preserved in immortal young and old HMEC, but the mechanotransductive mechanism was notably rejuvenated in older immortal cells, enabling them to proliferate increasingly as matrix modulus approached that of a tumor. YAP/TAZ were required for shifting production in favor of MEP in younger and LEP in older MPP on the stiffer surfaces. We hypothesize that the distinct differentiation responses of younger and older MPP reflect age-dependent epigenetic landscapes. Indeed, normal HMEC exhibit age-dependent gene expression patterns consistent with the concept of

age-dependent epigenetic states (Garbe et al., 2012). In addition, after older HMEC were made non-malignantly immortal, the Hippo pathway regained sensitivity that allowed them to increase proliferation as matrix rigidity approached an elastic modulus that was on a par with breast tumors. Stromal feedback loops can result in formation of stiffened regions; if such regions already contained an accumulation of aged progenitor cells carrying errors predisposing them to immortality, they could create an environment that promotes development of age-related luminal subtype breast tumors.

#### **5.4 The role of the Hippo pathway in age-related mechanoresponses**

The accumulation of cKit-progenitors with age could be attributed to the inefficient transduction of differentiation cues through the Hippo pathway. At low cell density, decreased LATS2 activity, which causes YAP and TAZ to translocate to the nucleus, depends upon F-actin SF formation (Wada et al., 2011). Young and old MPP formed SF and FA equally well in response to increasingly stiff substrata, within the physiologically relevant range. Therefore the stoichiometry of MST1/2, LATS2, and AMOT may change with age, dampening the activation of YAP and TAZ. In our hands, MST2 protein expression was consistently higher in post-menopause MPP. The Hippo pathway may have a rheostat-like mechanism that allows mesenchymal stem cells to distinguish between the relative stiffness of adipose, muscle, and bone tissues, and also allow mammary epithelial progenitors to respond to a much narrower range of elastic modulus. Each of these tissue microenvironments differs in their matrix composition as well as their elastic modular range, and there is a reasonable expectation that Hippo pathway activity is fine-tuned by combinations of ECM and growth factors.

Further study of the interaction between the Hippo pathway with combinations of microenvironmental elements may reveal components of the mechanical response rheostat and reveal the basis for its age-related dampening.

## 5.5 The paradox of mammographic density and breast cancer risk

Mammographic density is a major risk factor for a breast cancer subtype (Bertrand et al., 2013; Maskarinec et al., 2006). Paradoxically, while breast cancer risk increases, radiographic density of breast tissue tends to decrease with age, consistent with increased adipose and decreased connective tissues (Benz, 2008). This might be hypothetically explained by the fact that the local stiffness of the mammary epithelia may not correlate with the overall breast density. Indeed, with age, the breast undergoes sagging or ptosis. While the mammary gland experiences a decrease in stromal connective tissue, the epithelial sheets may feel a stretch due to a decrease in stromal support. This stretch may be translated as a stretch at the cellular level which has been shown to inhibit the Hippo pathway thus activate YAP/TAZ in the nucleus (Figure 21). This may explain why we observed higher level of YAP in the nucleus of HMEC from older women *in vivo*. We can speculate that with age, YAP/TAZ activation might result in a luminal differentiation with basal traits. This activation may lead to oncogenic pathway activation and malignancy.

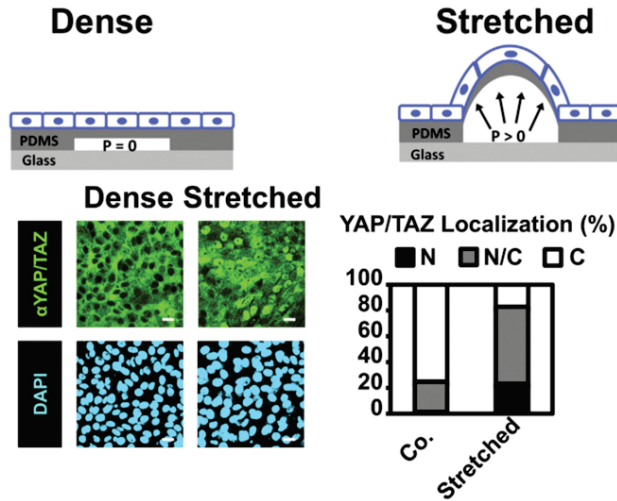


Figure 21: **Stretching of an epithelial monolayer overcomes YAP/TAZ inhibition and growth arrest in contact-inhibited cells.** Mammary epithelial cells were plated on the stretching device. After 2 days, cells were subjected to 6 hours of static stretching ( $p > 0$ ). The plot shows proportion of cells displaying preferential nuclear YAP/TAZ localization (N, black), even distribution of YAP/TAZ between the nucleus and the cytoplasm (N/C, gray), or prevalently cytoplasmic YAP/TAZ (C, white). Adapted from (Aragona et al., 2013).

## 5.6 The mammary gland exhibits an extensive range of heterogeneity

Adult tissues comprise populations of cells that can be heterogeneous in their phenotypic properties (Altschuler and Wu, 2010), and the mammary gland is a prototypical example of a heterogeneous tissue, possessing considerable spatial and temporal variability within both LEP and MEP populations. For example,

neighboring cells in healthy tissue can differ markedly with respect to their expression of adhesion molecules, cytoskeletal proteins, hormone receptors, and the activation of specific signaling pathways (Bloushtain-Qimron et al., 2008; Keller et al., 2010; Moreira et al., 2010; Shehata et al., 2012).

In Paper III, high-dimensional partitioning of HMEC from 44 women revealed four luminal and nine myoepithelial subpopulations, in addition to a double-positive (DP) progenitor subpopulation expressing both K14 and K19 markers previously observed *in vivo* (Villadsen et al., 2007). These subpopulations exhibit a high variability of surface and signaling marker expression, within their lineage-dependent range of expression. The mammary epithelium is more heterogeneous than initially perceived. An understanding of these different subpopulation of cells and their microenvironment regulation is essential for understanding the origins and the cellular context of human breast tumors.

## 5.7 Luminal cells exhibit basal characteristics with age

The basal cell types are not necessarily exclusive to myoepithelial cells, and may include luminal cells that express K14 and other basal-associated markers, which we and others have observed (Santagata et al., 2014). In Paper II, older progenitors needed to be stressed with extraphysiologically stiff substrata to reveal their YAP/TAZ-dependent bias towards LEP, which was consistent with our observation *in vivo* that YAP tended to be located more in LEP with increased age. In younger women, YAP was clearly in the nuclei of MEP. These new data suggest that age-dependent changes in the efficiency of YAP/TAZ-mediated mechanotransduction may help drive that phenotype of aging. In addition, forced expression of TAZ in luminal cells induces them to adopt basal characteristics, and depletion of TAZ in basal and/or myoepithelial cells leads to luminal differentiation (Skibinski et al., 2014).

In Paper III, subpopulations of LEP accumulating with age exhibited age-specific signatures. Strikingly, we observed a linear increase in YAP expression in LEP with age (Figure 22). Interestingly, no age-dependent subpopulations

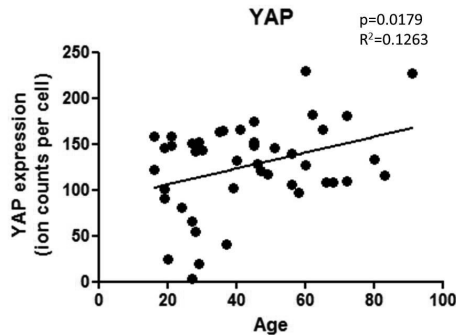


Figure 22: **YAP expression increases with age in LEP.** Using mass cytometry in Paper III we observed a linear increase of YAP marker expression with age in luminal cells.

where found in the MEP lineage. Specific age-related signatures in luminal clusters correlated with basal phenotype, migration and proliferation potential. Importantly, we built an unsupervised classification model that correctly assigned more than 80% of the samples into their correct age-group based on alterations in phenotypic diversity.

Altogether, high-dimensional partitioning of the mammary epithelia revealed luminal subpopulations with skewed differentiation and a basal phenotype that accumulate with age. These cells exhibit hallmarks of aging, and may be the progeny of altered luminal progenitors which have a skewed differentiation. This aging phenotype could be validated *in vivo*. A subpopulation of LEP accumulating with age with basal characteristics (increased K14 and decreased

---

K19 expression) was identified *in vivo* and these markers could be used to perform a morphometric context classification.

## 5.8 Evidence of age-dependent phenotypic divergence in HMEC progenitors

In Paper III, specific markers in the gene expression signatures were found in clusters of progenitors accumulating with age: K8/18, CD133, cKit, YAP and HER2. These markers are connected with stemness, stress, migration and malignancy. This finding correlates with the fact that *cKit* over-expression prevents normal differentiation (Regan et al., 2012) and may explain the accumulation of cKit progenitors with age. CD133 was the marker which changed the most with age. CD133 was found to be a luminal progenitor marker (Hilton et al., 2012; Raouf et al., 2008). In addition, CD133 is expressed in certain types of breast cancer, in which CD133-positivity seems to identify a restricted subgroup of tumor stem cells (Wright et al., 2008). As previously described, a high YAP expression in luminal biased-progenitors might result in a luminal differentiation with basal traits. Moreover, over-expression of *HER2* has been shown to play an important role in the development and progression of certain aggressive types of breast cancer (Ménard et al., 2000). More recently, a group showed that in luminal breast cancer, hormonal treatment lead to a reduction in ER levels promoting cancer stem cell phenotype (*CD133<sup>high</sup>* and *CD44<sup>low</sup>*) (Sansone et al., 2016). This results correlate well with the fact estradiol serum concentration decreases with age (van Landeghem et al., 1985) and we observed an increase in *CD133<sup>high</sup>* and *CD44<sup>low</sup>* cell proportion. These cells are highly suspected for the implication as cells-of-origin for breast cancers.

## 5.9 Breast cancer susceptibility and prevention

When we examined human mammary epithelia at high definition, aging was found to be associated with the accumulation of mammary epithelial progenitor cells, which are putative cells-of-origin for breast cancers, and with the presence of fewer myoepithelial cells, which can suppress malignant tumor-forming cells. Thus, during the aging process, the population of cells potentially targeted for transformation is increased, and there is a simultaneous decrease in tumor-suppressive cells, which suggests a mechanism that leads to increased susceptibility to malignant progression (Figure 23). Altogether, the reciprocal dynamic between the microenvironment and the progenitor is skewed, leading to an increase selection for adaptive mutations and a decrease in tumor suppressive mechanisms (Henry et al., 2011). Thus, with age, a higher susceptibility to breast cancer may be attributed to a mis-regulation of progenitors by their microenvironment, which is a previously unappreciated hallmark of aging. The ultimate goal would be to prevent breast cancer in a non-invasive way. However, the fact that seven out of eight women >50y will not be affected by breast cancer, reveals the difficulty of identifying susceptibility factors and not confounding them with normal aging markers.

The therapeutic targets for the current forms of prevention are hormone-related (Fisher et al., 1998; Powles et al., 2007). In addition, in Paper I, we observed that a cohort of post-menopausal women treated with warfarin had significantly reduced relative risk of developing breast cancer. This findings support preventative therapeutic intervention of the Gas6-Axl pathway to combat breast cancer. Using the breast tissue mimetic models which allow us to study the aging process at the molecular, cell and tissue levels, we hope to identify entirely new classes of therapeutic targets that will usher in a new

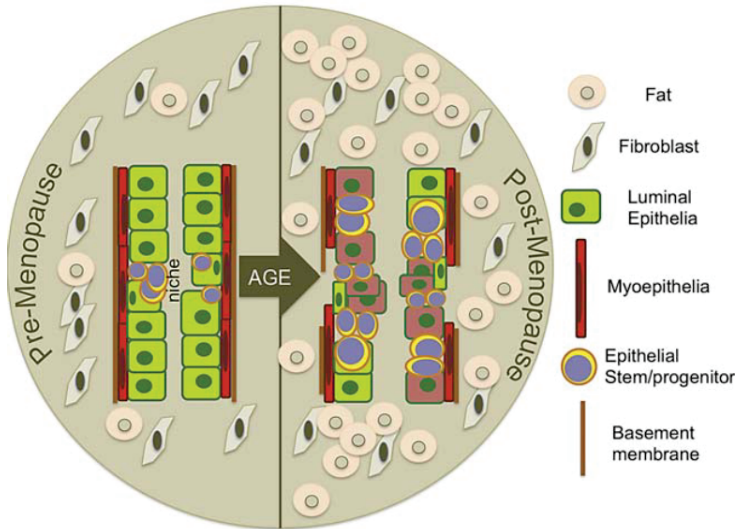


Figure 23: **A cartoon showing archetypical age-related states of breast tissue.** With age, the fat gradually replaces the connective tissue in the stroma that surrounds the mammary epithelia. Multipotent progenitors accumulate, luminal cells lose lineage fidelity and acquire the basal traits of the myoepithelial cells. The proportions of tumor-suppressive and contractile myoepithelial cells themselves also decreases with age. Reduction of myoepithelial cells might help explain putative discontinuities in the basement membrane that are thought to arise with age (LaBarge et al., 2015).

era of low toxicity chemoprevention. The ultimate achievement would be to identify a therapeutic approach to prevent breast cancers that is as safe as taking aspirin to ward off heart disease, for instance.

## 6 Concluding Remarks

We present an approach for interrogation of human aging that takes advantage of cultured strains of normal HMEC and engineered microenvironments to perform cell-based molecular and functional studies, which are validated by comparison with breast tissues. We identified a previously unappreciated mammary stem cell marker involved in breast homeostasis and breast cancer progression. We highlighted a novel hallmark of aging as a defect in microenvironmental stem cell regulation. Specifically, insensitivity of progenitors to mechanical cues may explain their accumulation with age. Finally, we revealed a high-dimensional age-related phenotypic divergence in the breast tissue that may contribute to the susceptibility to tumorigenesis and we built a robust age classification model. Moreover, distinct age-related phenotypic signatures were detectable in cKit-progenitor cells, considered the cell-of-origin for breast cancers.

Identifying pathways altered with age will enable the identification of entirely new classes of therapeutic targets that will usher in a new era of low toxicity chemoprevention.

## 7 Future Perspectives

Our results suggest that Axl receptor regulation is important for maintaining multipotent activity of normal stem/progenitor cells and surface receptor levels are restricted to rare suprabasal cells. Congruently, Axl expression is regulated at multiple levels. Axl has been previously identified as a YAP downstream target (Xu et al., 2011). We have shown that Axl expression correlated with YAP in MEP *in vitro*. This regulation of Axl by the Hippo pathway and its role in basal differentiation transcription program requires further investigation.

In addition, an *in situ* biomechanical characterization of mammary gland sections from women of differing age using Atomic Force Microscopy would be appreciated in order to compare the local epithelial stiffness with age at the cellular level.

We can speculate that with age, YAP/TAZ activation might result in a luminal differentiation with basal traits. This activation may lead to oncogenic pathway activation and malignancy. Further work is needed to target pathways altered with age, specifically the YAP/TAZ pathway, in order to assess if a "rejuvenation" of the older luminal cells would be observed via a decrease in basal traits. In future, this "rejuvenation" may be tested as a potential breast cancer prevention treatment.

Finally, we observed a population of cKit progenitors accumulating with age with a  $CD133^{high}$  and  $CD44^{low}$  phenotype. Others characterized these cells as cancer stem cells in luminal breast cancer (Sansone et al., 2016). These cells are highly suspected for the implication as cells-of-origin for breast cancers. Further investigation is needed to characterize these cells *in vivo*, to understand their role in breast cancer progression, and finally to target them as a preventive cure.

## 8 References

- Acerbi, I., Cassereau, L., Dean, I., Shi, Q., Au, A., Park, C., Chen, Y. Y., Liphardt, J., Hwang, E. S., and Weaver, V. M. (2015). Human breast cancer invasion and aggression correlates with ECM stiffening and immune cell infiltration. *Integrative Biology*, 7(10):1120–1134.
- Alexakis, C., Partridge, T., and Bou-Gharios, G. (2007). Implication of the satellite cell in dystrophic muscle fibrosis: a self-perpetuating mechanism of collagen overproduction. *American Journal of Physiology- Cell Physiology*, 293(2):C661–9.
- Altschuler, S. J. and Wu, L. F. (2010). Cellular Heterogeneity: Do Differences Make a Difference? *Cell*, 141(4):559–563.
- Amir, E.-a. D., Davis, K. L., Tadmor, M. D., Simonds, E. F., Levine, J. H., Bendall, S. C., Shenfeld, D. K., Krishnaswamy, S., Nolan, G. P., and Pe’er, D. (2013). viSNE enables visualization of high dimensional single-cell data and reveals phenotypic heterogeneity of leukemia. *Nature Biotechnology*, 31(6):545–52.
- Anderson, W. F., Chu, K. C., Chatterjee, N., Brawley, O., and Brinton, L. A. (2001). Tumor variants by hormone receptor expression in white patients with node-negative breast cancer from the surveillance, epidemiology, and end results database. *Journal of Clinical Oncology*, 19(1):18–27.
- Aragona, M., Panciera, T., Manfrin, A., Giullitti, S., Michielin, F., Elvassore, N., Dupont, S., and Piccolo, S. (2013). A mechanical checkpoint controls multicellular growth through YAP/TAZ regulation by actin-processing factors. *Cell*, 154(5):1047–59.
- Asiedu, M. K., Beauchamp-Perez, F. D., Ingle, J. N., Behrens, M. D., Radisky, D. C., and Knutson, K. L. (2014). AXL induces epithelial-to-mesenchymal transition and regulates the function of breast cancer stem cells. *Oncogene*, 33(10):1316–24.
- Asselin-Labat, M.-L., Vaillant, F., Sheridan, J. M., Pal, B., Wu, D., Simpson, E. R., Yasuda, H., Smyth, G. K., Martin, T. J., Lindeman, G. J., and Visvader, J. E. (2010). Control of mammary stem cell function by steroid hormone signalling. *Nature*, 465(7299):798–802.
- Atala, A., Bauer, S. B., Soker, S., Yoo, J. J., and Retik, A. B. (2006). Tissue-engineered autologous bladders for patients needing cystoplasty. *Lancet*, 367(9518):1241–6.
- Aubert, G. and Lansdorf, P. M. (2008). Telomeres and aging. *Physiological Reviews*, 88(2):557–79.
- Baker, D. J., Childs, B. G., Durik, M., Wijers, M. E., Sieben, C. J., Zhong, J., Saltness,

- 
- R. A., Jeganathan, K. B., Casaclang Verzosa, G., Pezeshki, A., Khazaie, K., Miller, J. D., and Van Deursen, J. M. (2016). Naturally occurring p16 Ink4a -positive cells shorten healthy lifespan. *Nature*, 530(7589):184–189.
- Bandura, D. R., Baranov, V. I., Ornatsky, O. I., Antonov, A., Kinach, R., Lou, X., Pavlov, S., Vorobiev, S., Dick, J. E., and Tanner, S. D. (2009). Mass cytometry: Technique for real time single cell multitarget immunoassay based on inductively coupled plasma time-of-flight mass spectrometry. *Analytical Chemistry*, 81(16):6813–6822.
- Barker, N., van Es, J. H., Kuipers, J., Kujala, P., van den Born, M., Cozijnsen, M., Haegebarth, A., Korving, J., Begthel, H., Peters, P. J., and Clevers, H. (2007). Identification of stem cells in small intestine and colon by marker gene *Lgr5*. *Nature*, 449(7165):1003–7.
- Barlow, C., Hirotsune, S., Paylor, R., Liyanage, M., Eckhaus, M., Collins, F., Shiloh, Y., Crawley, J. N., Ried, T., Tagle, D., and Wynshaw-Boris, A. (1996). Atm-Deficient Mice: A Paradigm of Ataxia Telangiectasia. *Cell*, 86(1):159–171.
- Beerman, I., Bhattacharya, D., Zandi, S., Sigvardsson, M., Weissman, I. L., Bryder, D., and Rossi, D. J. (2010). Functionally distinct hematopoietic stem cells modulate hematopoietic lineage potential during aging by a mechanism of clonal expansion. *Proceedings of the National Academy of Sciences*, 107(12):5465–70.
- Beerman, I., Bock, C., Garrison, B. S., Smith, Z. D., Gu, H., Meissner, A., and Rossi, D. J. (2013). Proliferation-dependent alterations of the DNA methylation landscape underlie hematopoietic stem cell aging. *Cell Stem Cell*, 12(4):413–25.
- Bendall, S. C., Simonds, E. F., Qiu, P., Amir, E.-a. D., Krutzik, P. O., Finck, R., Bruggner, R. V., Melamed, R., Trejo, A., Ornatsky, O. I., Balderas, R. S., Plevritis, S. K., Sachs, K., Pe, D., Tanner, S. D., and Nolan, G. P. (2011). Single-Cell Mass Cytometry of Differential Immune and Drug Responses Across a Human Hematopoietic Continuum. *Science*, 332(May):687–696.
- Beningo, K. A., Dembo, M., Kaverina, I., Small, J. V., and Wang, Y.-l. (2001). Nascent Focal Adhesions Are Responsible for the Generation of Strong Propulsive Forces in Migrating Fibroblasts. *The Journal of Cell Biology*, 153(4):881–888.
- Benz, C. C. (2008). Impact of aging on the biology of breast cancer. *Critical Reviews in Oncology/Hematology*, 66(1):65–74.
- Berdyeva, T. K., Woodworth, C. D., and Sokolov, I. (2005). Human epithelial cells increase their rigidity with ageing in vitro: direct measurements. *Physics in Medicine*

*and Biology*, 50(1):81–92.

- Bershadsky, A. D., Balaban, N. Q., and Geiger, B. (2003). Adhesion-dependent cell mechanosensitivity. *Annual Review of Cell and Developmental Biology*, 19(1):677–695.
- Bertrand, K. A., Tamimi, R. M., Scott, C. G., Jensen, M. R., Pankratz, V. S., Visscher, D., Norman, A., Couch, F., Shepherd, J., Fan, B., Chen, Y.-Y., Ma, L., Beck, A. H., Cummings, S. R., Kerlikowske, K., and Vachon, C. M. (2013). Mammographic density and risk of breast cancer by age and tumor characteristics. *Breast Cancer Research*, 15(6):R104.
- Bischofs, I. B. and Schwarz, U. S. (2003). Cell organization in soft media due to active mechanosensing. *Proceedings of the National Academy of Sciences*, 100(16):9274–9279.
- Bissell, M. J. and Labarge, M. A. (2005). Context, tissue plasticity, and cancer: Are tumor stem cells also regulated by the microenvironment? *Cancer Cell*, 7(1):17–23.
- Biteau, B., Hochmuth, C. E., and Jasper, H. (2008). JNK activity in somatic stem cells causes loss of tissue homeostasis in the aging *Drosophila* gut. *Cell Stem Cell*, 3(4):442–55.
- Blick, T., Hugo, H., Widodo, E., Waltham, M., Pinto, C., Mani, S. a., Weinberg, R. a., Neve, R. M., Lenburg, M. E., and Thompson, E. W. (2010). Epithelial mesenchymal transition traits in human breast cancer cell lines parallel the CD44HI/CD24lo/-stem cell phenotype in human breast cancer. *Journal of Mammary Gland Biology and Neoplasia*, 15(2):235–252.
- Bloustain-Qimron, N., Yao, J., Snyder, E. L., Shipitsin, M., Campbell, L. L., Mani, S. A., Hu, M., Chen, H., Ustyansky, V., Antosiewicz, J. E., Argani, P., Halushka, M. K., Thomson, J. A., Pharoah, P., Porgador, A., Sukumar, S., Parsons, R., Richardson, A. L., Stampfer, M. R., Gelman, R. S., Nikolskaya, T., Nikolsky, Y., and Polyak, K. (2008). Cell type-specific DNA methylation patterns in the human breast. *Proceedings of the National Academy of Sciences*, 105:14076–14081.
- Bodenmiller, B., Zunder, E. R., Finck, R., Chen, T. J., Savig, E. S., Bruggner, R. V., Simonds, E. F., Bendall, S. C., Sachs, K., Krutzik, P. O., and Nolan, G. P. (2012). Multiplexed mass cytometry profiling of cellular states perturbed by small-molecule regulators. *Nature Biotechnology*, 30(9):857–866.
- Bolinder, J., Ostman, J., and Arner, P. (1983). Influence of Aging on Insulin Receptor Binding and Metabolic Effects of Insulin on Human Adipose Tissue. *Diabetes*, 32(10):959–964.
- Bonnier, P., Romain, S., Lejeune, C., Tubiana, N., Martin, P.-m., and Piana, L. (1995).

- Age as a prognostic factor in breast cancer: relationship to pathologic and biologic features. *International Journal of Cancer*, 144:138–144.
- Bouchardy, C., Rapiti, E., Blagojevic, S., Vlastos, A. T., and Vlastos, G. (2007). Older female cancer patients: Importance, causes, and consequences of undertreatment. *Journal of Clinical Oncology*, 25(14):1858–1869.
- Boyd, N. F., Rommens, J. M., Vogt, K., Lee, V., Hopper, J. L., Yaffe, M. J., and Paterson, A. D. (2005). Mammographic breast density as an intermediate phenotype for breast cancer. *The Lancet. Oncology*, 6(10):798–808.
- Boyle, M., Wong, C., Rocha, M., and Jones, D. L. (2007). Decline in self-renewal factors contributes to aging of the stem cell niche in the *Drosophila* testis. *Cell Stem Cell*, 1(4):470–8.
- Brayton, C. F., Treuting, P. M., and Ward, J. M. (2012). Pathobiology of aging mice and GEM: background strains and experimental design. *Veterinary Pathology*, 49(1):85–105.
- Bruggner, R. V., Bodenmiller, B., Dill, D. L., Tibshirani, R. J., and Nolan, G. P. (2014). Automated identification of stratifying signatures in cellular subpopulations. *Proceedings of the National Academy of Sciences*, 111(26):E2770–7.
- Callister, W. D. and Rethwisch, D. G. (2000). *Fundamentals of Materials Science and Engineering: An Integrated Approach*. Wiley, Somerset, NJ, 5th edition.
- Campisi, J. and d’Adda di Fagagna, F. (2007). Cellular senescence: when bad things happen to good cells. *Nature Reviews Molecular Cell Biology*, 8(9):729–40.
- Caraux, A., Lu, Q., Fernandez, N., Riou, S., Di Santo, J. P., Raulet, D. H., Lemke, G., and Roth, C. (2006). Natural killer cell differentiation driven by Tyro3 receptor tyrosine kinases. *Nature Immunology*, 7(7):747–754.
- Carlson, B. and Faulkner, J. (1989). Muscle transplantation between young and old rats: age of host determines recovery. *American Journal of Physiology- Cell Physiology*.
- Carmel, R. (2001). Anemia and aging: an overview of clinical, diagnostic and biological issues. *Blood Reviews*, 15(1):9–18.
- Carter, A. J. R. and Nguyen, A. Q. (2011). Antagonistic pleiotropy as a widespread mechanism for the maintenance of polymorphic disease alleles. *BMC Medical Genetics*, 12(1):160.
- Cevenini, E., Invidia, L., Lescai, F., Salvioli, S., Tieri, P., Castellani, G., and Franceschi, C. (2015). Human models of aging and longevity. *Expert Opinion on Biological Therapy*, 8(9):1393–1405.

- Chakkalakal, J. V., Jones, K. M., Basson, M. A., and Brack, A. S. (2012). The aged niche disrupts muscle stem cell quiescence. *Nature*, 490(7420):355–60.
- Challen, G. A., Boles, N. C., Chambers, S. M., and Goodell, M. A. (2010). Distinct hematopoietic stem cell subtypes are differentially regulated by TGF-beta1. *Cell Stem Cell*, 6(3):265–78.
- Chandler, E. M., Seo, B. R., Califano, J. P., Andresen Eguiluz, R. C., Lee, J. S., Yoon, C. J., Tims, D. T., Wang, J. X., Cheng, L., Mohanan, S., Buckley, M. R., Cohen, I., Nikitin, A. Y., Williams, R. M., Gourdon, D., Reinhart-King, C. A., and Fischbach, C. (2012). Implanted adipose progenitor cells as physicochemical regulators of breast cancer. *Proceedings of the National Academy of Sciences*, 109(25):9786–91.
- Chang, C., Goel, H. L., Gao, H., Pursell, B., Shultz, L. D., Greiner, D. L., Ingerpuu, S., Patarroyo, M., Cao, S., Lim, E., Mao, J., McKee, K. K., Yurchenco, P. D., and Mercurio, A. M. (2015). A laminin 511 matrix is regulated by TAZ and functions as the ligand for the  $\alpha 6 \beta 1$  integrin to sustain breast cancer stem cells. *Genes & Development*, 29(1):1–6.
- Chanson, L., Brownfield, D., Garbe, J. C., Kuhn, I., Stampfer, M. R., Bissell, M. J., and LaBarge, M. A. (2011). Self-organization is a dynamic and lineage-intrinsic property of mammary epithelial cells. *Proceedings of the National Academy of Sciences*, 108(8):3264–3269.
- Chavez-MacGregor, M., Zhang, N., Buchholz, T. A., Zhang, Y., Niu, J., Elting, L., Smith, B. D., Hortobagyi, G. N., and Giordano, S. H. (2013). Trastuzumab-related cardiotoxicity among older patients with breast cancer. *Journal of Clinical Oncology*, 31(33):4222–8.
- Cheon, D.-J. and Orsulic, S. (2011). Mouse Models of Cancer. *Annual Review of Cell and Developmental Biology*.
- Cheung, T. H. and Rando, T. A. (2013). Molecular regulation of stem cell quiescence. *Nature reviews Molecular Cell Biology*, 14(6):329–40.
- Clark, G. M. (1992). The biology of breast cancer in older women. *Journal of gerontology*, 47 Spec No:19–23.
- Clark, G. M., Wenger, C. R., Beardslee, S., Owens, M. A., Pounds, G., Oldaker, T., Vendely, P., Pandian, M. R., Harrington, D., and McGuire, W. L. (1993). How to integrate steroid hormone receptor, flow cytometric, and other prognostic information in regard to primary breast cancer 5531. *Cancer*, 71(8):6–2162.
- Collins, C. A., Olsen, I., Zammit, P. S., Heslop, L., Petrie, A., Partridge, T. A., and Morgan, J. E. (2005). Stem cell function, self-renewal, and behavioral heterogeneity of

- cells from the adult muscle satellite cell niche. *Cell*, 122(2):289–301.
- Conboy, I. M., Conboy, M. J., Smythe, G. M., and Rando, T. A. (2003). Notch-mediated restoration of regenerative potential to aged muscle. *Science*, 302(5650):1575–7.
- Conboy, I. M., Conboy, M. J., Wagers, A. J., Girma, E. R., Weissman, I. L., and Rando, T. A. (2005). Rejuvenation of aged progenitor cells by exposure to a young systemic environment. *Nature*, 443(February).
- Conboy, I. M. and Rando, T. A. (2002). The regulation of Notch signaling controls satellite cell activation and cell fate determination in postnatal myogenesis. *Developmental Cell*, 3(3):397–409.
- Conn, M. (2011). *Handbook of Models for Human Aging*. Academic Press.
- Cosgrove, B. D., Gilbert, P. M., Porpiglia, E., Mourkioti, F., Lee, S. P., Corbel, S. Y., Llewellyn, M. E., Delp, S. L., and Blau, H. M. (2014). Rejuvenation of the muscle stem cell population restores strength to injured aged muscles. *Nature Medicine*, 20(3):255–64.
- Cotsarelis, G., Sun, T.-T., and Lavker, R. M. (1990). Label-retaining cells reside in the bulge area of pilosebaceous unit: Implications for follicular stem cells, hair cycle, and skin carcinogenesis. *Cell*, 61(7):1329–1337.
- d’Adda di Fagagna, F. (2008). Living on a break: cellular senescence as a DNA-damage response. *Nature Reviews Cancer*, 8(7):512–522.
- d’Adda di Fagagna, F., Reaper, P. M., Clay-Farrace, L., Fiegler, H., Carr, P., Von Zglinicki, T., Saretzki, G., Carter, N. P., and Jackson, S. P. (2003). A DNA damage checkpoint response in telomere-initiated senescence. *Nature*, 426(6963):194–8.
- Diab, S. G., Elledge, R. M., and Clark, G. M. (2000). Tumor Characteristics and Clinical Outcome of Elderly Women With Breast Cancer. *Journal of the National Cancer Institute*, 92(7).
- Dong, J., Feldmann, G., Huang, J., Wu, S., Zhang, N., Comerford, S. A., Gayyed, M. F., Anders, R. A., Maitra, A., and Pan, D. (2007). Elucidation of a universal size-control mechanism in *Drosophila* and mammals. *Cell*, 130(6):1120–33.
- Durbecq, V., Ameye, L., Veys, I., Paesmans, M., Desmedt, C., Sirtaine, N., Sotiriou, C., Bernard-Marty, C., Nogaret, J. M., Piccart, M., and Larsimont, D. (2008). A significant proportion of elderly patients develop hormone-dependant "luminal-B" tumours associated with aggressive characteristics. *Critical Reviews in Oncology/Hematology*, 67:80–92.
- Early Breast Cancer Trialists’ Collaborative Group, A. (2005). Effects of radiotherapy and

- of differences in the extent of surgery for early breast cancer on local recurrence and 15-year survival: An overview of the randomised trials. *Lancet*, 366(9503):2087–2106.
- Ellison, G., Klinowska, T., Westwood, R. F. R., Docter, E., French, T., and Fox, J. C. (2002). Further evidence to support the melanocytic origin of MDA-MB-435. *Molecular Pathology*, 55(5):294–9.
- Encinas, J. M., Michurina, T. V., Peunova, N., Park, J.-H., Tordo, J., Peterson, D. A., Fishell, G., Koulakov, A., and Enikolopov, G. (2011). Division-coupled astrocytic differentiation and age-related depletion of neural stem cells in the adult hippocampus. *Cell Stem Cell*, 8(5):566–79.
- Endogenous Hormones Breast Cancer Collaborative Group (2003). Body Mass Index, Serum Sex Hormones, and Breast Cancer Risk in Postmenopausal Women. *JNCI Journal of the National Cancer Institute*, 95(16):1218–1226.
- Engler, A., Sen, S., Sweeney, H., and Discher, D. (2006). Matrix elasticity directs stem cell lineage specification. *Cell*, 126(4):677–689.
- Eppenberger-Castori, S., Moore, D. H., Thor, A. D., Edgerton, S. M., Kueng, W., Eppenberger, U., and Benz, C. C. (2002). Age-associated biomarker profiles of human breast cancer. *The International Journal of Biochemistry and Cell Biology*, 34:1318–1330.
- Ergen, A. V., Boles, N. C., and Goodell, M. A. (2012). Rantes/Ccl5 influences hematopoietic stem cell subtypes and causes myeloid skewing. *Blood*, 119(11):2500–9.
- Ertel, A., Verghese, A., Byers, S. W., Ochs, M., and Tozeren, A. (2006). Pathway-specific differences between tumor cell lines and normal and tumor tissue cells. *Molecular Cancer*, 5(1):55.
- Esserman, L. J., Moore, D. H., Tsing, P. J., Chu, P. W., Yau, C., Ozanne, E., Chung, R. E., Tandon, V. J., Park, J. W., Baehner, F. L., Kreps, S., Tutt, A. N. J., Gillett, C. E., and Benz, C. C. (2011). Biologic markers determine both the risk and the timing of recurrence in breast cancer. *Breast Cancer Research and Treatment*, 129(2):607–16.
- Esteller, M., Silva, J. M., Dominguez, G., Bonilla, F., Matias-Guiu, X., Lerma, E., Bussaglia, E., Prat, J., Harkes, I. C., Repasky, E. A., Gabrielson, E., Schutte, M., Baylin, S. B., and Herman, J. G. (2000). Promoter hypermethylation and BRCA1 inactivation in sporadic breast and ovarian tumors. *Journal of the National Cancer Institute*, 92(7):564–9.
- Fast, R., Schütt, T., Toft, N., Møller, A., and Berendt, M. (2013). An observational study with long-term follow-up of canine cognitive dysfunction: clinical characteristics, survival, and risk factors. *Journal of Veterinary Internal Medicine*, 27(4):822–9.

- 
- Fienberg, H. G., Simonds, E. F., Fantl, W. J., Nolan, G. P., and Bodenmiller, B. (2012). A platinum-based covalent viability reagent for single-cell mass cytometry. *Cytometry Part A*, 81 A(6):467–475.
- Fisher, B., Costantino, J. P., Wickerham, D. L., Redmond, C. K., Kavanah, M., Cronin, W. M., Vogel, V., Robidoux, A., Dimitrov, N., Atkins, J., Daly, M., Wieand, S., Tan-Chiu, E., Ford, L., and Wolmark, N. (1998). Tamoxifen for Prevention of Breast Cancer: Report of the National Surgical Adjuvant Breast and Bowel Project P-1 Study. *JNCI Journal of the National Cancer Institute*, 90(18):1371–1388.
- Fuchs, E., Tumber, T., and Guasch, G. (2004). Socializing with the Neighbors. *Cell*, 116(6):769–778.
- Garbe, J. C., Bhattacharya, S., Merchant, B., Bassett, E., Swisshelm, K., Feiler, H. S., Wyrobek, A. J., and Stampfer, M. R. (2009). Molecular distinctions between stasis and telomere attrition senescence barriers shown by long-term culture of normal human mammary epithelial cells. *Cancer Research*, 69(19):7557–7568.
- Garbe, J. C., Pepin, F., Pelissier, F. A., Sputova, K., Fridriksdottir, A. J., Guo, D. E., Villadsen, R., Park, M., Petersen, O. W., Borowsky, A. D., Stampfer, M. R., and LaBarge, M. A. (2012). Accumulation of multipotent progenitors with a basal differentiation bias during aging of human mammary epithelia. *Cancer Research*, 72(14):3687–3701.
- Garbe, J. C., Vrba, L., Sputova, K., Fuchs, L., Novak, P., Brothman, A. R., Jackson, M., Chin, K., LaBarge, M. A., Watts, G., Futscher, B. W., and Stampfer, M. R. (2014). Immortalization of normal human mammary epithelial cells in two steps by direct targeting of senescence barriers does not require gross genomic alterations. *Cell Cycle*, 13(21):3423–3435.
- Garinis, G. A., van der Horst, G. T. J., Vijg, J., and Hoeijmakers, J. H. J. (2008). DNA damage and ageing: new-age ideas for an age-old problem. *Nature Cell Biology*, 10(11):1241–1247.
- Gehler, S., Baldassarre, M., Lad, Y., Leight, J. L., Wozniak, M. A., Riching, K. M., Eliceiri, K. W., Weaver, V. M., Calderwood, D. A., and Keely, P. J. (2009). Filamin A-beta1 integrin complex tunes epithelial cell response to matrix tension. *Molecular Biology of the Cell*, 20(14):3224–38.
- Geiger, H., de Haan, G., and Florian, M. C. (2013). The ageing haematopoietic stem cell compartment. *Nature Reviews Immunology*, 13(5):376–89.
- Gely-Pernot, A., Coronas, V., Harnois, T., Prestoz, L., Mandairon, N., Didier, A., Berjeaud,

- J. M., Monvoisin, A., Bourmeyster, N., De Frutos, P. G., Philippe, M., and Benzakour, O. (2012). An endogenous vitamin K-dependent mechanism regulates cell proliferation in the brain subventricular stem cell niche. *Stem Cells*, 30(4):719–731.
- Gil, J. and Peters, G. (2006). Regulation of the INK4b-ARF-INK4a tumour suppressor locus: all for one or one for all. *Nature Reviews Molecular Cell Biology*, 7(September):667–677.
- Gillet, J.-P., Calcagno, A. M., Varma, S., Marino, M., Green, L. J., Vora, M. I., Patel, C., Orina, J. N., Eliseeva, T. A., Singal, V., Padmanabhan, R., Davidson, B., Ganapathi, R., Sood, A. K., Rueda, B. R., Ambudkar, S. V., and Gottesman, M. M. (2011). Redefining the relevance of established cancer cell lines to the study of mechanisms of clinical anti-cancer drug resistance. *Proceedings of the National Academy of Sciences*, 108(46):18708–18713.
- Gjerdum, C., Tiron, C., Høiby, T., Stefansson, I., Haugen, H., Sandal, T., Collett, K., Li, S., McCormack, E., Gjertsen, B. T., Micklem, D. R., Akslen, L. A., Glackin, C., and Lorens, J. B. (2010). Axl is an essential epithelial-to-mesenchymal transition-induced regulator of breast cancer metastasis and patient survival. *Proceedings of the National Academy of Sciences*, 107(3):1124–9.
- Golji, J., Lam, J., and Mofrad, M. R. K. (2011). Vinculin activation is necessary for complete talin binding. *Biophysical Journal*, 100(2):332–40.
- Gomez, C. R., Boehmer, E. D., and Kovacs, E. J. (2005). The aging innate immune system. *Current Opinion in Immunology*, 17(5):457–462.
- Grayson, W. L., Fröhlich, M., Yeager, K., Bhumiratana, S., Chan, M. E., Cannizzaro, C., Wan, L. Q., Liu, X. S., Guo, X. E., and Vunjak-Novakovic, G. (2010). Engineering anatomically shaped human bone grafts. *Proceedings of the National Academy of Sciences*, 107(8):3299–304.
- Gudjonsson, T., Rønnov-Jessen, L., Villadsen, R., Rank, F., Bissell, M. J., and Petersen, O. W. (2002). Normal and tumor-derived myoepithelial cells differ in their ability to interact with luminal breast epithelial cells for polarity and basement membrane deposition. *Journal of Cell Science*, 115(Pt 1):39–50.
- Halder, G., Dupont, S., and Piccolo, S. (2012). Transduction of mechanical and cytoskeletal cues by YAP and TAZ. *Nature Reviews Molecular Cell Biology*, 13(9):591–600.
- Hannum, G., Guinney, J., Zhao, L., Zhang, L., Hughes, G., Sada, S., Klotzle, B., Bibikova, M., Fan, J.-B., Gao, Y., Deconde, R., Chen, M., Rajapakse, I., Friend, S., Ideker, T., and Zhang, K. (2013). Genome-wide methylation profiles reveal quantitative views of

- human aging rates. *Molecular Cell*, 49(2):359–67.
- Harvey, K. F., Zhang, X., and Thomas, D. M. (2013). The Hippo pathway and human cancer. *Nature Reviews Cancer*, 13(4):246–257.
- Hasanbasic, I., Rajotte, I., and Blostein, M. (2005). The role of gamma-carboxylation in the anti-apoptotic function of gas6. *Journal of Thrombosis and Haemostasis*, 3:2790–2797.
- Hayflick, L. (1965). The limited in vitro lifetime of human diploid cell strains. *Experimental Cell Research*, 37(3):614–636.
- Hayflick, L. and Moorhead, P. S. (1961). The serial cultivation of human diploid cell strains. *Experimental Cell Research*, 25:585–621.
- Henry, C. J., Marusyk, A., and DeGregori, J. (2011). Aging-associated changes in hematopoiesis and leukemogenesis: What’s the connection? *Aging*, 3(6):643–656.
- Herbig, U., Jobling, W. A., Chen, B. P. C., Chen, D. J., and Sedivy, J. M. (2004). Telomere shortening triggers senescence of human cells through a pathway involving ATM, p53, and p21(CIP1), but not p16(INK4a). *Molecular Cell*, 14(4):501–13.
- Hilton, H. N., Graham, J. D., Kantimm, S., Santucci, N., Cloosterman, D., Huschtscha, L. I., Mote, P. A., and Clarke, C. L. (2012). Progesterone and estrogen receptors segregate into different cell subpopulations in the normal human breast. *Molecular and Cellular Endocrinology*, 361(1-2):191–201.
- Hilton, H. N., Santucci, N., Silvestri, A., Kantimm, S., Huschtscha, L. I., Graham, J. D., and Clarke, C. L. (2014). Progesterone stimulates progenitor cells in normal human breast and breast cancer cells. *Breast cancer research and treatment*, 143(3):423–33.
- Holle, A. and Engler, A. (2011). More than a feeling: discovering, understanding, and influencing mechanosensing pathways. *Current Opinion in Biotechnology*, 22(5):648–654.
- Holliday, R. (2004). The close relationship between biological aging and age-associated pathologies in humans. *Journal of Gerontology: Biological Sciences*, 59(6):B547–50.
- Hong, J.-H., Hwang, E. S., McManus, M. T., Amsterdam, A., Tian, Y., Kalmukova, R., Mueller, E., Benjamin, T., Spiegelman, B. M., Sharp, P. A., Hopkins, N., and Yaffe, M. B. (2005). TAZ, a transcriptional modulator of mesenchymal stem cell differentiation. *Science*, 309(5737):1074–1078.
- Horvath, S., Zhang, Y., Langfelder, P., Kahn, R. S., Boks, M. P. M., van Eijk, K., van den Berg, L. H., and Ophoff, R. A. (2012). Aging effects on DNA methylation modules in human brain and blood tissue. *Genome Biology*, 13(10):R97.
- Howeedy, A. A., Virtanen, I., Laitinen, L., Gould, N. S., Koukoulis, G. K., and Gould,

- V. E. (1990). Differential distribution of tenascin in the normal, hyperplastic, and neoplastic breast. *Laboratory investigation; a journal of technical methods and pathology*, 63(6):798–806.
- Hutson, S., Cowen, P., and Bird, C. (1985). Morphometric studies of age related changes in normal human breast and their significance for evolution of mammary cancer. *Journal of Clinical Pathology*, 38(3):281–287.
- Ishizaki, T., Naito, M., Fujisawa, K., Maekawa, M., Watanabe, N., Saito, Y., and Narumiya, S. (1997). p160ROCK, a Rho-associated coiled-coil forming protein kinase, works downstream of Rho and induces focal adhesions. *FEBS Letters*, 404(2-3):118–124.
- Issa, J. P., Ottaviano, Y. L., Celano, P., Hamilton, S. R., Davidson, N. E., and Baylin, S. B. (1994). Methylation of the oestrogen receptor CpG island links ageing and neoplasia in human colon. *Nature Genetics*, 7(4):536–540.
- Iwasa, H., Maimaiti, S., Kuroyanagi, H., Kawano, S., Inami, K., Timalisina, S., Ikeda, M., Nakagawa, K., and Hata, Y. (2013). Yes-associated protein homolog, YAP-1, is involved in the thermotolerance and aging in the nematode *Caenorhabditis elegans*. *Experimental Cell Research*, 319(7):931–45.
- Jaramillo-Rodríguez, Y., Cerda-Flores, R. M., Ruiz-Ramos, R., López-Márquez, F. C., and Calderón-Garcidueñas, A. L. (2014). YAP expression in normal and neoplastic breast tissue: an immunohistochemical study. *Archives of Medical Research*, 45(3):223–8.
- Jarvis, J. U. (1981). Eusociality in a mammal: cooperative breeding in naked mole-rat colonies. *Science*, 212(4494):571–3.
- Jenkins, E. O., Deal, A. M., Anders, C. K., Prat, A., Perou, C. M., Carey, L. A., and Muss, H. B. (2014). Age-Specific Changes in Intrinsic Breast Cancer Subtypes: A Focus on Older Women. *The Oncologist*.
- Ji, H., Goode, R. J. A., Vaillant, F., Mathivanan, S., Kapp, E. A., Mathias, R. A., Lindeman, G. J., Visvader, J. E., and Simpson, R. J. (2011). Proteomic profiling of secretome and adherent plasma membranes from distinct mammary epithelial cell subpopulations. *Proteomics*, 11(20):4029–39.
- Kanai, F., Marignani, P. A., Sarbassova, D., Yagi, R., Hall, R. A., Donowitz, M., Hisaminato, A., Fujiwara, T., Ito, Y., Cantley, L. C., and Yaffe, M. B. (2000). TAZ: a novel transcriptional co-activator regulated by interactions with 14-3-3 and PDZ domain proteins. *The EMBO journal*, 19(24):6778–91.
- Keller, P. J., Lin, A., Arendt, L. M., Klebba, I., Jones, A. D., Rudnick, J. A., DiMeo,

- 
- T. A., Gilmore, H., Jefferson, D. M., Graham, R. A., Naber, S. P., Schnitt, S., and Kuperwasser, C. (2010). Mapping the cellular and molecular heterogeneity of normal and malignant breast tissues and cultured cell lines. *Breast Cancer Research*, 12(5):R87.
- Kim, J. E., Finlay, G. J., and Baguley, B. C. (2013). The Role of the Hippo Pathway in Melanocytes and Melanoma. *Frontiers in Oncology*, 3(May):1–7.
- Kimura, K., Ito, M., Amano, M., Chihara, K., Fukata, Y., Nakafuku, M., Yamamori, B., Feng, J., Nakano, T., Okawa, K., Iwamatsu, A., and Kaibuchi, K. (1996). Regulation of myosin phosphatase by Rho and Rho-associated kinase (Rho-kinase). *Science*, 273(5272):245–248.
- Kirane, A., Ludwig, K. F., Sorrelle, N., Haaland, G., Sandal, T., Ranaweera, R., Toombs, J. E., Wang, M., Dineen, S. P., Micklem, D., Dellinger, M. T., Lorens, J. B., and Brekken, R. A. (2015). Warfarin Blocks Gas6-Mediated Axl Activation Required for Pancreatic Cancer Epithelial Plasticity and Metastasis. *Cancer Research*, 75(18).
- Klass, M. R. (1983). A method for the isolation of longevity mutants in the nematode *Caenorhabditis elegans* and initial results. *Mechanisms of Ageing and Development*, 22(3-4):279–86.
- Kodaka, M. and Hata, Y. (2015). The mammalian Hippo pathway: regulation and function of YAP1 and TAZ. *Cellular and Molecular Life Sciences*, pages 285–306.
- Kovanen, V., Suominen, H., Risteli, J., and Risteli, L. (1988). Type IV collagen and laminin in slow and fast skeletal muscle in rats—effects of age and life-time endurance training. *Collagen and Related Research*, 8(2):145–53.
- LaBarge, M. A., Mora-Blanco, E. L., Samson, S., and Miyano, M. (2015). Breast Cancer beyond the Age of Mutation. *Gerontology*.
- LaBarge, M. A., Nelson, C. M., Villadsen, R., Fridriksdottir, A., Ruth, J. R., Stampfer, M. R., Petersen, O. W., and Bissell, M. J. (2009). Human mammary progenitor cell fate decisions are products of interactions with combinatorial microenvironments. *Integrative Biology*, 1(1):70–79.
- LaBarge, M. A., Petersen, O. W., and Bissell, M. J. (2007). Of microenvironments and mammary stem cells. *Stem Cell Reviews*, 3(2):137–146.
- Lacroix, M. (2009). MDA-MB-435 cells are from melanoma, not from breast cancer. *Cancer Chemotherapy and Pharmacology*, 63(3):567.
- Lavelle, K., Todd, C., Moran, A., Howell, A., Bundred, N., and Campbell, M. (2007). Non-standard management of breast cancer increases with age in the UK: a population

- based cohort of women  $>$  or  $=65$  years. *British Journal of Cancer*, 96(8):1197–1203.
- Lee, J. K., Garbe, J. C., Vrba, L., Miyano, M., Futscher, B. W., Stampfer, M. R., and LaBarge, M. A. (2015). Age and the means of bypassing stasis influence the intrinsic subtype of immortalized human mammary epithelial cells. *Frontiers in Cell and Developmental Biology*, 3(March):1–9.
- Levental, I., Georges, P., and Janmey, P. (2007). Soft biological materials and their impact on cell function. *Soft Matter*, 3(3):299.
- Levental, K. R., Yu, H., Kass, L., Lakins, J. N., Egeblad, M., Erler, J. T., Fong, S. F., Csizsar, K., Giaccia, A., Weninger, W., Yamauchi, M., Gasser, D. L., and Weaver, V. M. (2009). Matrix Crosslinking Forces Tumor Progression by Enhancing Integrin Signaling. *Cell*, 139(5):891–906.
- Levine, J. H., Simonds, E. F., Bendall, S. C., Davis, K. L., Amir, E.-a. D., Tadmor, M. D., Litvin, O., Fienberg, H. G., Jager, A., Zunder, E. R., Finck, R., Gedman, A. L., Radtke, I., Downing, J. R., Pe'er, D., and Nolan, G. P. (2015). Data Driven Phenotypic Dissection of AML Reveals Progenitor like Cells that Correlate with Prognosis. *Cell*, 162(1):184–197.
- Liang, H., Masoro, E. J., Nelson, J. F., Strong, R., McMahan, C., and Richardson, A. (2003). Genetic mouse models of extended lifespan. *Experimental Gerontology*, 38(11-12):1353–1364.
- Lifshitz, E. and Kramer, L. (2000). Outpatient Urine Culture. Does Collection Technique Matter? *Archives of Internal Medicine*, 160(16):2537.
- Lim, E., Vaillant, F., Wu, D., Forrest, N. C., Pal, B., Hart, A. H., Asselin-Labat, M.-L., Gyorki, D. E., Ward, T., Partanen, A., Feleppa, F., Huschtscha, L. I., Thorne, H. J., Fox, S. B., Yan, M., French, J. D., Brown, M. A., Smyth, G. K., Visvader, J. E., and Lindeman, G. J. (2009). Aberrant luminal progenitors as the candidate target population for basal tumor development in BRCA1 mutation carriers. *Nature Medicine*, 15(8):907–13.
- Lin, C., Pelissier, F. A., Zhang, H., Lakins, J., Weaver, V. M., Park, C., and LaBarge, M. A. (2015). Microenvironment rigidity modulates responses to the HER2 receptor tyrosine kinase inhibitor lapatinib via YAP and TAZ transcription factors. *Molecular Biology of the Cell*, 26(22):3946–3953.
- Lin, C.-H., Yu, M.-C., Tung, W.-H., Chen, T.-T., Yu, C.-C., Weng, C.-M., Tsai, Y.-J., Bai, K.-J., Hong, C.-Y., Chien, M.-H., and Chen, B.-C. (2013). Connective tissue

- growth factor induces collagen I expression in human lung fibroblasts through the Rac1/MLK3/JNK/AP-1 pathway. *Biochimica et Biophysica Acta*, 1833(12):2823–33.
- Linger, R. M. A., Keating, A. K., Earp, H. S., and Graham, D. K. (2008). TAM Receptor Tyrosine Kinase: Biological Functions, Signaling, and Potential Therapeutics Targeting in human Cancer. *Advanced Cancer Research*, 100(08):35–83.
- Liu, S., Ginestier, C., Charafe-Jauffret, E., Foco, H., Kleer, C. G., Merajver, S. D., Dontu, G., and Wicha, M. S. (2008). BRCA1 regulates human mammary stem/progenitor cell fate. *Proceedings of the National Academy of Sciences*, 105(5):1680–5.
- López-Otín, C., Blasco, M. A., Partridge, L., Serrano, M., and Kroemer, G. (2013). The hallmarks of aging. *Cell*, 153(6):1194–217.
- Lou, X., Zhang, G., Herrera, I., Kinach, R., Ornatsky, O., Baranov, V., Nitz, M., and Winnik, M. A. (2007). Polymer-based elemental tags for sensitive bioassays. *Angewandte Chemie (International ed. in English)*, 46(32):6111–4.
- Lu, P., Takai, K., Weaver, V. M., and Werb, Z. (2011). Extracellular matrix degradation and remodeling in development and disease. *Cold Spring Harbor Perspectives in Biology*, 3(12).
- Lu, P., Weaver, V. M., and Werb, Z. (2012). The extracellular matrix: A dynamic niche in cancer progression. *Journal of Cell Biology*, 196(4):395–406.
- Lugert, S., Basak, O., Knuckles, P., Haussler, U., Fabel, K., Götz, M., Haas, C. A., Kempermann, G., Taylor, V., and Giachino, C. (2010). Quiescent and active hippocampal neural stem cells with distinct morphologies respond selectively to physiological and pathological stimuli and aging. *Cell Stem Cell*, 6(5):445–56.
- Lui, C., Lee, K., and Nelson, C. (2012). Matrix compliance and RhoA direct the differentiation of mammary progenitor cells. *Biomechanics and Modeling in Mechanobiology*, 11(8):1241–1249.
- Lutz, W., Sanderson, W., and Scherbov, S. (2008). The coming acceleration of global population ageing. *Nature*, 451(7179):716–9.
- Mansilla, E., Díaz Aquino, V., Zambón, D., Marin, G. H., Mártire, K., Roque, G., Ichim, T., Riordan, N. H., Patel, A., Sturla, F., Larsen, G., Spretz, R., Núñez, L., Soratti, C., Ibar, R., van Leeuwen, M., Tau, J. M., Drago, H., and Maceira, A. (2011). Could metabolic syndrome, lipodystrophy, and aging be mesenchymal stem cell exhaustion syndromes? *Stem Cells International*, 2011:943216.
- Martin, K., Potten, C., Roberts, S., and Kirkwood, T. (1998). Altered stem cell regeneration

- in irradiated intestinal crypts of senescent mice. *Journal of Cell Science*, 111(16):2297–2303.
- Maskarinec, G., Pagano, I., Lurie, G., and Kolonel, L. (2006). A longitudinal investigation of mammographic density: the multiethnic cohort. *Cancer Epidemiology Biomarkers & Prevention*, 15(4):732–739.
- McCay, C., Crowell, M. F., and Maynard, L. A. (1935). The Effect of Retarded Growth upon the Length of Life Span and upon the Ultimate Body Size. *The journal of nutrition*.
- McCormack, V. A., Perry, N. M., Vinnicombe, S. J., and Dos Santos Silva, I. (2010). Changes and tracking of mammographic density in relation to Pike’s model of breast tissue aging: a UK longitudinal study. *International journal of cancer*, 127(2):452–61.
- Melk, A., Mansfield, E. S., Hsieh, S.-C., Hernandez-Boussard, T., Grimm, P., Rayner, D. C., Halloran, P. F., and Sarwal, M. M. (2005). Transcriptional analysis of the molecular basis of human kidney aging using cDNA microarray profiling. *Kidney International*, 68(6):2667–2679.
- Ménard, S., Tagliabue, E., Campiglio, M., and Pupa, S. M. (2000). Role of HER2 gene overexpression in breast carcinoma. *Journal of Cellular Physiology*, 182(2):150–162.
- Millar, T., Walker, R., Arango, J.-C., Ironside, J., Harrison, D., MacIntyre, D., Blackwood, D., Smith, C., and Bell, J. (2007). Tissue and organ donation for research in forensic pathology: the MRC Sudden Death Brain and Tissue Bank. *The Journal of Pathology*, 213(4):369–375.
- Mitra, A., Mishra, L., and Li, S. (2013). Technologies for deriving primary tumor cells for use in personalized cancer therapy. *Trends in Biotechnology*, 31(6):347–354.
- Moerman, E. J., Teng, K., Lipschitz, D. A., and Lecka-Czernik, B. (2004). Aging activates adipogenic and suppresses osteogenic programs in mesenchymal marrow stroma/stem cells: the role of PPAR- $\gamma$ 2 transcription factor and TGF- $\beta$ /BMP signaling pathways. *Aging Cell*, 3(6):379–389.
- Moreira, J. M., Cabezón, T., Gromova, I., Gromov, P., Timmermans-Wielenga, V., Machado, I., Llombart-Bosch, A., Kroman, N., Rank, F., and Celis, J. E. (2010). Tissue proteomics of the human mammary gland: Towards an abridged definition of the molecular phenotypes underlying epithelial normalcy. *Molecular Oncology*, 4(6):539–561.
- Mortensen, M., Soilleux, E. J., Djordjevic, G., Tripp, R., Lutteropp, M., Sadighi-Akha, E., Stranks, A. J., Glanville, J., Knight, S., Jacobsen, S.-E. W., Kranc, K. R., and Simon, A. K. (2011). The autophagy protein Atg7 is essential for hematopoietic stem

- cell maintenance. *The Journal of Experimental Medicine*, 208(3):455–67.
- Moskalev, A. A., Shaposhnikov, M. V., Plyusnina, E. N., Zhavoronkov, A., Budovsky, A., Yanai, H., and Fraifeld, V. E. (2013). The role of DNA damage and repair in aging through the prism of Koch-like criteria. *Ageing Research Reviews*, 12(2):661–84.
- Mouse Genome Consortium Sequencing (2002). Initial sequencing and comparative analysis of the mouse genome. *Nature*, 420(December).
- Muir, A. R., Kanji, A. H., and Allbrook, D. (1965). The structure of the satellite cells in skeletal muscle. *Journal of Anatomy*, 99(Pt 3):435–44.
- Muss, H. B., Woolf, S., Berry, D., Cirrincione, C., Weiss, R. B., Budman, D., Wood, W. C., Henderson, I. C., Hudis, C., Winer, E., Cohen, H., Wheeler, J., and Norton, L. (2005). Adjuvant chemotherapy in older and younger women with lymph node-positive breast cancer. *JAMA*, 293(9):1073–81.
- Mustacchi, G., Cazzaniga, M. E., Pronzato, P., De Matteis, a., Di Costanzo, F., and Floriani, I. (2007). Breast cancer in elderly women: A different reality? Results from the NORA study. *Annals of Oncology*, 18(6):991–996.
- Nakano, T., Kawamoto, K., Kishino, J., Nomura, K., Higashino, K.-i., and Arita, H. (1997). Requirement of gamma-carboxyglutamic acid residues for the biological activity of Gas6: contribution of endogenous Gas6 to the proliferation of vascular smooth muscle cells. *The Biochemical Journal*, 323 ( Pt 2):387–92.
- Narod, S. A. and Foulkes, W. D. (2004). BRCA1 and BRCA2: 1994 and beyond. *Nature Reviews Cancer*, 4(9):665–76.
- Navasesh, M. (1993). Methods for Collecting Saliva. *Annals of the New York Academy of Sciences*, 694(1 Saliva as a D):72–77.
- Neve, R. M., Chin, K., Fridlyand, J., Yeh, J., Baehner, F. L., Fevr, T., Clark, L., Bayani, N., Coppe, J. P., Tong, F., Speed, T., Spellman, P. T., DeVries, S., Lapuk, A., Wang, N. J., Kuo, W. L., Stilwell, J. L., Pinkel, D., Albertson, D. G., Waldman, F. M., McCormick, F., Dickson, R. B., Johnson, M. D., Lippman, M., Ethier, S., Gazdar, A., and Gray, J. W. (2006). A collection of breast cancer cell lines for the study of functionally distinct cancer subtypes. *Cancer Cell*, 10(6):515–527.
- Niemann, C. and Watt, F. M. (2002). Designer skin: lineage commitment in postnatal epidermis. *Trends in Cell Biology*, 12(4):185–192.
- Nilsson, S. K., Johnston, H. M., and Coverdale, J. A. (2001). Spatial localization of transplanted hemopoietic stem cells : inferences for the localization of stem cell niches

- Spatial localization of transplanted hemopoietic stem cells : inferences for the localization of stem cell niches. *Blood*, 97(8):2293–2299.
- Nishimura, E. K., Jordan, S. A., Oshima, H., Yoshida, H., Osawa, M., Moriyama, M., Jackson, I. J., Barrandon, Y., Miyachi, Y., and Nishikawa, S.-I. (2002). Dominant role of the niche in melanocyte stem-cell fate determination. *Nature*, 416(6883):854–60.
- Oh, J., Lee, Y. D., and Wagers, A. J. (2014). Stem cell aging: mechanisms, regulators and therapeutic opportunities. *Nature Medicine*, 20(8):870–880.
- Ornatsky, O., Bandura, D., Baranov, V., Nitz, M., Winnik, M. a., and Tanner, S. (2010). Highly multiparametric analysis by mass cytometry. *Journal of Immunological Methods*, 361(1-2):1–20.
- Pan, L., Chen, S., Weng, C., Call, G., Zhu, D., Tang, H., Zhang, N., and Xie, T. (2007). Stem cell aging is controlled both intrinsically and extrinsically in the *Drosophila* ovary. *Cell Stem Cell*, 1(4):458–69.
- Park, I.-K., Giovenzana, C., Hughes, T. L., Yu, J., Trotta, R., and Caligiuri, M. A. (2009). The Axl / Gas6 pathway is required for optimal cytokine signaling during human natural killer cell development. *Blood*, 113(11):2470–2477.
- Pashai, N., Hao, H., All, A., Gupta, S., Chaerkady, R., de Los Angeles, A., Gearhart, J. D., and Kerr, C. L. (2012). Genome-wide profiling of pluripotent cells reveals a unique molecular signature of human embryonic germ cells. *PLoS ONE*, 7(6).
- Paszek, M. J., Zahir, N., Johnson, K. R., Lakins, J. N., Rozenberg, G. I., Gefen, A., Reinhart-King, C. a., Margulies, S. S., Dembo, M., Boettiger, D., Hammer, D. a., and Weaver, V. M. (2005). Tensional homeostasis and the malignant phenotype. *Cancer Cell*, 8(3):241–254.
- Patra, C., Talukdar, S., Novoyatleva, T., Velagala, S. R., Mühlfeld, C., Kundu, B., Kundu, S. C., and Engel, F. B. (2012). Silk protein fibroin from *Antheraea mylitta* for cardiac tissue engineering. *Biomaterials*, 33(9):2673–2680.
- Peer, P. G., van Dijck, J. A., Hendriks, J. H., Holland, R., and Verbeek, A. L. (1993). Age-dependent growth rate of primary breast cancer. *Cancer*, 71(11):3547–3551.
- Pelissier, F. A., Garbe, J. C., Ananthanarayanan, B., Miyano, M., Lin, C., Jokela, T., Kumar, S., Stampfer, M. R., Lorens, J. B., and LaBarge, M. A. (2014). Age-related dysfunction in mechanotransduction impairs differentiation of human mammary epithelial progenitors. *Cell Reports*, 7(6):1926–39.
- Pervaiz, S., Taneja, R., and Ghaffari, S. (2009). Oxidative Stress Regulation of Stem and

- Progenitor Cells. *Antioxidants & Redox Signaling*, 11(11):2777–2789.
- Petersen, T. H., Calle, E. A., Zhao, L., Lee, E. J., Gui, L., Raredon, M. B., Gavrillov, K., Yi, T., Zhuang, Z. W., Breuer, C., Herzog, E., and Niklason, L. E. (2010). Tissue-engineered lungs for in vivo implantation. *Science*, 329(5991):538–41.
- Pinder, M. C., Duan, Z., Goodwin, J. S., Hortobagyi, G. N., and Giordano, S. H. (2007). Congestive heart failure in older women treated with adjuvant anthracycline chemotherapy for breast cancer. *Journal of clinical oncology : official journal of the American Society of Clinical Oncology*, 25(25):3808–15.
- Pobbati, A. and Hong, W. (2013). Emerging roles of TEAD transcription factors and its coactivators in cancers. *Cancer Biology & Therapy*, 14(5):390–8.
- Powles, T. J., Ashley, S., Tidy, A., Smith, I. E., and Dowsett, M. (2007). Twenty-year follow-up of the Royal Marsden randomized, double-blinded tamoxifen breast cancer prevention trial. *Journal of the National Cancer Institute*, 99(4):283–290.
- Prat, A. and Perou, C. M. (2011). Deconstructing the molecular portraits of breast cancer. *Molecular Oncology*, 5(1):5–23.
- Prowse, K. R. and Greider, C. W. (1995). Developmental and tissue-specific regulation of mouse telomerase and telomere length. *Proceedings of the National Academy of Sciences*, 92(11):4818–22.
- Qian, X., Goderie, S. K., Shen, Q., Stern, J. H., and Temple, S. (1998). Intrinsic programs of patterned cell lineages in isolated vertebrate CNS ventricular zone cells. *Development*, 125(16):3143–52.
- Qin, Z., Voorhees, J. J., Fisher, G. J., and Quan, T. (2014). Age-associated reduction of cellular spreading/mechanical force up-regulates matrix metalloproteinase-1 expression and collagen fibril fragmentation via c-Jun/AP-1 in human dermal fibroblasts. *Aging Cell*, (August):1–10.
- Raouf, A., Zhao, Y., To, K., Stingl, J., Delaney, A., Barbara, M., Iscove, N., Jones, S., McKinney, S., Emerman, J., Aparicio, S., Marra, M., and Eaves, C. (2008). Transcriptome analysis of the normal human mammary cell commitment and differentiation process. *Cell Stem Cell*, 3(1):109–18.
- Regan, J. L., Kendrick, H., Magnay, F.-a., Vafaizadeh, V., Groner, B., and Smalley, M. (2012). c-Kit is required for growth and survival of the cells of origin of Brca1-mutation-associated breast cancer. *Oncogene*, 31(7):869–883.
- Reid, D. M., Doughty, J., Eastell, R., Heys, S. D., Howell, A., McCloskey, E. V., Powles,

- T., Selby, P., and Coleman, R. E. (2008). Guidance for the management of breast cancer treatment-induced bone loss: a consensus position statement from a UK Expert Group. *Cancer Treatment Reviews*, 34 Suppl 1:S3–18.
- Rera, M., Bahadorani, S., Cho, J., Koehler, C. L., Ulgherait, M., Hur, J. H., Ansari, W. S., Lo, T., Jones, D. L., and Walker, D. W. (2011). Modulation of longevity and tissue homeostasis by the *Drosophila* PGC-1 homolog. *Cell Metabolism*, 14(5):623–34.
- Ryu, B.-Y., Orwig, K. E., Oatley, J. M., Avarbock, M. R., and Brinster, R. L. (2006). Effects of Aging and Niche Microenvironment on Spermatogonial Stem Cell Self-Renewal. *Stem Cells*, 24(6):1505–1511.
- Sacco, A., Doyonnas, R., Kraft, P., Vitorovic, S., and Blau, H. M. (2008). Self-renewal and expansion of single transplanted muscle stem cells. *Nature*, 456(7221):502–6.
- Sansone, P., Ceccarelli, C., Berishaj, M., Chang, Q., Rajasekhar, V. K., Perna, F., Bowman, R. L., Vidone, M., Daly, L., Nnoli, J., Santini, D., Taffurelli, M., Shih, N. N. C., Feldman, M., Mao, J. J., Colameco, C., Chen, J., DeMichele, A., Fabbri, N., Healey, J. H., Cricca, M., Gasparre, G., Lyden, D., Bonafé, M., and Bromberg, J. (2016). Self-renewal of CD133hi cells by IL6-Notch3 signalling regulates endocrine resistance in metastatic breast cancer. *Nature Communications*, 7:10442.
- Santagata, S., Thakkar, A., Ergonul, A., Wang, B., Woo, T., Hu, R., Harrell, J. C., McNamara, G., Schwede, M., Culhane, A. C., Kindelberger, D., Rodig, S., Richardson, A., Schnitt, S. J., Tamimi, R. M., and Ince, T. A. (2014). Taxonomy of breast cancer based on normal cell phenotype predicts outcome. *The Journal of Clinical Investigation*, 124(2):859–70.
- Schaefer, G., Rosen, P. P., Lesser, M. L., Kinne, D. W., and Beattie, E. J. (1984). Breast carcinoma in elderly women: pathology, prognosis, and survival. *Pathology Annual*, 19 Pt 1:195–219.
- Schonberg, M. A., Marcantonio, E. R., Li, D., Silliman, R. A., Ngo, L., and McCarthy, E. P. (2010). Breast cancer among the oldest old: tumor characteristics, treatment choices, and survival. *Journal of Clinical Oncology*, 28(12):2038–2045.
- Schwartz, M. A. (2010). Integrins and extracellular matrix in mechanotransduction. *Cold Spring Harbor Perspectives in Biology*, 2(12):a005066.
- Serrano, M., Lin, A. W., McCurrach, M. E., Beach, D., and Lowe, S. W. (1997). Oncogenic ras Provokes Premature Cell Senescence Associated with Accumulation of p53 and p16INK4a. *Cell*, 88(5):593–602.

- 
- Shehata, M., Teschendorff, A., Sharp, G., Novcic, N., Russell, I. A., Avril, S., Prater, M., Eirew, P., Caldas, C., Watson, C. J., and Stingl, J. (2012). Phenotypic and functional characterisation of the luminal cell hierarchy of the mammary gland. *Breast Cancer Research*, 14(5):R134.
- Shuster, S., Black, M. M., and McVitie, E. (1975). The influence of age and sex on skin thickness, skin collagen and density. *British Journal of Dermatology*, 93(6):639–643.
- Signer, R. and Morrison, S. (2013). Mechanisms that regulate stem cell aging and life span. *Cell Stem Cell*, 12(2):152–165.
- Skibinski, A., Breindel, J. L., Prat, A., Galván, P., Smith, E., Rolfs, A., Gupta, P. B., LaBaer, J., and Kuperwasser, C. (2014). The Hippo Transducer TAZ Interacts with the SWI/SNF Complex to Regulate Breast Epithelial Lineage Commitment. *Cell Reports*, 6:1059–1072.
- Soen, Y., Mori, A., Palmer, T. D., and Brown, P. O. (2006). Exploring the regulation of human neural precursor cell differentiation using arrays of signaling microenvironments. *Molecular Systems Biology*, 2:37.
- Son, M.-Y., Seol, B., Han, Y.-M., and Cho, Y. S. (2013). Comparative receptor tyrosine kinase profiling identifies a novel role for AXL in human stem cell pluripotency. *Human Molecular Genetics*, 23(7):1802–16.
- Sørlie, T., Perou, C. M., Tibshirani, R., Aas, T., Geisler, S., Johnsen, H., Hastie, T., Eisen, M. B., van de Rijn, M., Jeffrey, S. S., Thorsen, T., Quist, H., Matese, J. C., Brown, P. O., Botstein, D., Lønning, P. E., and Børresen-Dale, A. L. (2001). Gene expression patterns of breast carcinomas distinguish tumor subclasses with clinical implications. *Proceedings of the National Academy of Sciences*, 98(19):10869–74.
- Soule, H. D., Maloney, T. M., Wolman, S. R., Peterson, W. D., Brenz, R., McGrath, C. M., Russo, J., Pauley, R. J., Jones, R. F., and Brooks, S. C. (1990). Isolation and characterization of a spontaneously immortalized human breast epithelial cell line, MCF-10. *Cancer Research*, 50(18):6075–86.
- Sputova, K., Garbe, J. C., Pelissier, F. A., Chang, E., Stampfer, M. R., and Labarge, M. A. (2013). Aging phenotypes in cultured normal human mammary epithelial cells are correlated with decreased telomerase activity independent of telomere length. *Genome Integrity*, 4(1):4.
- Stampfer, M. R., Labarge, M. A., and Garbe, J. C. (2013). *An Integrated Human Mammary Epithelial Cell Culture System for Studying Carcinogenesis and Aging*. Humana Press,

Totowa, NJ.

- Stein, W. D., Litman, T., Fojo, T., and Bates, S. E. (2004). A serial analysis of gene expression (SAGE) database analysis of chemosensitivity: comparing solid tumors with cell lines and comparing solid tumors from different tissue origins. *Cancer Research*, 64:2805–2815.
- Stenderup, K. (2003). Aging is associated with decreased maximal life span and accelerated senescence of bone marrow stromal cells. *Bone*, 33(6):919–926.
- Stephens, P. J., Tarpey, P. S., Davies, H., Van Loo, P., Greenman, C., Wedge, D. C., Nik-Zainal, S., Martin, S., Varela, I., Bignell, G. R., Yates, L. R., Papaemmanuil, E., Beare, D., Butler, A., Cheverton, A., Gamble, J., Hinton, J., Jia, M., Jayakumar, A., Jones, D., Latimer, C., Lau, K. W., McLaren, S., McBride, D. J., Menzies, A., Mudie, L., Raine, K., Rad, R., Chapman, M. S., Teague, J., Easton, D., Langerød, A., Lee, M. T. M., Shen, C.-Y., Tee, B. T. K., Huimin, B. W., Broeks, A., Vargas, A. C., Turashvili, G., Martens, J., Fatima, A., Miron, P., Chin, S.-F., Thomas, G., Boyault, S., Mariani, O., Lakhani, S. R., van de Vijver, M., van 't Veer, L., Foekens, J., Desmedt, C., Sotiriou, C., Tutt, A., Caldas, C., Reis-Filho, J. S., Aparicio, S. A. J. R., Salomon, A. V., Børresen-Dale, A.-L., Richardson, A. L., Campbell, P. J., Futreal, P. A., and Stratton, M. R. (2012). The landscape of cancer genes and mutational processes in breast cancer. *Nature*, 486(7403):400–4.
- Sudol, M. (1994). Yes-associated protein (YAP65) is a proline-rich phosphoprotein that binds to the SH3 domain of the Yes proto-oncogene product. *Oncogene*, 9(8):2145–52.
- Swindell, W. R., Johnston, A., Sun, L., Xing, X., Fisher, G. J., Bulyk, M. L., Elder, J. T., and Gudjonsson, J. E. (2012). Meta-profiles of gene expression during aging: Limited similarities between mouse and human and an unexpectedly decreased inflammatory signature. *PLoS One*, 7(3).
- Takeda, T. (1999). Senescence-accelerated mouse (SAM): A biogerontological resource in aging research. *Neurobiology of Aging*, 20(2):105–110.
- Takubo, K., Nagamatsu, G., Kobayashi, C. I., Nakamura-Ishizu, A., Kobayashi, H., Ikeda, E., Goda, N., Rahimi, Y., Johnson, R. S., Soga, T., Hirao, A., Suematsu, M., and Suda, T. (2013). Regulation of Glycolysis by Pdk Functions as a Metabolic Checkpoint for Cell Cycle Quiescence in Hematopoietic Stem Cells. *Cell Stem Cell*, 12(1):49–61.
- Tamada, M., Sheetz, M. P., and Sawada, Y. (2004). Activation of a signaling cascade by cytoskeleton stretch. *Developmental Cell*, 7(5):709–18.

- 
- Tanabe, K., Nagata, K., Ohashi, K., Nakano, T., Arita, H., and Mizuno, K. (1997). Roles of  $\gamma$ -carboxylation and a sex hormone-binding globulin-like domain in receptor-binding and in biological activities of Gas6. *FEBS Letters*, 408(3):306–310.
- Taylor, E. J., Adams, C., and Neville, R. (1995). Some nutritional aspects of ageing in dogs and cats. *Proceedings of the Nutrition Society*, 54(03):645–656.
- Thurlbeck, W. M. (1975). Growth and aging of the normal human lung. *Chest Journal*, 67(2\_Supplement):3S.
- Titus, S., Li, F., Stobezki, R., Akula, K., Unsal, E., Jeong, K., Dickler, M., Robson, M., Moy, F., Goswami, S., and Oktay, K. (2013). Impairment of BRCA1-related DNA double-strand break repair leads to ovarian aging in mice and humans. *Science Translational Medicine*, 5(172):172ra21.
- Tsai, H.-T., Isaacs, C., Fu, a. Z., Warren, J. L., Freedman, a. N., Barac, A., Huang, C.-Y., and Potosky, a. L. (2014). Risk of cardiovascular adverse events from trastuzumab (Herceptin®) in elderly persons with breast cancer: a population-based study. *Breast Cancer Research and Treatment*, 144(1):163–70.
- Tse, J. and Engler, A. (2010). Preparation of hydrogel substrates with tunable mechanical properties. *Current Protocols in Cell Biology*, Chapter 10(June):Unit 10.16.
- Tuck, M. K., Chan, D. W., Chia, D., Godwin, A. K., Grizzle, W. E., Krueger, K. E., Rom, W., Sanda, M., Sorbara, L., Stass, S., Wang, W., and Brenner, D. E. (2009). Standard operating procedures for serum and plasma collection: Early detection research network consensus statement standard operating procedure integration working group. *Journal of Proteome Research*, 8(1):113–117.
- Tumlin, J., Wali, R., Williams, W., Murray, P., Tolwani, A. J., Vinnikova, A. K., Szerlip, H. M., Ye, J., Paganini, E. P., Dworkin, L., Finkel, K. W., Kraus, M. A., and Humes, H. D. (2008). Efficacy and safety of renal tubule cell therapy for acute renal failure. *Journal of the American Society of Nephrology*, 19(5):1034–40.
- Turner, N. C., Reis-Filho, J. S., Russell, A. M., Springall, R. J., Ryder, K., Steele, D., Savage, K., Gillett, C. E., Schmitt, F. C., Ashworth, A., and Tutt, A. N. (2007). BRCA1 dysfunction in sporadic basal-like breast cancer. *Oncogene*, 26(14):2126–32.
- Turrentine, F. E., Wang, H., Simpson, V. B., and Jones, R. S. (2006). Surgical risk factors, morbidity, and mortality in elderly patients. *Journal of the American College of Surgeons*, 203(6):865–77.
- van Deursen, J. M. (2014). The role of senescent cells in ageing. *Nature*, 509(7501):439–446.

- van Landeghem, A. A., Poortman, J., Nabuurs, M., and Thijssen, J. H. H. (1985). Endogenous concentration and subcellular distribution of estrogens in normal and malignant human breast tissue. *Cancer Research*, 45(June):2900–2906.
- Varani, J., Dame, M. K., Rittie, L., Fligel, S. E. G., Kang, S., Fisher, G. J., and Voorhees, J. J. (2006). Decreased collagen production in chronologically aged skin: roles of age-dependent alteration in fibroblast function and defective mechanical stimulation. *The American journal of pathology*, 168(6):1861–1868.
- Villadsen, R., Fridriksdottir, A. J., Rønnov-Jessen, L., Gudjonsson, T., Rank, F., LaBarge, M. A., Bissell, M. J., and Petersen, O. W. (2007). Evidence for a stem cell hierarchy in the adult human breast. *Journal of Cell Biology*, 177(1):87–101.
- Visvader, J. E. (2009). Keeping abreast of the mammary epithelial hierarchy and breast tumorigenesis. *Genes & Development*, 15(23):2563–2577.
- Vlug, E., van de Ven, R., and Vermeulen, J. (2013). Nuclear localization of the transcriptional coactivator YAP is associated with invasive lobular breast cancer. *Cellular Oncology*, pages 375–384.
- Vogel, V. and Sheetz, M. (2006). Local force and geometry sensing regulate cell functions. *Nature Reviews Molecular Cell Biology*, 7(4):265–275.
- Wada, K.-I., Itoga, K., Okano, T., Yonemura, S., and Sasaki, H. (2011). Hippo pathway regulation by cell morphology and stress fibers. *Development*, 138(18):3907–3914.
- Waki, T., Tamura, G., Sato, M., and Motoyama, T. (2003). Age-related methylation of tumor suppressor and tumor-related genes: an analysis of autopsy samples. *Oncogene*, 22(26):4128–4133.
- Wang, J., Zhang, H., Young, A. G., Qiu, R., Argalian, S., Li, X., Wu, X., Lemke, G., and Lu, Q. (2011). Transcriptome analysis of neural progenitor cells by a genetic dual reporter strategy. *Stem Cells*, 29(10):1589–1600.
- Warr, M. R., Binnewies, M., Flach, J., Reynaud, D., Garg, T., Malhotra, R., Debnath, J., and Passegué, E. (2013). FOXO3A directs a protective autophagy program in haematopoietic stem cells. *Nature*, 494(7437):323–7.
- Weismann, A. (1889). *Essays Upon Heredity and Kindred Biological Problems*.
- Well, D., Yang, H., Houseni, M., Iruvuri, S., Alzeair, S., Sansovini, M., Wintering, N., Alavi, A., and Torigian, D. A. (2007). Age-related structural and metabolic changes in the pelvic reproductive end organs. *Seminars in Nuclear Medicine*, 37(3):173–84.
- Williams, G. C. (1957). Pleiotropy, natural selection, and the evolution of senescence.

- Evolution*, 11(4):398–411.
- Woodward, W. A., Chen, M. S., Behbod, F., and Rosen, J. M. (2005). On mammary stem cells. *Journal of Cell Science*, 118(16):3585–3594.
- Wright, M. H., Calcagno, A. M., Salcido, C. D., Carlson, M. D., Ambudkar, S. V., and Varticovski, L. (2008). Brca1 breast tumors contain distinct CD44+/CD24- and CD133+ cells with cancer stem cell characteristics. *Breast Cancer Research*, 10(1):R10.
- Wu, S., Huang, J., Dong, J., and Pan, D. (2003). hippo encodes a Ste-20 family protein kinase that restricts cell proliferation and promotes apoptosis in conjunction with salvador and warts. *Cell*, 114(4):445–456.
- Wyld, L. and Reed, M. (2007). The role of surgery in the management of older women with breast cancer. *European Journal of Cancer*, 43(15):2253–63.
- Xu, M. Z., Chan, S. W., Liu, a. M., Wong, K. F., Fan, S. T., Chen, J., Poon, R. T., Zender, L., Lowe, S. W., Hong, W., and Luk, J. M. (2011). AXL receptor kinase is a mediator of YAP-dependent oncogenic functions in hepatocellular carcinoma. *Oncogene*, 30(10):1229–1240.
- Yang, S.-H., Cheng, P.-H., Banta, H., Piotrowska-Nitsche, K., Yang, J.-J., Cheng, E. C. H., Snyder, B., Larkin, K., Liu, J., Orkin, J., Fang, Z.-H., Smith, Y., Bachevalier, J., Zola, S. M., Li, S.-H., Li, X.-J., and Chan, A. W. S. (2008). Towards a transgenic model of Huntington’s disease in a non-human primate. *Nature*, 453(7197):921–4.
- Yau, C., Fedele, V., Roydasgupta, R., Fridlyand, J., Hubbard, A., Gray, J. W., Chew, K., Dairkee, S. H., Moore, D. H., Schittulli, F., Tommasi, S., Paradiso, A., Albertson, D. G., and Benz, C. C. (2007). Aging impacts transcriptomes but not genomes of hormone-dependent breast cancers. *Breast Cancer Research*, 9(5):R59.
- Yu, H., Mouw, J. K., and Weaver, V. M. (2011). Forcing form and function: biomechanical regulation of tumor evolution. *Trends in Cell Biology*, 21(1):47–56.
- Yu, W.-M., Liu, X., Shen, J., Jovanovic, O., Pohl, E. E., Gerson, S. L., Finkel, T., Broxmeyer, H. E., and Qu, C.-K. (2013). Metabolic regulation by the mitochondrial phosphatase PTPMT1 is required for hematopoietic stem cell differentiation. *Cell Stem Cell*, 12(1):62–74.
- Zhang, H., Liu, C. Y., Zha, Z. Y., Zhao, B., Yao, J., Zhao, S., Xiong, Y., Lei, Q. Y., and Guan, K. L. (2009). TEAD transcription factors mediate the function of TAZ in cell growth and epithelial-mesenchymal transition. *Journal of Biological Chemistry*, 284(20):13355–13362.

- Zhao, B., Li, L., Lu, Q., Wang, L. H., Liu, C. Y., Lei, Q., and Guan, K. L. (2011). Angiomotin is a novel Hippo pathway component that inhibits YAP oncoprotein. *Genes and Development*, 25(1):51–63.
- Zhao, B., Wei, X., Li, W., Udan, R. S., Yang, Q., Kim, J., Xie, J., Ikenoue, T., Yu, J., Li, L., Zheng, P., Ye, K., Chinnaiyan, A., Halder, G., Lai, Z.-C., and Guan, K.-L. (2007). Inactivation of YAP oncoprotein by the Hippo pathway is involved in cell contact inhibition and tissue growth control. *Genes & Development*, 21(21):2747–61.
- Zhao, B., Ye, X., Yu, J., Li, L., Li, W., Li, S., Yu, J., Lin, J. D., Wang, C.-y., Chinnaiyan, A. M., Lai, Z.-c., and Guan, K.-l. (2008). TEAD mediates YAP-dependent gene induction and growth control. *Genes & Development*, pages 1962–1971.









# Age-Related Dysfunction in Mechanotransduction Impairs Differentiation of Human Mammary Epithelial Progenitors

Fanny A. Pelissier,<sup>1,2</sup> James C. Garbe,<sup>1</sup> Badriprasad Ananthanarayanan,<sup>4</sup> Masaru Miyano,<sup>1</sup> ChunHan Lin,<sup>1,3</sup> Tiina Jokela,<sup>1,2</sup> Sanjay Kumar,<sup>4</sup> Martha R. Stampfer,<sup>1</sup> James B. Lorens,<sup>2</sup> and Mark A. LaBarge<sup>1,\*</sup>

<sup>1</sup>Life Science Division, Lawrence Berkeley National Laboratory, Berkeley, CA 94720, USA

<sup>2</sup>Center for Cancer Biomarkers, Department of Biomedicine, University of Bergen, Bergen 5009, Norway

<sup>3</sup>Department of Comparative Biochemistry

<sup>4</sup>Department of Bioengineering

University of California, Berkeley, Berkeley, CA 94720, USA

\*Correspondence: [malabarge@lbl.gov](mailto:malabarge@lbl.gov)

<http://dx.doi.org/10.1016/j.celrep.2014.05.021>

This is an open access article under the CC BY-NC-ND license (<http://creativecommons.org/licenses/by-nc-nd/3.0/>).

## SUMMARY

Dysfunctional progenitor and luminal cells with acquired basal cell properties accumulate during human mammary epithelial aging for reasons not understood. Multipotent progenitors from women aged <30 years were exposed to a physiologically relevant range of matrix elastic modulus (stiffness). Increased stiffness causes a differentiation bias towards myoepithelial cells while reducing production of luminal cells and progenitor maintenance. Lineage representation in progenitors from women >55 years is unaffected by physiological stiffness changes. Efficient activation of Hippo pathway transducers YAP and TAZ is required for the modulus-dependent myoepithelial/basal bias in younger progenitors. In older progenitors, YAP and TAZ are activated only when stressed with extraphysiologically stiff matrices, which bias differentiation towards luminal-like phenotypes. In vivo YAP is primarily active in myoepithelia of younger breasts, but localization and activity increases in luminal cells with age. Thus, aging phenotypes of mammary epithelia may arise partly because alterations in Hippo pathway activation impair microenvironment-directed differentiation and lineage specificity.

## INTRODUCTION

The aging process is often correlated with changes in stem cell activity with consequences ranging from reduced regenerative capacity to increased cancer incidence. Human hematopoietic stem cells accumulate with age (Kuranda et al., 2011; Pang et al., 2011) and exhibit a differentiation bias toward defective myeloid lineages (Cho et al., 2008), making individuals more prone to autoimmune problems and myeloid leukemias (Henry

et al., 2011). In mice, the proportion of mitotic neural stem cells increases with age, whereas numbers of adult-born neurons decrease (Stoll et al., 2011). Human hippocampus shows patterns of age-related changes similar to mice that may underlie age-related cognitive decline (Knoth et al., 2010). Transit amplifying cells, not stem cells, accumulate in epidermis with age and delay wound healing (Charruyer et al., 2009). Mammary epithelium is maintained by a hierarchy of lineage-biased and multipotent progenitor and stem cells (Nguyen et al., 2014; Rios et al., 2014; Villadsen et al., 2007). In human mammary gland, differentiation-defective cKit-expressing multipotent progenitors (MPPs) accumulate with age, and proportions of daughter myoepithelial (MEP) and luminal epithelial (LEP) cells shift with age. We hypothesized that these age-associated changes make aged breast tissue susceptible to malignant progression (Garbe et al., 2012). Accumulation of defective stem or progenitor cells may be a common phenotype among aging tissues, and we hypothesize that aged MPPs accumulate because they do not correctly perceive microenvironmental differentiation cues.

The molecular composition of microenvironments impose specific cell fate decisions in normal and immortal nonmalignant mammary MPP (LaBarge et al., 2009). Cell culture substrata tuned to elastic moduli that mimicked normal breast tissue also biased the differentiation of an immortal nonmalignant MPP cell line into LEP (Lui et al., 2012). Matrix stiffness is mechanistically important in breast cancer progression as well; rigid breast tissue correlates with high breast cancer risk and drives malignant phenotypes in breast cancer cell lines (Yu et al., 2011). The physiological range of elastic modulus in breast likely plays an instructive role in the differentiation of normal mammary epithelial progenitors.

Membrane and cytoskeleton proteins sense mechanical cues and trigger transduction cascades that relay information throughout the cytoskeleton and to the nucleus. Responses can include changes in morphology and gene expression (Vogel and Sheetz, 2006). Sensing matrix elasticity occurs through cell-cell and cell-extracellular matrix (ECM) interactions mediated by adherens, integrins, vinculin, focal adhesion kinase (FAK), and others (Beningo et al., 2001; Bershadsky et al., 2003; Tamada

et al., 2004). The actinomyosin network includes RhoA, which regulates the actin cytoskeleton in the formation of stress fibers (SFs) and focal adhesions (FAs). Activation of ROCK1/ROCK2 causes increased activity of the motor protein myosin II by phosphorylation of the myosin light chain (MLC) and inactivation of the MLC phosphatase (Ishizaki et al., 1997; Kimura et al., 1996). YAP and TAZ are Hippo pathway transcriptional coactivators that are thought to interact with the Rho pathway to transduce mechanical information about the microenvironment to the nucleus (Halder et al., 2012). As stiffness increases, YAP/TAZ relocates from cytoplasm into nucleus, where they generate gene expression patterns that underlie cellular functions like proliferation, migration, epithelial-to-mesenchymal transition, and differentiation (Dupont et al., 2011; Kanai et al., 2000; Zhao et al., 2007).

Differentiation of mesenchymal stem cells down neurogenic, myogenic, or osteogenic pathways was directed by exposure to a wide range of tissue-relevant elastic moduli, from 100 to ~40,000 Pa (Engler et al., 2006). In comparison, mammary MPP differentiation should be responsive to a much narrower range of modulus relevant to normal and malignant breast (100~4,000 Pa; Paszek et al., 2005). The impact of aging on modulus-directed differentiation is unknown. Addressing these issues required a culture-based platform for functional analyses of primary normal human mammary MPP from many individuals. Here, we used such an approach to demonstrate that differentiation patterns of MPP from women aged <30 years cultured on tunable 2D and 3D substrata were exquisitely responsive to a physiologically relevant range of elastic modulus in a YAP/TAZ-dependent manner, whereas MPP from women >55 years were relatively unresponsive to changes in rigidity due to inefficient activation of the Hippo pathway transducers.

## RESULTS

### Aging Alters Modulus-Dependent Differentiation

To test whether microenvironment rigidity directed differentiation in MPP, we enriched receptor tyrosine kinase cKit-expressing (cKit+) human mammary epithelial cells (HMECs) by flow cytometry (fluorescence-activated cell sorting [FACS]) from fourth passage primary prestasis HMEC (strains) derived from five women aged <30 years and five from women >55 years (Figure S1; Table S1). Prestasis HMEC strains are normal and not treated with any immortalizing agents, have finite lifespans, and we previously demonstrated that they retain molecular, biochemical, and functional properties consistent with chronological aging in vivo (Garbe et al., 2012). The cKit+ MPP were cultured for 48 hr on type 1 collagen-coated polyacrylamide (PA) gels. The Young's elastic modulus [E(Pa)] of the PA gels was tuned from 200 Pa to 2,350 Pa. The lineage of each daughter cell was confirmed by immunofluorescence (IF) of intermediate filament proteins keratin (K)14 and K19, CD227 (sialomucin-1), and CD10 (Calla; Figures 1A, 1B, 1E, and 1F). Computer image analysis identified the different lineages; LEP are CD227+/CD10-/K14-/K19+, MEP are CD227-/CD10+/K14+/K19-, and K14+K19+ expression is consistent with MPP states (Villadsen et al., 2007). cKit+ MPP from women <30 years generated proportionately more LEP on soft substrata, but gen-

eration of MEP increased with higher E (Figures 1C, 1C', 1G, and S2A). cKit+ MPP from women >55 years did not generate different lineage proportions in response to changes in E (Figures 1D, 1D', 1H, and S2B). Primary first passage cKit+ MPP from three women <30 years, embedded in tunable 3D hydrogels with some type 1 collagen for 7 days (Figure S3A; Ananthanarayanan et al., 2011), gave rise to more LEP at 120 Pa versus more MEP at 3,800 Pa (Figures 1K, 1M, 1M', and S3B). In contrast, cKit+ MPP from three women >55 years did not display modulus-dependent differentiation patterns (Figures 1L, 1N, 1N', and S3C). The proportion of K14+/K19+ MPP decreased with elastic modulus on 2D PA gels and in 3D gels <30 years HMEC (Figures S4A–S4C), but no change in proportions of MPP was observed in >55 years HMEC (Figures S4B, S4D, and S4F). These results suggested that differentiation was modulus dependent in younger MPP and that this response was lost with age.

To test if changes in lineage proportions were due to lineage-biased proliferation, incorporation of 5-ethynyl-2'-deoxyuridine (EdU) into DNA was measured as a proxy for proliferation. All lineages derived after 48 hr from cKit+ MPP on PA gels exhibited similar proportions of EdU incorporation (EdU\*), irrespective of substrate rigidity or age (Figure 1I). In contrast, EdU incorporation in unsorted HMEC strains, which are primarily composed of more mature LEP and MEP, revealed age- and lineage-specific replicative behaviors. Proportions of EdU+ MEP from <30 years HMEC significantly increased with greater E whereas EdU+ LEP trended downward (Figure 1J). Unsorted HMEC from women >55 years exhibited neither lineage- nor modulus-dependent proliferation (Figure 1J), underscoring the lack of mechanoreponse with age. Thus, changes in lineage proportions exhibited by <30 years MPP after 48 hr were likely due to modulus-dependent differentiation, and only after the lineages matured in <30 years HMEC strains, did they show evidence of modulus-dependent proliferation.

### Mechanosensing Functions Were Unaltered by Age

To determine whether mechanosensing was age dependent, F-actin SF formation and FA assembly activities were measured in cKit+ MPP from three <30 years and three >55 years strains. Irrespective of age, SF formation increased with greater E (Figure 2A). Homogeneity measurements were used to quantify formation of the F-actin cables (Haralick et al., 1973; Pantic et al., 2012); SF homogeneity was inversely proportional to E in both age groups, which showed similar slopes (Figures 2B and 2C). Progenitors from both age groups were stained for pFAK and vinculin, which colocalize at FA. More FA assemblies were observed with increased E at the interfaces of MPP and gels, and FA formation was not impaired with age (Figures 2D and 2E). FA homogeneity was inversely proportional to E with comparable slopes in both age groups (Figures 2F and 2G). Thus, similar SF and FA phenotypes were observed both in younger and older cKit+ MPP.

Extracellular signal-regulated kinase (ERK) is phosphorylated in response to increased elastic modulus in some adherent cell lines (Provenzano et al., 2009), and because it is a key effector of serum responses, changes in its modulation could cause pleiotropic cellular responses. Both young and old cKit+ MPP exhibited a low level of ERK phosphorylation on 200 Pa PA

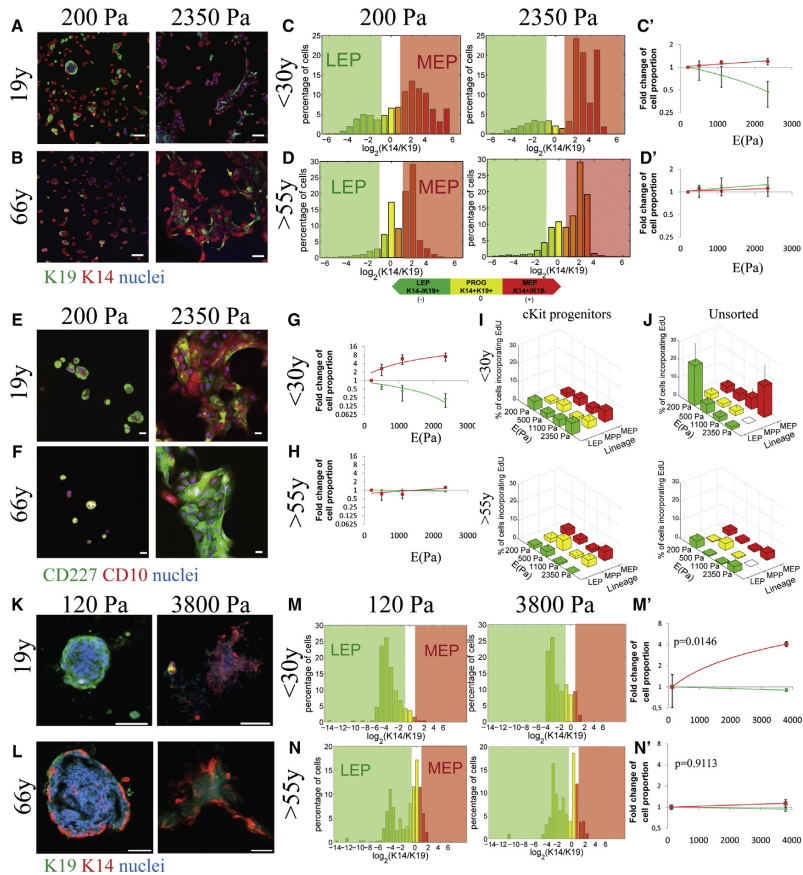


**Figure 1. Aging Alters Differentiation Patterns in Response to Matrix Stiffness**

(A and B) Representative IF images of progenitors from young (240L; 19 years) and (B) an older (122L; 66 years) strains stained for K19 (green), K14 (red), and DAPI (blue) after 48 hr of culture on PA gels with increasing elastic modulus (E[Pa]). Bars represent 100  $\mu$ m.

(C and D) Histograms represent  $\log_2$ -transformed ratios of K14 to K19 protein expression in single cells on 2D PA gels with increasing stiffness; histograms are heat mapped to indicate cells with the phenotypes of K14+/K19+ LEPs (green), K14+/K19+ progenitors (yellow), and K14+/K19- MEPs (red).

(C' and D') Corresponding linear regression plots of LEP and MEP proportions as a function of modulus are shown for (C') women <30 years (LEP:  $p = 0.0429$ ,  $r^2 = 0.2086$ ; MEP:  $p = 0.0475$ ,  $r^2 = 0.2009$ ,  $n = 5$ ) and (D') women >55 years (LEP:  $p = 0.4812$ ,  $r^2 = 0.0296$ ; MEP:  $p = 0.5138$ ,  $r^2 = 0.0240$ ,  $n = 5$ ). Regressions are fold change of lineage proportions compared to cKit+ on 200 Pa condition  $\pm$  SEM.

(E and F) Representative IF images of progenitors from (E) young (240L; 19 years) and (F) older (122L; 66 years) strains stained for CD227 (green), CD10 (red), and DAPI (blue) after 48 hr of culture on PA gels with increasing elastic modulus. Bars represent 20  $\mu$ m.

(G and H) Linear regression of fold change of LEP (CD227+/CD10-) and MEP (CD227-/CD10+) proportions as function of elastic modulus in (G) women <30 years (LEP:  $p = 0.0080$ ,  $r^2 = 0.5219$ ; MEP:  $p = 0.0198$ ,  $r^2 = 0.4340$ ,  $n = 3$ ) and (H) women >55 years (LEP:  $p = 0.4689$ ,  $r^2 = 0.0536$ ; MEP:  $p = 0.1937$ ,  $r^2 = 0.5219$ ,  $n = 3$ ). Linear regressions are of fold change of lineage proportions normal to 200 Pa condition  $\pm$  SEM.

(I and J) Percentage of cells incorporating EdU as function of lineages and stiffness in (I) cKit+ HMEC and (J) unsorted HMEC (MEP from women <30 years linear regression,  $p = 0.0270$ ,  $r^2 = 0.9467$ ; LEP from women <30 years t test 200 Pa versus 2,350 Pa,  $p = 0.0153$ ,  $n = 5$ ). Data are means  $\pm$  SEM.

(K and L) Representative IF of K19 (green), K14 (red), and DAPI (blue) of passage 1 cKit+ HMEC from a 19-year-old and a 65-year-old woman after 7 days of culture encapsulated in 3D hyaluronic acid (HA) gels. Bars represent 20  $\mu$ m.

(legend continued on next page)

gels but increased up to 15-fold on 2,350 Pa PA gels (Figures 2H and 2I). Differences in pERK were not significant between age groups, and mitogen-activated protein kinase (MAPK) inhibitor PD98059 prevented ERK phosphorylation. By these measures, modulus-dependent activity in serum response was independent of age.

If mechanosensing was unaffected by aging, then perturbations of actinomyosin regulators that are known to alter FA or SF formation should elicit parallel phenotypes in young and old MPP. Independent of age, we observed that inhibitors of ROCK1/ROCK2 (Y27632) and MLC kinase (ML-7) tended to disrupt SF on 2,350 Pa substrata and showed little effect at 200 Pa, whereas the MLC phosphatase inhibitor calyculin A (calA) caused SF formation at 200 Pa (Figures 3A and 3B). Patterns of changes in F-actin homogeneity were parallel in both age groups (Figures 3C and 3D). Y27632 and ML-7 disrupted the FA assemblies on 2,350 Pa substrata, whereas calA promoted FA assembly on 200 Pa substrata (Figures 3E and 3F) and measurements of FA homogeneity showed parallel changes in both age groups (Figures 3G and 3H). Mechanosensing of substrata in the physiologically relevant range was age independent, evaluated by these measures, and thus was unlikely to account for age-dependent differences in mechanically directed differentiation.

Analysis of the effects of actinomyosin network modulation on differentiation in three young and three old cKit+ MPP revealed surprising age-dependent responses. FA and SF in cells treated with Y27632 and ML-7 on 2,350 Pa gels were similar to untreated cells on 200 Pa gels, whereas calA increased the SF and FA as if cells were on stiffer substrata. Thus, SF and FA phenotypes were pharmacologically manipulated irrespective of the actual substrate E. Younger cKit+ MPP treated with Y27632 or ML-7 significantly increased proportions of K19+ LEP compared to DMSO-treated cells on 2,350 Pa gels. In contrast, older MPP were unaffected by Y27632 or ML-7 treatment (Figure S5). Interestingly, calA increased MEP generation from young MPP but caused older MPP to give rise to significantly more LEP. No changes in proportion were observed on 200 Pa gels, suggesting that addition of calA was insufficient to trigger cell differentiation on such a soft substrata. Older progenitors did not respond to chemically decreased perception of stiffness, but they responded to artificially higher stiffness oppositely to that of young progenitors, suggesting that age-dependent transcriptional programs were operative.

### Aging Alters the Ability of YAP and TAZ to Transduce Mechanical Information to the Nucleus

We next determined whether the mechanotransductive transcription factors YAP and TAZ were involved in modulus-dependent differentiation. IF staining of YAP and TAZ in cKit+ MPP from three HMEC strains <30 years exhibited increased YAP/TAZ nuclear translocation as PA gel E increased from 200 to 2,350 Pa (Figures 4A and 4B). However, significant nu-

clear translocation of YAP/TAZ was not observed in older progenitors in the same range (Figures 4C and 4D). The ability to activate YAP/TAZ by changes in substrate E was age dependent.

To determine the extent to which YAP/TAZ was unresponsive to changes in E in older progenitors, we evaluated their activation in response to extraphysiological stiffness. cKit+ MPP from three young and three old strains were cultured on type 1 collagen-coated glass (>3 GigaPa) or 200 Pa gels. YAP/TAZ translocated to the nucleus in young cKit+ MPP on glass (Figures 4A and 4B), gave rise to fewer LEP (Figure 4E), and those LEP incorporated less EdU on glass compared to 200 Pa gels (Figure 4F). In older cKit+ MPP on glass, YAP/TAZ was nuclear (Figures 4C and 4D), but cells gave rise to more LEP (Figure 4G), which incorporated more EdU on glass than on 200 Pa gels (Figure 4H). Both calA treatment and culture on extraphysiologically rigid substrata elicited more LEP differentiation in older MPP, which was the opposite of younger MPP. Thus, the Hippo pathway mechanoresponse in older progenitors was shifted to an extraphysiological "trigger point".

To determine if YAP and TAZ were required for modulus-dependent differentiation, both in the physiological and extraphysiological ranges, cKit+ MPP were transfected with small interfering RNAs (siRNAs), siYAP or siTAZ, which achieved >70% knockdown of the respective mRNAs (Figure 4K). K14 and K19 proteins were measured by IF in each cell after 48 hr on PA gels. Younger MPP harboring either siYAP or siTAZ were unable to give rise to more MEP on 2,350 Pa PA gels and glass substrata compared to controls (Figure 4I). In older MPP, siYAP and siTAZ had no effect at 200 Pa or 2,350 Pa, but they prevented the generation of more LEP on glass (Figure 4J). Thus, YAP and TAZ were required for modulus-dependent differentiation in progenitors irrespective of age.

### YAP Localization Changes with Age In Vivo

That YAP and TAZ activity correlated with a bias toward MEP in younger women prompted us to evaluate normal breast tissue sections from reduction mammoplasty. K14, K19, and YAP were evaluated by IF in sections from four women aged 34 years, 40 years, 50 years, and 54 years (Figure 5A). Multiple fields from each section were analyzed to account for heterogeneity, and marker-based watershed cell segmentation identified levels of YAP in nuclear and cytoplasmic domains of MEP, LEP, and K14+/K19+ putative MPP. YAP staining was localized mainly to the nuclei of MEP and MPP in the 34 years and 40 years glands (Figure 5B). In the 34 years gland, we also observed a number of occurrences of K14+/K19- cells that we assumed were LEP based on their luminal location. Upon measuring the YAP signal intensity, it was determined that the K14+ cells always correlated with higher YAP expression (Figure 5C). In contrast to younger epithelia, the 50 years and 54 years glands exhibited no inequality in YAP localization between the different lineages (Figure 5B),

(M and N) Histograms represent  $\log_2$ -transformed ratios of K14 to K19 protein expression in single cells in 3D HA gels; histograms are heat mapped to indicate cells with the phenotypes of K14-/K19+ LEPs (green), K14+/K19+ progenitors (yellow), and K14+/K19- MEPs (red).

(M' and N') Fold changes of lineage proportions normal to 120 Pa condition (chi-square test women <30 years,  $p = 0.0146$ ; women >55 years,  $p = 0.9113$ ). See also Figures S2, S3, and S4 and Table S2.

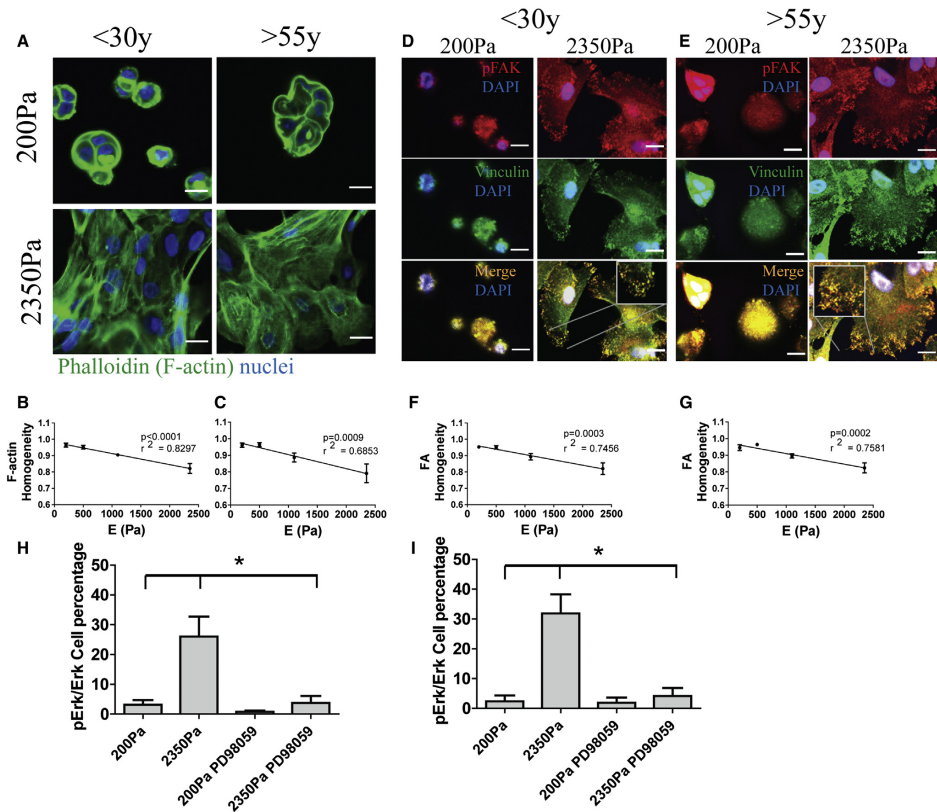


**Figure 2. Mechanosensing Apparatuses Function Independently of Age to Generate Actin Stress Fibers, Focal Adhesions, and ERK Activation**

(A) Representative IF images of F-actin (green) in cKit+ HMEC from a young strain (240L; 19 years) and an older strain (122L; 66 years) on PA gels of increasing stiffness.

(B and C) Quantification of F-actin homogeneity using feature detection (B,  $p < 0.0001$  and  $r^2 = 0.8297$ , slope =  $-6.805 \times 10^{-5} \pm 9.749 \times 10^{-6}$ ,  $n = 3$ ; C,  $p < 0.001$  and  $r^2 = 0.6853$ , slope =  $-8.454 \times 10^{-5} \pm 1.811 \times 10^{-5}$ ,  $n = 3$ ). The slopes are not significantly different ( $p = 0.5699$ ).

(D and E) Representative IF images of pFAK (red) and vinculin (green), which overlapped (yellow), from confocal microscopy are shown in cKit+ HMEC from (D) a young strain (240L; 19 years) and (E) an older strain (122L; 66 years). Cells are shown at the substrata interface. Bars represent 20  $\mu$ m.

(F and G) Quantification of vinculin and pFAK homogeneity (F,  $p < 0.001$  and  $r^2 = 0.7456$ , slope =  $-6.512 \times 10^{-5} \pm 1.203 \times 10^{-5}$ ,  $n = 3$ ; G,  $p < 0.001$  and  $r^2 = 0.7581$ , slope =  $-6.356 \times 10^{-5} \pm 1.136 \times 10^{-5}$ ,  $n = 3$ ). The slopes are not significantly different ( $p = 0.8124$ ). Data are means  $\pm$  SEM.

(H and I) Ratio of pERK positive to ERK positive cell number in cKit+ HMEC from <30 years ( $n = 3$ ) and >55 years ( $n = 3$ ) strains on 200 Pa and 2,350 Pa.

and qualitatively, the even-appearing distribution of YAP in the nuclei and cytoplasm of the LEP and MEP in older women was reminiscent of YAP staining in >55 years HMEC (Figure 5C). YAP distribution in vivo was age dependent consistent with our findings in primary cultures. Overall, the data suggest that YAP activity is associated with MEP/basal phenotypes, even in the case of LEP in older women that acquire

some traits of MEP. That impression was strengthened by our analysis of breast cancer data from The Cancer Genome Atlas data (Cancer Genome Atlas, 2012), which showed that YAP/TAZ mRNA expression negatively correlated with levels of LEP-related proteins and mRNAs and positively correlated with markers of MEP and with YAP/TAZ target genes (Figures S6A and S6B).

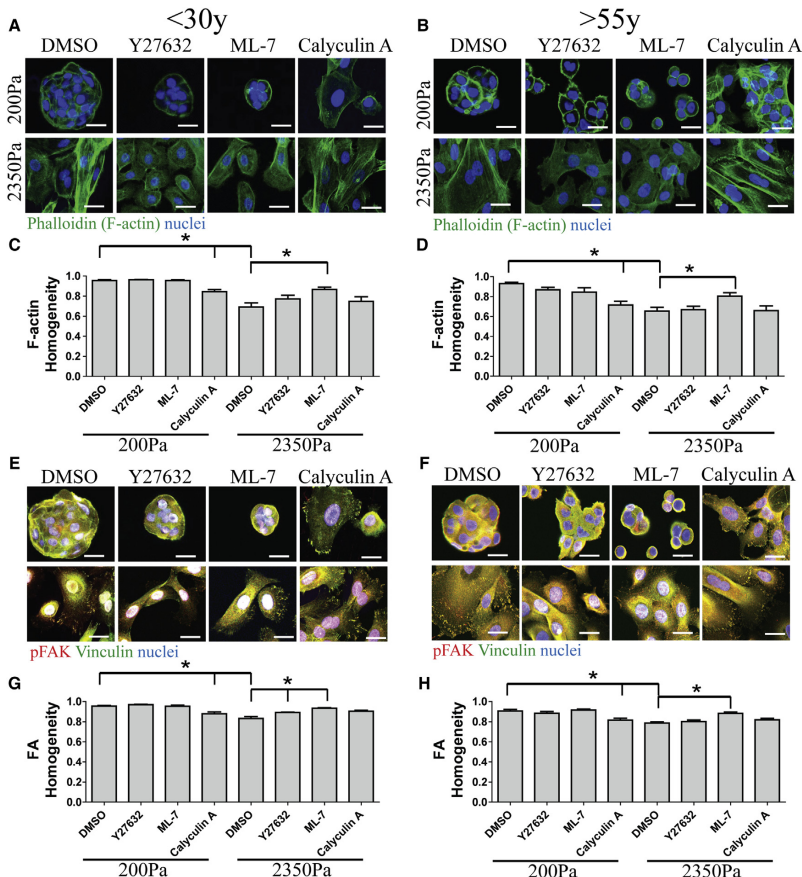


**Figure 3. Perturbations of Actinomyosin Regulators Elicit Parallel Phenotypes in Progenitors from Young and Old Age Groups**

(A and B) Representative IF images of F-actin with phalloidin (green) in cKit<sup>+</sup> HMEC from (A) a young strain (240L; 19 years) and (B) an older strain (122L; 66 years).

(C and D) Quantification of F-actin homogeneity in (C) younger cKit<sup>+</sup> (n = 3) and (D) older cKit<sup>+</sup> (n = 3).

(E and F) Merged images of IF of pFAK (red) and vinculin (green), overlap is (yellow), in cKit<sup>+</sup> HMEC from (E) the young strain and (F) the older strain. Bars represent 20  $\mu$ m.

(G and H) Quantification of vinculin and pFAK homogeneity in (G) young cKit<sup>+</sup> (n = 3) and (H) older cKit<sup>+</sup> (n = 3).

See also Figure S5.

#### Levels of Hippo Pathway Components Changed with Age

To better understand why the trigger point for YAP/TAZ was increased in older MPP, we determined whether Hippo pathway components showed age-dependent expression patterns. Mst1/Mst2, Lats2, and angiostatins (AMOT) phosphorylate and sequester YAP/TAZ in the cytoplasm, which would prevent YAP/TAZ from associating with DNA-binding cofactors TEAD1–

TEAD4 and transcribing target genes, like connective tissue growth factor (CTGF) (Zhao et al., 2007, 2011). Analysis with quantitative real-time PCR (qRT-PCR) revealed that, in almost all cases, *MST1/MST2*, *LATS2*, *AMOT*, *AMOTL1*, *TEAD1–TEAD4*, and *CTGF* were significantly correlated between women <30 years and women >55 years on 200 Pa (Figure 6A;  $p = 0.0110$ ;  $R = 0.7283$ ) and 2,350 Pa (Figure 6B;

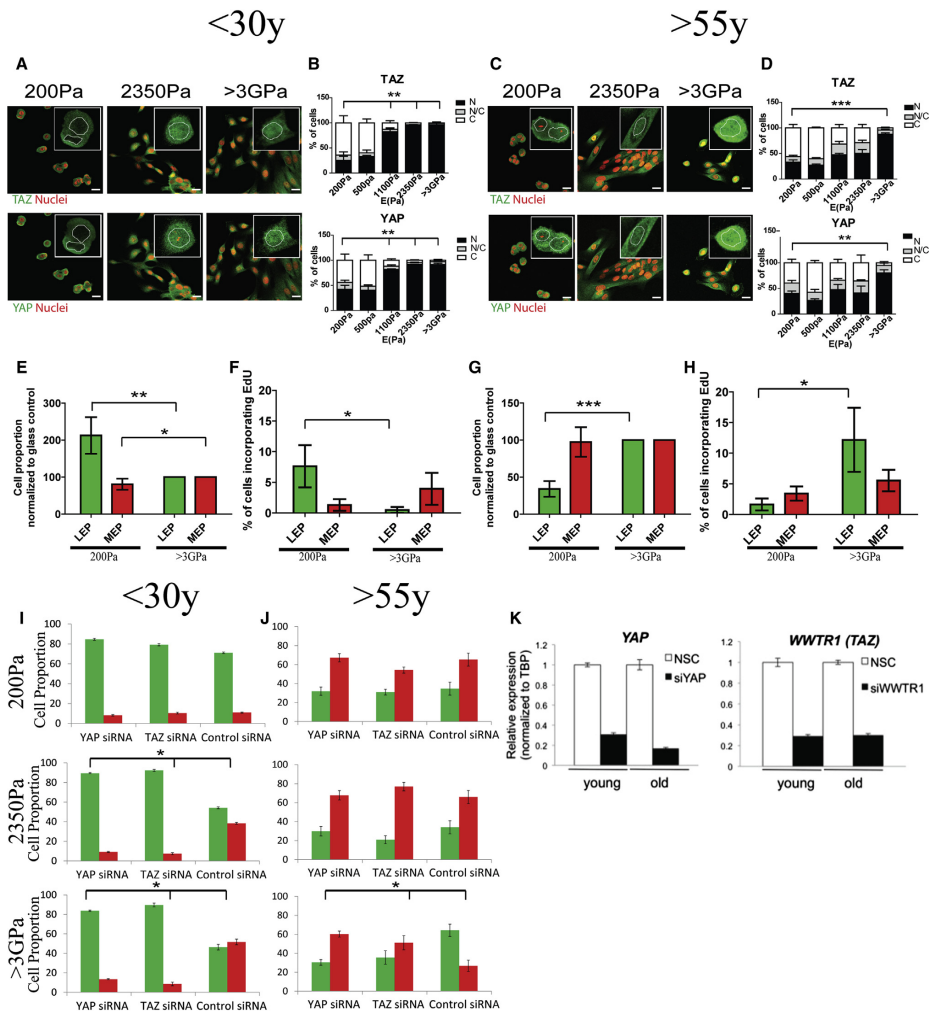


**Figure 4. YAP and TAZ Activation Are Altered during Aging**

(A and C) Representative IF images of TAZ, YAP (green), and DAPI (red) in cKit+ HMEC from (A) a young strain (240L; 19 years) and (C) an older strain (353P; 72 years). Bars represent 20  $\mu$ m.

(B and D) Bar plots represent the distribution of YAP and TAZ (N, predominantly in the nucleus; N/C, equally distributed; C, predominantly in the cytoplasm) from over 100 cells/strain in (B) younger (n = 3) and (D) older (n = 3) strains.

(E and G) K19+LEP and K14+MEP proportions derived from cKit+ HMEC from (E) younger (n = 5) and (G) older (n = 5) women. Data are fold change of cell proportions compared to glass control  $\pm$  SEM.

(F and H) Percentage of EdU+ LEP and MEP derived from cKit+ HMEC from (F) younger (n = 5) and (H) older (n = 5) women. Data are means  $\pm$  SEM.

(I and J) K19+LEP and K14+MEP proportions derived from cKit+ HMEC from (I) younger and (J) older strains transfected with YAP or TAZ siRNA.

(K) Bar graphs of YAP and TAZ transcript knockdown following siRNA treatment and NSC scrambled control siRNA.

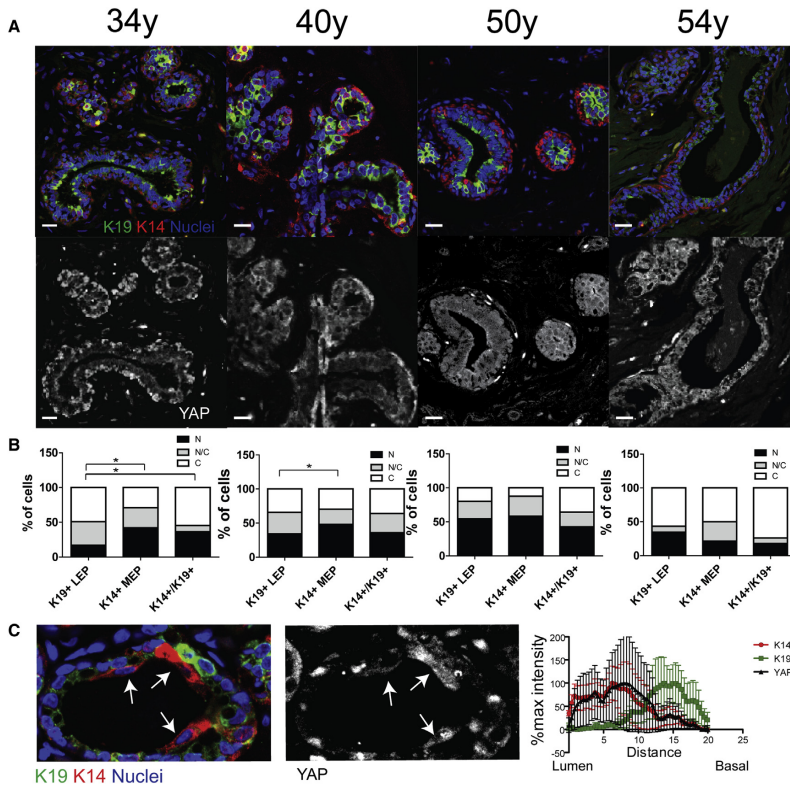


**Figure 5. YAP Localization Changes with Age In Vivo**

(A) Representative IF images of K14 (red), K19 (green), YAP (white), and DAPI (blue) in human mammary breast sections from four women (aged 34 years, 40 years, 50 years, and 54 years). Bars represent 20  $\mu$ m.

(B) Bar plots represent the distribution of YAP (N, predominantly in the nucleus; N/C, equally distributed; C, predominantly in the cytoplasm) from over 100 cells/woman.

(C) YAP signal isolation from the immunofluorescence of K14 (red), K19 (green), YAP (white), and DAPI (blue) from the 34-year-old woman. Arrows identify luminal-positioned K14<sup>+</sup>/K19<sup>low/-</sup> cells. The line graph shows mean pixel intensities from the lumen to the basal side of the structure in ten different examples of K14<sup>+</sup> luminal cells.

See also Figure S6.

$p = 0.0083$ ;  $R = 0.7464$ ) gels. On glass, the correlation was less pronounced (Figure 6C;  $p = 0.0543$ ;  $R = 0.5934$ ). Because differences in Hippo gene expression were not strikingly age dependent in physiological conditions, we examined protein levels of MST1 and MST2. MST1 levels from three women <30 years and three women >55 years were not significantly different (Figures 6D–6G). MST2 protein levels were 3-fold greater in MPP from women >55 years compared to <30 years on 2,350 Pa gels (Figure 6E). Thus, it is tempting to speculate that age-dependent stoichiometry of Hippo pathway regulators

can lead to insensitivity to mechanical cues and activation of YAP/TAZ.

#### Immortalization of Aged HMECs Restored Responsiveness to Physiological Stiffness

Cellular responses to mechanical stimuli are often examined with mesenchymal stem cells or immortal malignant and nonmalignant cell lines. Whereas immortal cell lines tend to proliferate more on stiffer substrata, we showed that normal <30 years HMEC exhibited lineage-dependent responses and that

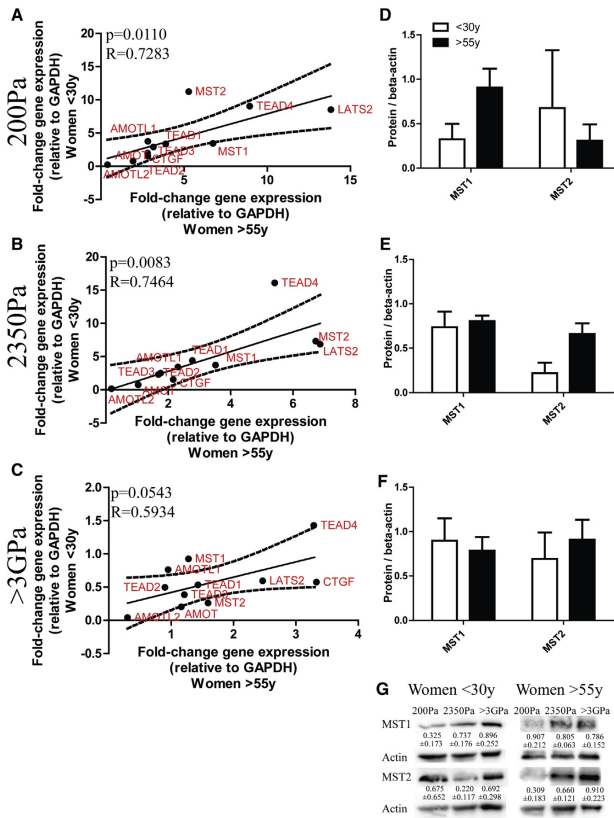


**Figure 6. Age-Dependent Patterns of Hippo Pathway Components**

(A–C) Correlation of gene expression between cKit+ HMEC from younger (n = 3) and older (n = 3) strains after 24 hr on (A) 200 Pa, (B) 2,350 Pa PA gels, and (C) >3 GPa substrate. Data are normalized to GAPDH expression.

(D–F) Western blot densitometric analysis of MST1 and MST2 from cKit+ HMEC from younger (n = 3) and older (n = 3) strains after 24 hr on (D) 200 Pa, (E) 2,350 Pa PA gels, and (F) >3 GPa substrate. Data are normalized to beta-actin protein content and are mean ± SEM.

(G) Representative western blot with quantification from a young (240L; 19 years) and an older strain (122L; 66 years).

cell lines on PA gels from 200 to 2,350 Pa (Figures 7G–7N). Thus, immortalization of older HMEC restored sensitivity of the Hippo pathway to the physiological stiffness range, albeit abnormally because proliferation was no longer lineage-dependent. The propensity of immortal cell lines to generate more MEP or LEP on extraphysiological substrata was consistent with the chronological age of the HMEC, suggesting that the intrinsic age-related changes were stable.

## DISCUSSION

Matrix rigidity is a determinant of mammary epithelial progenitor differentiation. Exposure of progenitors to mechanically tuned culture substrata revealed two fundamental changes that arise in MPP with age: (1) the mechanical trigger point for activation of YAP/TAZ increases, and (2) the YAP/TAZ-dependent differentiation programs become distinct. Culture of MPP from <30-year-old women in the most compliant 2D or 3D conditions (100–200 Pa) enhanced LEP differentiation, whereas stiffer substrata (2,300–3,800 Pa) favored MEP production. Older progenitors stochastically differentiated when exposed to a physiologically relevant elastic modulus range. Our results document the role of YAP/TAZ transcription factors as drivers of modulus-dependent differentiation in human mammary epithelial MPP and suggest that YAP/TAZ activity favors differentiation into MEP and other basal cell types. The basal cell types are not exclusive to MEP and may include LEP that express K14 or other basal-associated markers, which we and others have observed (Santagata et al., 2014). Older MPP needed to be stressed with extraphysiologically stiff substrata to reveal their YAP/TAZ-dependent bias toward LEP, which was consistent with our observation in vivo that YAP tended to be located in LEP with increased age. In younger women, YAP was in the nuclei of

<55 years HMEC were nonresponsive to a physiological range of E (Figure 1). To better understand the differences between the normal and immortal nonmalignant states as a function of age, we examined immortal nonmalignant cell lines derived from two young and two old primary HMEC strains with targeted inactivation of senescence barriers combined with unknown genomic errors (Stamper et al., 2013). The cell lines, 240LMY (19 years), 184Fp16s (21 years), 122LMY (66 years), and 805Pp16s (91 years; Figure S7) were cultured atop PA gels tuned from 200 to 2,350 Pa. cKit+ MPP from 240LMY and 184Fp16s cell lines gave rise to more K14+ MEP than LEP on glass compared to 200 Pa PA gels (Figure 7A). cKit+ MPP from 122LMY and 805Pp16s gave rise to more K19+ LEP than MEP on glass compared to 200 Pa PA gels (Figure 7B). Independent of age, all lineages of the immortal cell lines incorporated more EdU as rigidity increased (Figures 7C–7F). YAP/TAZ nuclear translocation was detected both in <30 years and >55 years

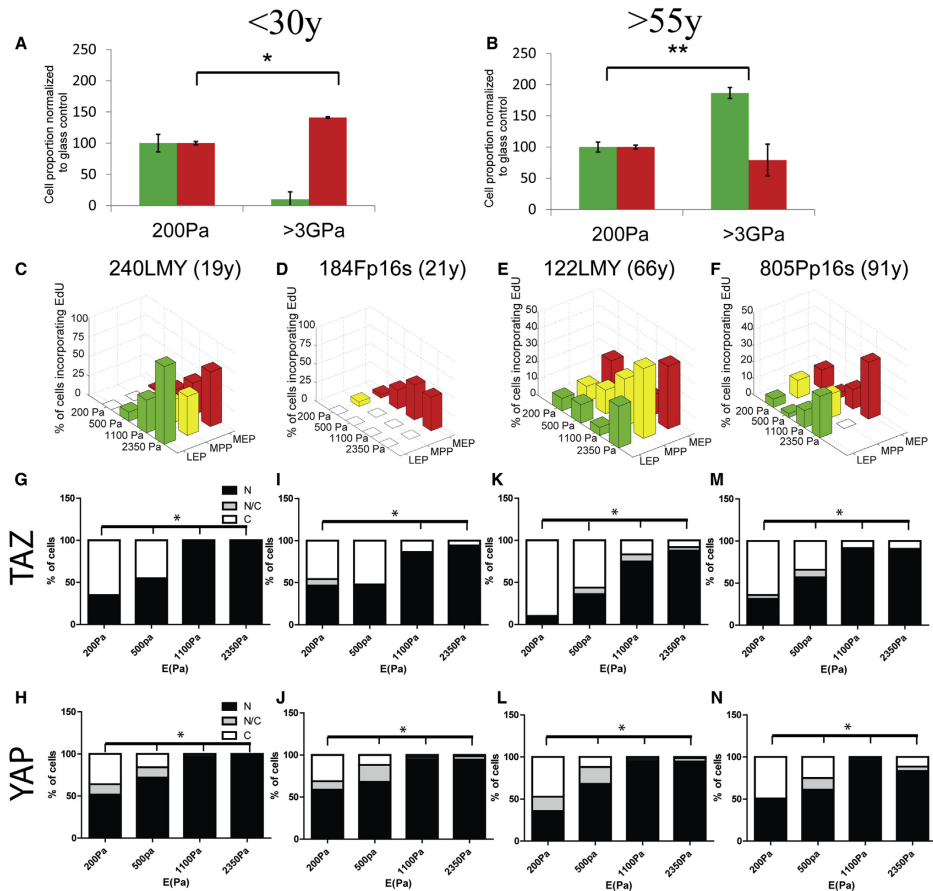


**Figure 7. Immortalization Restores Responsiveness to Physiological Stiffness in Older HMEC**

(A and B) K19+LEP and K14+MEP proportions derived from immortalized cell lines from (A) younger ( $p = 0.0111$ ;  $n = 2$  individuals in triplicate) and (B) older ( $p = 0.0056$ ;  $n = 2$  individuals in triplicate) women. Data are fold change of cell proportions compared to glass control  $\pm$  SEM.

(C–F) Percentage of cells from immortalized cell lines derived from primary strains 240LMY at passage 25, 184Fp16s at passage 31, 122LMY at passage 19, and 805Pp16s at passage 29 incorporating EdU as a function of lineage, as defined by K14 and K19 expression, and stiffness.

(G–N) Bar plots represent the distribution of YAP and TAZ (N, predominantly in the nucleus; N/C, equally distributed; C, predominantly in the cytoplasm) from over 100 cells/lineage in immortalized cell lines. By comparison to the other cell lines, 184F derivatives are known to be mainly basal at the expense of LEP and progenitor phenotypes. See also Figure S7.

K14-expressing MEP, as well as the apical snouts of LEP. We previously demonstrated that postmenopausal LEP tend to express some K14, as well as other markers associated with MEP, and these new data suggest that age-dependent changes in YAP/TAZ activity may underlie that phenotype of aging.

Radiographic density of breast tissue tends to decrease with age suggesting that the mechanical environment is also altered (Benz, 2008), but mechanical forces do not exclusively govern YAP/TAZ regulation. Our experimental approach took advantage of tuned mechanical perturbations of matrix to functionally

probe the HMEC, but more broadly these results revealed that aging fundamentally alters Hippo pathway regulation. The role of cell-cell contact in Hippo pathway regulation should be further investigated in the context of chronological age. Both Wnt/ $\beta$ -catenin and NF2 are known to regulate YAP/TAZ *in vivo* (Cockburn et al., 2013; Imajo et al., 2012), and changes to both pathways have been implicated in different age-related cancers (Evans et al., 2005; Seidler et al., 2004). Little is known about whether YAP/TAZ play a role in other phenotypes of aging. Deficiency in *C. elegans yap-1* resulted in overall healthier aging relative to controls (Iwasa et al., 2013). Disrupted Hippo signaling in human and mouse ovarian follicles, which caused YAP activation, promoted growth and oocyte maturation, which are processes typically defective with age (Kawamura et al., 2013). Indirect evidence suggests mesenchymal stem cells also have dampened modulus-dependent differentiation responses with age. Bone is magnitudes stiffer than adipose tissue and the osteogenic potential of mesenchymal stem cells decreases and a bias toward adipogenesis increases with age (Moerman et al., 2004), but the role of Hippo is unclear.

Accumulation of MPP with age may be attributed to inefficient transduction of differentiation cues through the Hippo pathway. At low cell density, decreased Lats2 activity dependent on SF formation causes YAP/TAZ to translocate to the nucleus (Wada et al., 2011), but <30 years and >55 years MPP formed SF and FA comparably in response to changes in matrix stiffness. Thus, we explored the potential for stoichiometric imbalances in Hippo kinases with age that could dampen activation of YAP/TAZ. In our hands, MST2 protein was higher in >55 years MPP, suggestive of a damping mechanism. The Hippo pathway is implicated in differentiation of different progenitors into adipose, breast, muscle, and bone tissues, representing a wide range of elastic modulus and predicting a marvelously adaptable molecular rheostat. Each of these tissues differs in their matrix composition as well as physical attributes, and there is a reasonable expectation that combinations of ECM and growth factors tune Hippo pathway activity. Further study of microenvironment regulation of the Hippo pathway may identify components of the activation rheostat and reveal the basis for its age-related dampening.

Changes to the mechanical microenvironment affect multiple cell types in breast. High breast stiffness and density are correlated with increased risk and cancer progression (Yu et al., 2011). Increased stiffness also can induce adipocyte progenitors to differentiate into fibroblasts, which can positively feedback to further increase tissue stiffness (Chandler et al., 2012). MPP from women <30 years responded to increasingly rigid matrices by increased production of MEP, which are thought to be tumor suppressive (Gudjonsson et al., 2002; Hu et al., 2008), and proportionately decreased numbers of cells with the MPP phenotype, which are hypothesized to be breast cancer cells of origin (Lim et al., 2009), suggestive of a protective mechanism from tumor progression in younger epithelia. However, this putative protective mechanism falters with age, as demonstrated when aged HMEC were essentially unresponsive to physiological changes in matrix rigidity.

We speculate that the prevalence of luminal subtype breast cancers in postmenopausal women may be the result of age-

acquired epigenetic states. When older MPP were exposed to extraphysiologically stiff substrata, they exhibited LEP-biased differentiation—the exact opposite of the younger progenitors. Age-dependent differentiation patterns were preserved in immortal young and old HMEC, but the mechanotransductive mechanism was notably rejuvenated in older immortal cells, enabling them to proliferate increasingly as matrix modulus approached that of a tumor. YAP/TAZ were required for shifting production in favor of MEP in younger and LEP in older MPP on the stiffer surfaces. We hypothesize that the distinct differentiation responses of younger and older MPP reflect age-dependent epigenetic landscapes. Indeed, normal HMEC exhibit age-dependent gene expression patterns consistent with the concept of age-dependent epigenetic states (Garbe et al., 2012). A precedent was set in hematopoietic stem cells where DNA and histone modifications were shown to correlate with age-related functional phenotypes (Chambers et al., 2007). Stromal feedback loops can result in formation of stiffened regions; if such regions already contained an accumulation of aged progenitor cells carrying errors predisposing them to immortality, they could create an environment that promotes development of age-related luminal subtype breast tumors.

Finally, it is important to be able to empirically examine the cell and molecular consequences of aging in normal human epithelia because most carcinomas are age-related. Wild-type mice are typically resistant to cancers, murine models of breast cancer do not completely model the steps of cancer progression in HMEC (Stampfer et al., 2013), and most inbred strains exhibit tumor incidence curves consistent with sporadic tumor genesis; thus, mice may not be an optimal model for studying the genesis of age-related breast cancers. Here, we present an approach for interrogation of human aging that takes advantage of cultured strains of normal HMEC and engineered microenvironments to perform cell-based molecular and functional studies, which are validated by comparison with breast tissues. Most studies that have drawn conclusions from breast cancer cell lines or mouse studies have used three methods to establish relevance of their results to human *in vivo*: an experiment with primary HMEC that recapitulates the main findings, examination of tissue sections for *in vivo* evidence that correlates with the findings, and correlation with large gene/protein expression data sets derived from patient samples. We have followed these three conventions. We find it striking that many of the molecular and biochemical phenotypes of aging persist in our early passage strains in spite of the imperfect microenvironment, which reinforces our impression that age-associated epigenetic changes are stabilizing those phenotypes. However, limitations and challenges are intrinsic to every experimental system. Early pregnancy has a detectable protective effect against breast cancer, and the balance of epithelial lineages and gene expression patterns in mice and humans are affected by parity (Choudhury et al., 2013). Our current strain collection is not annotated for parity information, and focused studies should be conducted to determine how parity modifies the aging phenotype in breast. There is an impressive level of heterogeneity among human mammary epithelia as was beautifully shown by detailed examinations of luminal lineages (Santagata et al., 2014; Shehata et al., 2012). Our method for establishing primary strains

encompasses a significant amount of the total heterogeneity in given surgical specimen, and low stress culture conditions maintain MPP activity in early passages (Labarge et al., 2013). We also addressed this issue of heterogeneity and potential for interindividual variation by using strains established from 17 different women, with any given experiment comparing thousands of independent measurements from groups comprised of three to five strains each. We find repeatedly that the functional, molecular, and biochemical phenotypes often differ between the pre- and postmenopausal age groups, underscoring the importance of chronological age as an experimental variable.

## EXPERIMENTAL PROCEDURES

### Cell Culture

All cell culture was in M87A medium with cholera toxin at 0.5 ng/ml and oxytocin (X) at 0.1 nM (Bachem; Garbe et al., 2009). Primary HMEC strains were generated and maintained as described (Labarge et al., 2013); all tissues were obtained with proper oversight from the Lawrence Berkeley National Laboratory institutional review board. Modulus-dependent effects were measured in sub-confluent cultures. Table S1 shows the strains used for each experiment.

### Reagents

Cells were treated with Y27632 (10  $\mu$ M; Sigma), ML-7 (10  $\mu$ M; Sigma), or calyculin A (2 nM; Calbiochem) 2 hr after adhesion. Cells were treated with PD98059 (50  $\mu$ M; Cell Signaling Technology) 24 hr after adhesion. Cells were transfected with YAPsi, WWTR1 (TAZsi), or nontargeting control siRNA SMARTpools (Dharmacon/Thermo) plus a fluorescein isothiocyanate (FITC) label with DharmaFECT reagent according to manufacturer 24 hr prior to FACS enrichment.

### Flow Cytometry

Anti-CD227-FITC (BD; clone HMPV; 1:50), anti-CD10-phycocerythrin (BioLegend; clone HI10a; 1:100), and anti-CD117-antigen-presenting cell (BioLegend; clone 104D2; 1:50) were added to cells in media for 25 min on ice, washed in PBS, and sorted with a FACS Vantage DIVA (Becton Dickinson).

### PA Gels

PA gels were made on circular, 12 mm coverslips etched in 0.1 M NaOH following an adapted protocol (Tse and Engler, 2010). Sulfo-SANPAH (0.4 mM) was activated by UV light, and then collagen was added (0.1 mg/ml in 50 mM HEPES; Sigma). ddH<sub>2</sub>O washed gels were placed in polyHema-treated (0.133 ml at 12 mg/ml in 95% EtOH) 24-well plates. Gel modulus was confirmed with atomic force microscopy.

### Immunofluorescence

HMEC were fixed in methanol:acetone (1:1) at  $-20^{\circ}\text{C}$  for 15 min, blocked with PBS, 5% normal goat serum, 0.1% Triton X-100, and incubated with anti-K14 (1:1,000; Covance; polyclonal rabbit) and anti-K19 (1:20; Developmental Studies Hybridoma Bank; clone Troma-III) overnight at  $4^{\circ}\text{C}$  and then visualized with fluorescent secondary antibodies (Invitrogen) incubated for 2 hr at room temperature. EdU was added to culture media 4 hr prior to fixing cells and was imaged with Alexa 647 click reagents (Invitrogen). Paraformaldehyde (2.5%) was used for fixation for phalloidin (1:50; Invitrogen), anti-pFAK (1:1,000; Invitrogen; monoclonal antibody [mAb]), anti-vinculin (1:400; Sigma; mAb), anti-YAP (1:100; Santa Cruz Biotechnology; SC-15407), anti-TAZ (1:200; CST; polyclonal), phospho-p44/42 MAPK (Erk1/Erk2; 1:100; CST mAb), and p44/42 MAPK (Erk1/Erk2; 1:100; CST mAb). Paraformaldehyde (1.6%) was used for fixation for anti-CD227 (1:200; Abcam; polyclonal) and anti-CD10 (1:100; BD Biosciences; clone HI10a). Paraffin-embedded sections were deparaffinized and antigen retrieved (Vector Laboratories) and stained with primary antibodies to K14 (1:1,000; Covance; PRB-155P; visualized with A647 Zenon probes from Invitrogen), K19 (1:100; Abcam; AAH07628) and YAP (1:100; Santa Cruz; SC-15407). Cells were imaged with LSM710 confocal microscope (Carl Zeiss). Image analyses were conducted using a

modified watershed method in Matlab software (Mathworks); see Supplemental Information for detailed code.

### Real-Time PCR

Total RNA was purified with Trizol (Invitrogen) followed by RNeasy prep (QiAGEN). cDNA was synthesized with SuperScript III RT (Invitrogen). Transcripts levels were measured by qRT-PCR using iTaq SYBR Green Supermix (BioRad) and LightCycler480 (Roche). Primer sequences are in the Supplemental Information.

### Generation of Immortal Cell Lines

Finite lifespan HMEC from specimens 184, 240L, 122L, and 805P were grown in M87A. Retroviral vectors: the p16 small hairpin RNA was in MSCV vector, and c-Myc was in pBabe-hygro (BH2) or LXSN vector. Retroviral stocks were generated from supernatants collected in M87A medium. Strains 240L, 122L, and 805P at passage 3 or and 184 at passage 4 were transduced with MSCV-p16sh or MSCV control and selected with puromycin. At the next passage, after puromycin selection, the p16sh-transduced cells were transduced with c-Myc pBabe-hygro (c-myc LXSN for 184) and selected with hygromycin. Vector-only control prestasis cells entered stasis at passages 12–15, whereas the immortalized lines continued to grow.

### Western Blot

The following antibodies were used: MST1 CST no. 3682 rabbit 1:1,000, MST2 CST no. 3952 rabbit 1:1,000, beta-actin Abcam no. 8227 rabbit 1:500, and visualized with goat anti-rabbit immunoglobulin G (H + L)-horseradish peroxidase conjugate no. 170-6515 1:10,000.

### TCGA Database

All data were obtained from the The Cancer Genome Atlas (TCGA) breast cancer online portal ([https://tcga-data.nci.nih.gov/docs/publications/brca\\_2012/](https://tcga-data.nci.nih.gov/docs/publications/brca_2012/); Cancer Genome Atlas, 2012). The following files were used: for microarray gene expression data: "BRCA.exp.547.med.txt" and for reverse-phase protein array expression data: "rppaData-403Samp-171Ab-Trimmed.txt."

### Statistical Analysis

Graphpad Prism 5.0 for PC and Matlab were used for all statistical analysis. Standard linear regression was used. Grouped analyses were performed with Bonferroni's test for multiple comparisons. To compare two population distributions, chi-square and t tests were performed. Significance was established when \* $p < 0.05$ , \*\* $p < 0.01$ , and \*\*\* $p < 0.001$ .

## SUPPLEMENTAL INFORMATION

Supplemental Information includes Supplemental Experimental Procedures, seven figures, and two tables and can be found with this article at <http://dx.doi.org/10.1016/j.celrep.2014.05.021>.

## AUTHOR CONTRIBUTIONS

F.A.P. and M.A.L. designed the research; F.A.P., J.C.G., B.A., M.M., C.L., T.J., J.B.L., and M.A.L. performed experiments; J.C.G., M.R.S., S.K., and M.A.L. provided cell strains and other key reagents; and F.A.P., J.B.L., and M.A.L. wrote the manuscript.

## ACKNOWLEDGMENTS

We thank Prof. Matthias Lutolf, Gurkaran S. Buxi, and Thibault Vatter for expert advice. M.A.L. is supported by the NIH (NIA R00AG033176 and R01AG040081; NCI U54CA143836) and the US Department of Energy (DE-AC02-05CH11231). B.A. is supported by a postdoctoral fellowship from the California Institute for Regenerative Medicine (TG2-01164).

Received: March 20, 2013

Revised: April 15, 2014

Accepted: May 8, 2014

Published: June 5, 2014

REFERENCES

- Ananthanarayanan, B., Kim, Y., and Kumar, S. (2011). Elucidating the mechanobiology of malignant brain tumors using a brain matrix-mimetic hyaluronic acid hydrogel platform. *Biomaterials* 32, 7913–7923.
- Beningo, K.A., Dembo, M., Kaverina, I., Small, J.V., and Wang, Y.L. (2001). Nascent focal adhesions are responsible for the generation of strong propulsive forces in migrating fibroblasts. *J. Cell Biol.* 153, 881–888.
- Benz, C.C. (2008). Impact of aging on the biology of breast cancer. *Crit. Rev. Oncol. Hematol.* 66, 65–74.
- Bershady, A.D., Balaban, N.Q., and Geiger, B. (2003). Adhesion-dependent cell mechanosensitivity. *Annu. Rev. Cell Dev. Biol.* 19, 677–695.
- Cancer Genome Atlas, N.; Cancer Genome Atlas Network (2012). Comprehensive molecular portraits of human breast tumours. *Nature* 490, 61–70.
- Chambers, S.M., Shaw, C.A., Gatzka, C., Fisk, C.J., Donehower, L.A., and Goodell, M.A. (2007). Aging hematopoietic stem cells decline in function and exhibit epigenetic dysregulation. *PLoS Biol.* 5, e201.
- Chandler, E.M., Seo, B.R., Califano, J.P., Andresen Eguliz, R.C., Lee, J.S., Yoon, C.J., Tims, D.T., Wang, J.X., Cheng, L., Mohanan, S., et al. (2012). Implanted adipose progenitor cells as physicochemical regulators of breast cancer. *Proc. Natl. Acad. Sci. USA* 109, 9786–9791.
- Charruyer, A., Barland, C.O., Yue, L., Wessendorf, H.B., Lu, Y., Lawrence, H.J., Mancianti, M.L., and Ghadially, R. (2009). Transit-amplifying cell frequency and cell cycle kinetics are altered in aged epidermis. *J. Invest. Dermatol.* 129, 2574–2583.
- Cho, R.H., Sieburg, H.B., and Muller-Sieburg, C.E. (2008). A new mechanism for the aging of hematopoietic stem cells: aging changes the clonal composition of the stem cell compartment but not individual stem cells. *Blood* 111, 5553–5561.
- Choudhury, S., Almendro, V., Merino, V.F., Wu, Z., Maruyama, R., Su, Y., Martins, F.C., Fackler, M.J., Bessarabova, M., Kowalczyk, A., et al. (2013). Molecular profiling of human mammary gland links breast cancer risk to a p27(+) cell population with progenitor characteristics. *Cell Stem Cell* 13, 117–130.
- Cockburn, K., Biechele, S., Garner, J., and Rossant, J. (2013). The Hippo pathway member Nf2 is required for inner cell mass specification. *Curr. Biol.* 23, 1195–1201.
- Dupont, S., Morsut, L., Aragona, M., Enzo, E., Giulitti, S., Cordenonsi, M., Zanconato, F., Le Digabel, J., Forcato, M., Bicciato, S., et al. (2011). Role of YAP/TAZ in mechanotransduction. *Nature* 474, 179–183.
- Engler, A.J., Sen, S., Sweeney, H.L., and Discher, D.E. (2006). Matrix elasticity directs stem cell lineage specification. *Cell* 126, 677–689.
- Evans, D.G., Maher, E.R., and Baser, M.E. (2005). Age related shift in the mutation spectra of germline and somatic NF2 mutations: hypothetical role of DNA repair mechanisms. *J. Med. Genet.* 42, 630–632.
- Garbe, J.C., Bhattacharya, S., Merchant, B., Bassett, E., Swisshelm, K., Feiler, H.S., Wyrobek, A.J., and Stampfer, M.R. (2009). Molecular distinctions between stasis and telomere attrition senescence barriers shown by long-term culture of normal human mammary epithelial cells. *Cancer Res.* 69, 7557–7568.
- Garbe, J.C., Pepin, F., Pelissier, F.A., Sputova, K., Fridriksdottir, A.J., Guo, D.E., Villadsen, R., Park, M., Petersen, O.W., Borowsky, A.D., et al. (2012). Accumulation of multipotent progenitors with a basal differentiation bias during aging of human mammary epithelia. *Cancer Res.* 72, 3687–3701.
- Gudjonsson, T., Rennov-Jessen, L., Villadsen, R., Rank, F., Bissell, M.J., and Petersen, O.W. (2002). Normal and tumor-derived myoepithelial cells differ in their ability to interact with luminal breast epithelial cells for polarity and basement membrane deposition. *J. Cell Sci.* 115, 39–50.
- Halder, G., Dupont, S., and Piccolo, S. (2012). Transduction of mechanical and cytoskeletal cues by YAP and TAZ. *Nat. Rev. Mol. Cell Biol.* 13, 591–600.
- Haralick, R.M., Shanmugam, K., and Dinstein, I. (1973). Textural features for image classification. *IEEE Trans. Syst. Man Cybern.* SMC-3, 610–621.
- Henry, C.J., Marusyk, A., and DeGregori, J. (2011). Aging-associated changes in hematopoiesis and leukemogenesis: what's the connection? *Aging (Albany, N.Y. Online)* 3, 643–656.
- Hu, M., Yao, J., Carroll, D.K., Weremowicz, S., Chen, H., Carrasco, D., Richardson, A., Violette, S., Nikolaskaya, T., Nikolsky, Y., et al. (2008). Regulation of in situ invasive breast carcinoma transition. *Cancer Cell* 13, 394–406.
- Imaji, M., Miyatake, K., Iimura, A., Miyamoto, A., and Nishida, E. (2012). A molecular mechanism that links Hippo signalling to the inhibition of Wnt/ $\beta$ -catenin signalling. *EMBO J.* 31, 1109–1122.
- Ishizaki, T., Naito, M., Fujisawa, K., Maekawa, M., Watanabe, N., Saito, Y., and Narumiya, S. (1997). p160ROCK, a Rho-associated coiled-coil forming protein kinase, works downstream of Rho and induces focal adhesions. *FEBS Lett.* 404, 118–124.
- Iwasa, H., Maimaiti, S., Kuroyanagi, H., Kawano, S., Inami, K., Timalsina, S., Ikeda, M., Nakagawa, K., and Hata, Y. (2013). Yes-associated protein homolog, YAP-1, is involved in the thermotolerance and aging in the nematode *Caenorhabditis elegans*. *Exp. Cell Res.* 319, 931–945.
- Kanai, F., Marignani, P.A., Sarbassova, D., Yagi, R., Hall, R.A., Donowitz, M., Hisaminato, A., Fujiwara, T., Ito, Y., Cantley, L.C., and Yaffe, M.B. (2000). TAZ: a novel transcriptional co-activator regulated by interactions with 14-3-3 and PDZ domain proteins. *EMBO J.* 19, 6778–6791.
- Kawamura, K., Cheng, Y., Suzuki, N., Deguchi, M., Sato, Y., Takae, S., Ho, C.H., Kawamura, N., Tamura, M., Hashimoto, S., et al. (2013). Hippo signaling disruption and Akt stimulation of ovarian follicles for infertility treatment. *Proc. Natl. Acad. Sci. USA* 110, 17474–17479.
- Kimura, K., Ito, M., Amano, M., Chihara, K., Fukata, Y., Nakafuku, M., Yamamori, B., Feng, J., Nakano, T., Okawa, K., et al. (1996). Regulation of myosin phosphatase by Rho and Rho-associated kinase (Rho-kinase). *Science* 273, 245–248.
- Knoth, R., Singec, I., Ditter, M., Pantazis, G., Capetian, P., Meyer, R.P., Horvat, V., Volk, B., and Kempermann, G. (2010). Murine features of neurogenesis in the human hippocampus across the lifespan from 0 to 100 years. *PLoS ONE* 5, e8809.
- Kuranda, K., Vargaftig, J., de la Rochere, P., Dosquet, C., Charron, D., Bardin, F., Tonnelle, C., Bonnet, D., and Goodhardt, M. (2011). Age-related changes in human hematopoietic stem/progenitor cells. *Aging Cell* 10, 542–546.
- LaBarge, M.A., Nelson, C.M., Villadsen, R., Fridriksdottir, A., Ruth, J.R., Stampfer, M.R., Petersen, O.W., and Bissell, M.J. (2009). Human mammary progenitor cell fate decisions are products of interactions with combinatorial microenvironments. *Integr. Biol. (Camb.)* 1, 70–79.
- Labarge, M.A., Garbe, J.C., and Stampfer, M.R. (2013). Processing of human reduction mammoplasty and mastectomy tissues for cell culture. *J. Vis. Exp.* (71), pii: 50011.
- Lim, E., Vaillant, F., Wu, D., Forrest, N.C., Pal, B., Hart, A.H., Asselin-Labat, M.L., Gyorki, D.E., Ward, T., Partanen, A., et al.; hConFab (2009). Aberrant luminal progenitors as the candidate target population for basal tumor development in BRCA1 mutation carriers. *Nat. Med.* 15, 907–913.
- Lui, C., Lee, K., and Nelson, C.M. (2012). Matrix compliance and RhoA direct the differentiation of mammary progenitor cells. *Biomech. Model. Mechanobiol.* 11, 1241–1249.
- Moerman, E.J., Teng, K., Lipschitz, D.A., and Lecka-Czernik, B. (2004). Aging activates adipogenic and suppresses osteogenic programs in mesenchymal marrow stroma/stem cells: the role of PPAR-gamma2 transcription factor and TGF-beta/BMP signaling pathways. *Aging Cell* 3, 379–389.
- Nguyen, L.V., Makarem, M., Carles, A., Moksá, M., Kannan, N., Pandoh, P., Eirew, P., Osako, T., Kardel, M., Cheung, A.M., et al. (2014). Clonal analysis via barcoding reveals diverse growth and differentiation of transplanted mouse and human mammary stem cells. *Cell Stem Cell* 14, 253–263.
- Pang, W.W., Price, E.A., Sahoo, D., Beeram, I., Maloney, W.J., Rossi, D.J., Schrier, S.L., and Weissman, I.L. (2011). Human bone marrow hematopoietic stem cells are increased in frequency and myeloid-biased with age. *Proc. Natl. Acad. Sci. USA* 108, 20012–20017.

- Pantic, I., Pantic, S., and Basta-Jovanovic, G. (2012). Gray level co-occurrence matrix texture analysis of germinal center light zone lymphocyte nuclei: physiology viewpoint with focus on apoptosis. *Microsc. Microanal.* *18*, 470–475.
- Paszek, M.J., Zahir, N., Johnson, K.R., Lakins, J.N., Rozenberg, G.I., Gefen, A., Reinhart-King, C.A., Margulies, S.S., Dembo, M., Boettiger, D., et al. (2005). Tensional homeostasis and the malignant phenotype. *Cancer Cell* *8*, 241–254.
- Provenzano, P.P., Inman, D.R., Eliceiri, K.W., and Keely, P.J. (2009). Matrix density-induced mechanoregulation of breast cell phenotype, signaling and gene expression through a FAK-ERK linkage. *Oncogene* *28*, 4326–4343.
- Rios, A.C., Fu, N.Y., Lindeman, G.J., and Visvader, J.E. (2014). In situ identification of bipotent stem cells in the mammary gland. *Nature* *506*, 322–327.
- Santagata, S., Thakkar, A., Ergonul, A., Wang, B., Woo, T., Hu, R., Harrell, J.C., McNamara, G., Schwede, M., Culhane, A.C., et al. (2014). Taxonomy of breast cancer based on normal cell phenotype predicts outcome. *J. Clin. Invest.* *124*, 859–870.
- Seidler, H.B., Utsuyama, M., Nagaoka, S., Takemura, T., Kitagawa, M., and Hirokawa, K. (2004). Expression level of Wnt signaling components possibly influences the biological behavior of colorectal cancer in different age groups. *Exp. Mol. Pathol.* *76*, 224–233.
- Shehata, M., Teschendorff, A., Sharp, G., Novcic, N., Russell, A., Avril, S., Prater, M., Eirew, P., Caldas, C., Watson, C.J., and Stingl, J. (2012). Phenotypic and functional characterization of the luminal cell hierarchy of the mammary gland. *Breast Cancer Res.* *14*, R134.
- Stampfer, M.M., LaBarge, M.A., and Garbe, J.C. (2013). An Integrated Human Mammary Epithelial Cell Culture System for Studying Carcinogenesis and Aging. In *Cell and Molecular Biology of Breast Cancer*, H. Schatten, ed. (New York: Springer), pp. 323–361.
- Stoll, E.A., Habibi, B.A., Mikheev, A.M., Lasiene, J., Massey, S.C., Swanson, K.R., Rostomily, R.C., and Horner, P.J. (2011). Increased re-entry into cell cycle mitigates age-related neurogenic decline in the murine subventricular zone. *Stem Cells* *29*, 2005–2017.
- Tamada, M., Sheetz, M.P., and Sawada, Y. (2004). Activation of a signaling cascade by cytoskeleton stretch. *Dev. Cell* *7*, 709–718.
- Tse, J.R., and Engler, A.J. (2010). Preparation of hydrogel substrates with tunable mechanical properties. *Curr. Protoc. Cell Biol.* *Chapter 10*, Unit 10.16.
- Villadsen, R., Fridriksdottir, A.J., Rennov-Jessen, L., Gudjonsson, T., Rank, F., LaBarge, M.A., Bissell, M.J., and Petersen, O.W. (2007). Evidence for a stem cell hierarchy in the adult human breast. *J. Cell Biol.* *177*, 87–101.
- Vogel, V., and Sheetz, M. (2006). Local force and geometry sensing regulate cell functions. *Nat. Rev. Mol. Cell Biol.* *7*, 265–275.
- Wada, K., Itoga, K., Okano, T., Yonemura, S., and Sasaki, H. (2011). Hippo pathway regulation by cell morphology and stress fibers. *Development* *138*, 3907–3914.
- Yu, H., Mouw, J.K., and Weaver, V.M. (2011). Forcing form and function: biomechanical regulation of tumor evolution. *Trends Cell Biol.* *21*, 47–56.
- Zhao, B., Wei, X., Li, W., Udan, R.S., Yang, Q., Kim, J., Xie, J., Ikenoue, T., Yu, J., Li, L., et al. (2007). Inactivation of YAP oncoprotein by the Hippo pathway is involved in cell contact inhibition and tissue growth control. *Genes Dev.* *21*, 2747–2761.
- Zhao, B., Li, L., Lu, Q., Wang, L.H., Liu, C.Y., Lei, Q., and Guan, K.L. (2011). Angiomotin is a novel Hippo pathway component that inhibits YAP oncoprotein. *Genes Dev.* *25*, 51–63.

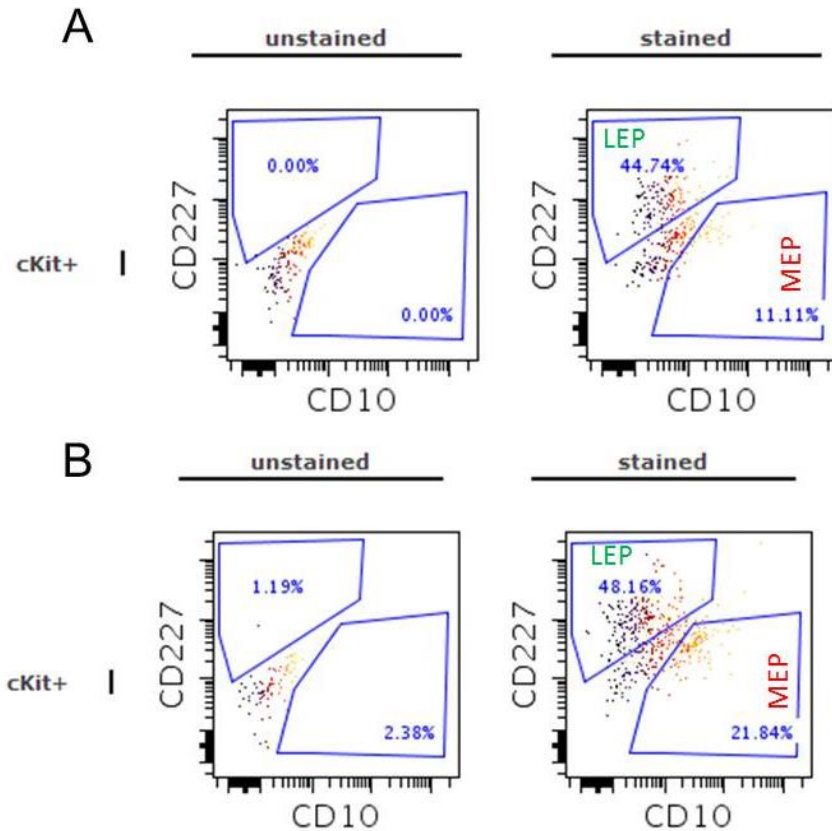
**Supplemental Table S1, related to Experimental Procedures:** Primary cell strains and immortal cell lines

Figure		1	1	1	2	3	4	4	4	5	6	6	7	S4	S5
Strain	Age (years)	A-D' I, J	E-H	K-N'			A-D	E-H	I-K		A-C	D-G			
160	16			1p	4p	4p									
240L	19	4p	4p		4p	4p	4p	4p	4p *		4p	4p		4p	4p
168R	19	4p	4p		4p	4p	4p	4p			4p	4p		4p	4p
53R	19			1p											
184	21	4p						4p			4p			4p	
51R	27			1p											
123	27	4p						4p			4p			4p	
124	29	4p	4p					4p			4p	4p		4p	4p
1030P	30						4p								
BR048	34									0p					
BR038	40									0p					
BR039	50									0p					
BR040	54									0p					
96L	61			1p											
71C	65			1p											
881P	65	4p						4p			4p			4p	
122L	66	4p	4p		4p	4p	4p	4p	4p *		4p	4p		4p	4p
29	68		4p	1p								4p			4p
429ER	72				4p	4p									
353P	72	4p	4p				4p	4p			4p	4p		4p	4p
464P	80	4p			4p	4p	4p	4p			4p			4p	
451P	83	4p						4p			4p			4p	

**Immortal cell lines**

240LMY	19												25p		
184Fp16s	21												31p		
122LMY	66												19p		
805Pp16s	91												29p		

\*: Technical triplicates p: Passage



**Figure S1, related to Experimental Procedures.** (A) Representative FACS analyses showing CD227 and CD10 expression in fourth-passage cKit-enriched HMEC isolated from one woman younger than 30 years (160 16y) and (B) one older than 55 years (429ER 72y). Left, unstained controls; right, the CD10- and CD227-stained samples.

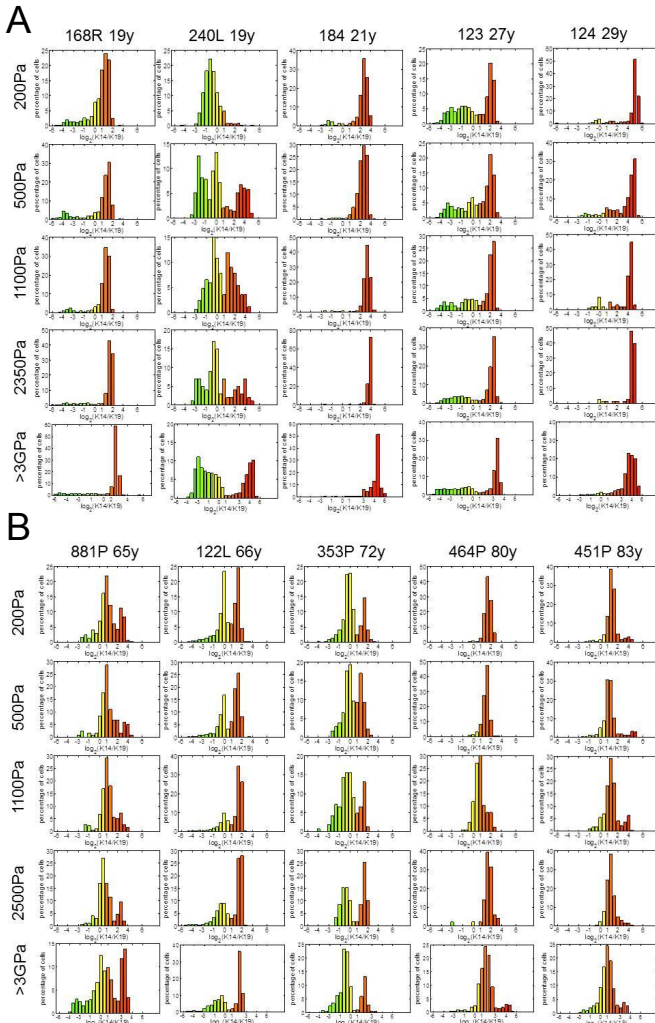


**Figure S2, related to Figure 1 (A)** Histograms represent  $\log_2$ -transformed ratios of K14 to K19 protein expression in single cells for each donor <30y under each condition. (B) Histograms represent  $\log_2$ -transformed ratios of K14 to K19 protein expression in single cells for each donor >55y under each condition.

Supplemental Table S2 related to Figure S2: p-values obtained with a Chi-squared test.

Conditions	Strain	168R	240L	184	123	124	881P	122L	353P	464P	451P
200Pa vs 500Pa		0.127	0.000	0.688	0.846	0.008	0.492	0.202	0.357	0.417	0.281
200Pa vs 1100Pa		0.054	0.003	0.010	0.096	0.000	0.459	0.235	0.162	0.166	0.124
200Pa vs 2350Pa		0.001	0.036	0.001	0.007	0.013	0.053	0.051	0.054	0.392	0.522
200Pa vs >3GPa		0.003	0.000	0.044	0.039	0.000	0.035	0.002	0.001	0.023	0.000

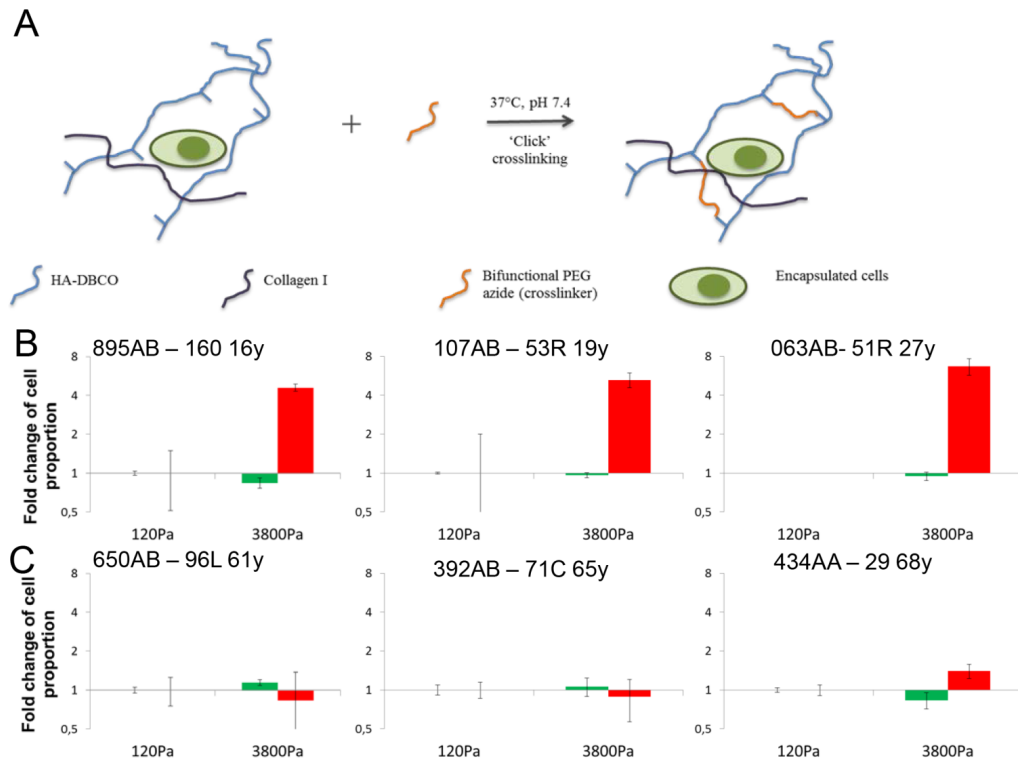


**Figure S3, related to Figure 1.** (A) Cartoon schematic of 3D encapsulation in click-crosslinked hyaluronic acid (HA) hydrogels. Fold change of lineage proportions in passage 1 cKit<sup>+</sup> HMEC from donors (B) <30y and (C) >55y in HA gels with increasing stiffness.

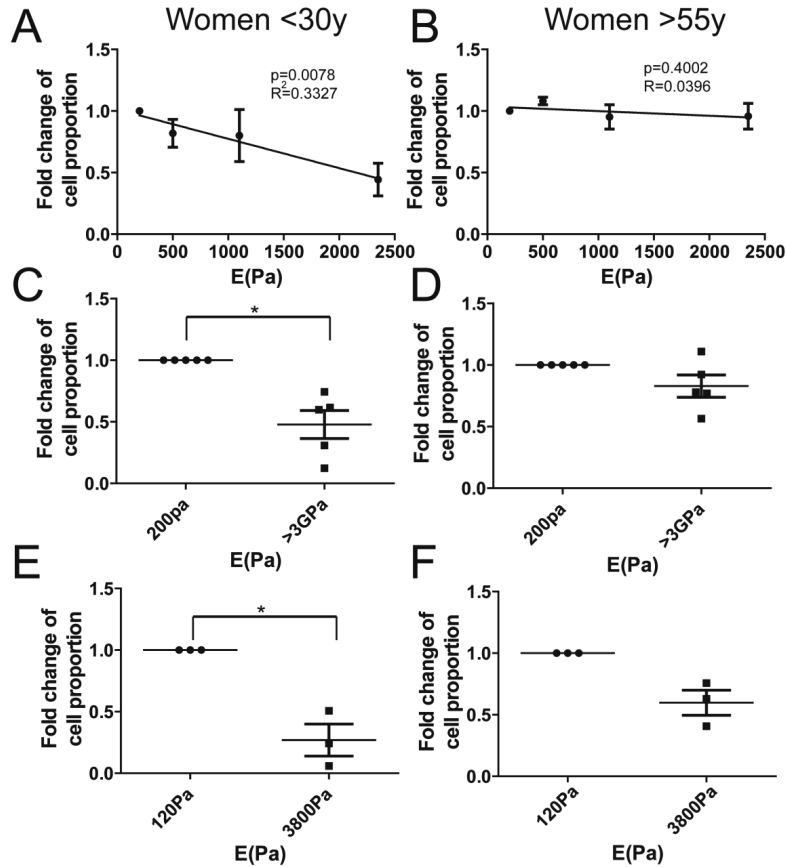


**Figure S4, related to Figure 1.** (A) Linear regression plots of K14+/K19+ HMEC proportion as a function of modulus are shown for women <30y ( $p=0.0078$ ,  $r^2=0.3327$ ,  $n=5$ ) and (B) women >55 ( $p=0.4002$ ,  $r^2=0.0396$ ,  $n=5$ ). (C) K14+/K19+ HMEC proportion as a function of modulus is shown for women <30y ( $p=0.0101$ ,  $n=5$ ) and (D) women >55 ( $p=0.0577$ ,  $n=5$ ). Regressions and plots are fold change of proportions compared to 200Pa condition  $\pm$  s.e.m. (E) Fold changes of K14+/K19+ HMEC proportion normal to 120Pa condition after 7 days of culture encapsulated in 3D hyaluronic acid (HA) gels (women <30y  $p=0.0301$ ,  $n=3$ , F, women >55y  $p=0.0587$ ).

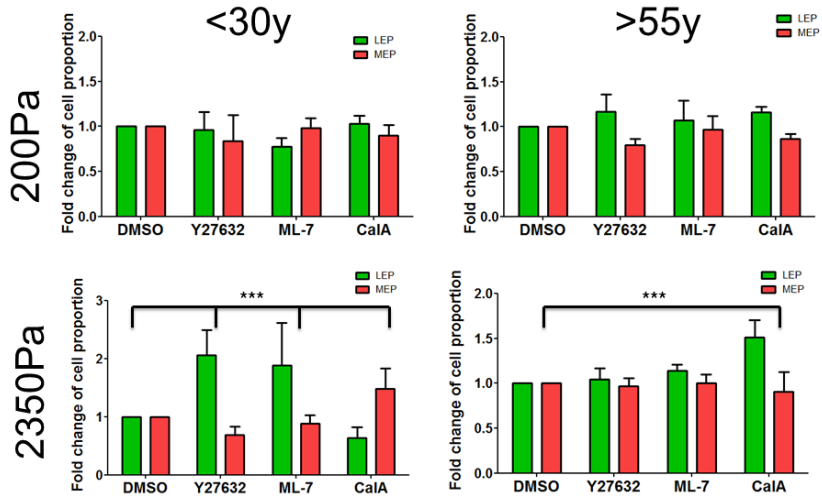


**Figure S5, related to Figure 3.** Fold change of lineage proportions in cKit+ HMEC from women <30y and >55y on 200Pa and 2350Pa PA gels treated with mechano-sensing inhibitors.

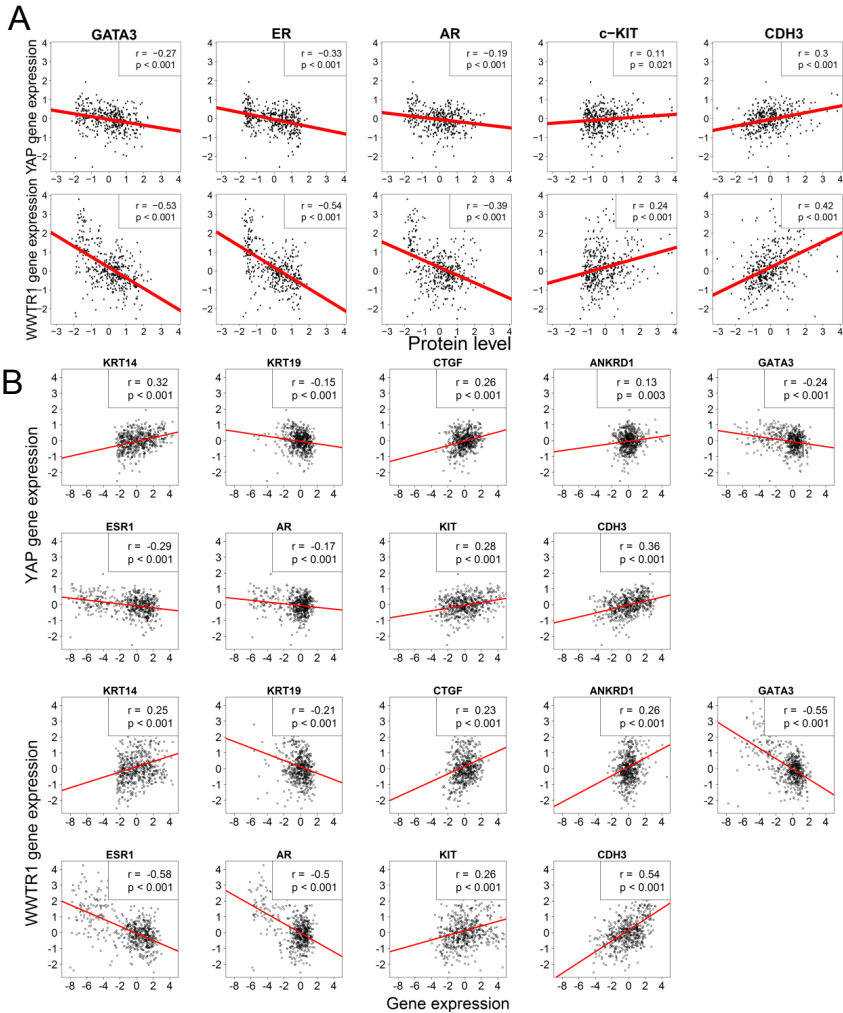


**Figure S6 related to Figure 5.** (A) Correlation between YAP and TAZ gene expression and the protein expression of various biomarkers in TCGA dataset (Pearson's  $r$  statistic is shown). (B) Correlation between YAP and TAZ gene expression and various biomarkers gene expression from the TCGA dataset.

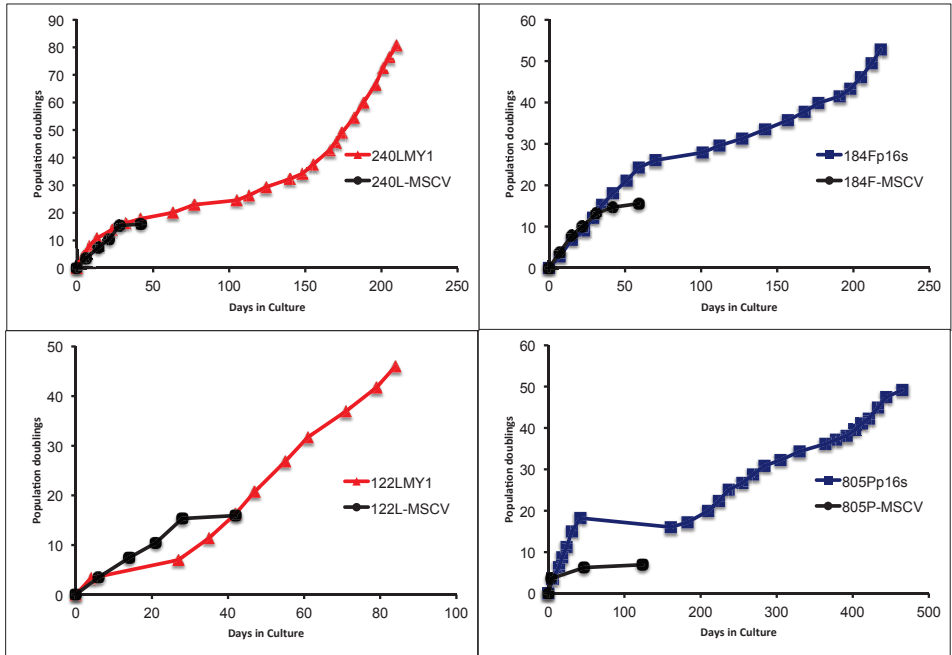


**Figure S7, related to Figure 7.** Growth curves for the four immortal lines used and the MSCV-vector only controls that entered stasis.

## Supplemental Experimental Procedures:

### Primers used for qRT-PCR:

The primer sets were designed to target two different exons of the gene.

GAPDH	AAGGTGAAGGTCGGAGTCAAC, GGGGTCATTGATGGCAACAATA
TEAD1	GGCCGGGAATGATTCAAACAG, CAATGGAGCGACCTTGCCA
TEAD2	GCCTCCGAGAGCTATATGATCG, TCACTCCGTAGAAGCCACCA
TEAD3	TCATCCACAAGCTGAAGCAC, CAATGACAAGCAGGGTCTCC
TEAD4	GGACATCCGCCAAATCTATG, TCCTCGATGTTGGTGTGAG
MST1	CCTCCACATTCCGAAAACCA, GCACTCCTGACAAATGGGTG
MST2	AGGAACAGCAACGAGAATTGG, CCCCTTCACTCATCGTGCTT
LATS2	CAGCTGGAGCAAGAAATGG, TGGCCCTCTTAACTGTG
AMOT	AGGCAAGAGTTGGAAGGATG, TTGGAGGATGACTTCACGAG
AMOTL1	TGCATGTGAGAAGCGAGAAC, CATTGTATTCCGGCATGTTG
AMOTL2	ACCATGCGGAACAAGATGGAC, GGCGGCGATTTGCAGATTC
CTGF	CGGGTTACCAATGACAACG, TGGAGATTTGGGAGTACGG

**3D encapsulation in Hyaluronic Acid (HA) gels** - Passage 1 cKit<sup>+</sup> HMEC were encapsulated in click-crosslinked HA hydrogels (Figure S3A). Details will be published elsewhere, but briefly, HA-dibenzocyclooctyne (HA-DBCO) was synthesized as follows: HA-COOH (65 kDa molecular weight, Lifecore Biomedical) was dissolved in water, activated by EDC/NHS (N-(3-Dimethylaminopropyl)-N'-ethylcarbodiimide/N-hydroxysuccinimide, Sigma-Aldrich) and reacted with DBCO-amine (Sigma-Aldrich) dissolved in dimethyl sulfoxide for 48h at room temperature, followed by dialysis and freeze-drying to obtain HA-DBCO with approximately 10% of the HA disaccharide units modified by DBCO (from <sup>1</sup>H NMR data, not shown). HA-DBCO was crosslinked by 'click' chemistry using bifunctional PEG-azide (1 kDa molecular weight, Creative Pegworks) to form hydrogels rapidly via the Strain-Promoted Azide-Alkyne Cycloaddition (SPAAC) reaction (Ning, Guo et al. 2008). The elastic modulus of the hydrogels was modified similar to that described previously (Ananthanarayanan, Kim et al. 2011) by

varying HA content and the ratio ( $r$ ) of azide groups to HA disaccharide units. The two formulations chosen were 1.5 wt% HA,  $r = 0.15$  and 3 wt% HA,  $r = 0.09$ , corresponding to Young's moduli of  $123 \pm 37$  Pa and  $3843 \pm 306$  Pa respectively as measured by oscillatory shear rheology. For 3D cell encapsulation, hydrogels were prepared on glass chamber-slides treated with a hydrophobic solution. HA-DBCO was mixed with Collagen I (PureCol bovine collagen, Advanced Biomatrix) to 0.03 wt%. PEG-azide was added just prior to mixing with the cell pellet, and the solution was allowed to gel for 1h at 37 °C before adding media. Cell-gel constructs were maintained for 7d before immunofluorescent quantification of K14/K19 expression.

### Cell segmentation with Matlab:

This function imports a directory of pictures, segments cells and cells incorporating EdU from each picture.

Each cell from the cell mode script should be run one after each other.

#### Initializing cell:

```
input_directory = uigetdir('C:\','Select INPUT directory');
if (input_directory == 0)
error('This directory does not exist');
end
output_directory = input_directory;

%Create excel file names
res_ratio = strcat(output_directory,'/ratio.xls');
res_intensity = strcat(output_directory,'/intensity.xls');
size = 1;
size2 = 1;
count1 =1;
count2 =1;
n1 =1;
n2 =1;
EdU_cKit = zeros(3,2);
EdU_unso = zeros(3,2);
files = dir(input_directory);
```

#### Cell number 1: Segmenting cells from a picture

```
for i = 1:length(files)
% Name of the current picture must contain the population name (cKit,
% or unsorted) and the stiffness (L, M, H, VH, or G)
name = char(files(i).name);

% The directory should contain only pictures, if not, you can select for
% tif or lsm files.

% if length(name) > 3
% strin = char(name(length(name)-2:length(name)));
% % Consider tif files only
% if strcmp(strin, 'lsm') || strcmp(strin, 'LSM')

disp(strcat('Processing tif stack -',files(i).name,':', num2str(i),'',...
num2str(length(files))));
```

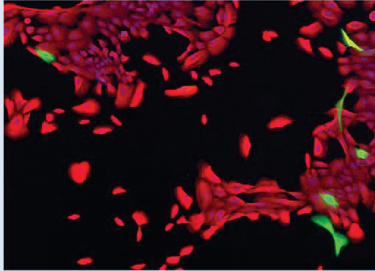
The `coor` function finds the population (cKit or unsorted) and the condition (L, M, H, VH, G)

```
[position1,position2] = coor(name);
currentFile = strcat(input_directory, '/', files(i).name);

% Open the current picture
test = imread(currentFile);
% Attribute each channel to a single picture
I_blue = test(:,,1);
I_red = test(:,,2);
I_green = test(:,,3);
```

```
I_cy = test(:,:,4);
```

```
MyRGB = cat(3,Ired,Igreen, I_blue);  
MyGray = rgb2gray(MyRGB);  
MyEdU = cat(3,Ired,Igreen, I_cy);  
I = MyGray;
```



Original picture showing the first three channels (RGB)

The next step is applying a threshold to the picture

```
bw = im2bw(I, 0.08); %This value is flexible
```

```
%figure, imshow(bw);  
% Fill holes  
bw2 = imfill(bw,'holes');  
% Remove the objects under 40 pixels  
bw4 = bwareaopen(bw2, 40);
```



Original picture converted to binary image using a threshold

Getting the perimeter of each object

```
bw4_perim = bwperim(bw4);
```

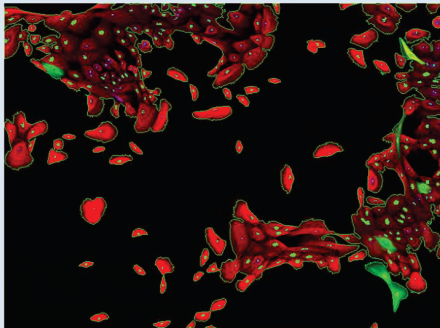
Finding the nucleus

```
mask_em = imextendedmax(I_blue, 20); %This value is flexible  
mask_em = imfill(mask_em, 'holes');  
% mask_em = bwareaopen(mask_em, 5);
```



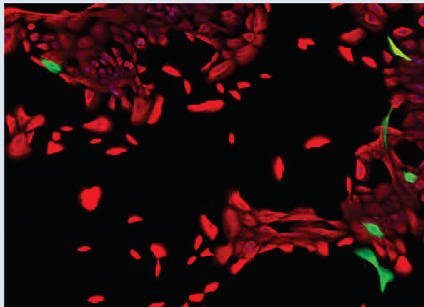
Mask containing the cell nucleus

```
%overlay3 = imoverlay(MyRGB, bw4_perim | mask_em, [.3 1 .3]);  
%figure, imshow(overlay3);
```

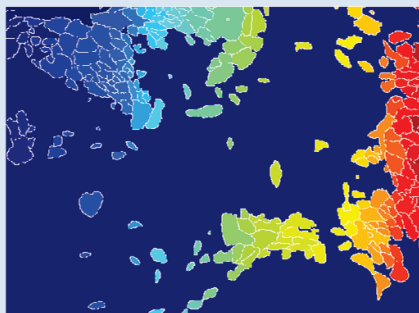


Overlay of the original picture with the perimeter and the marked nucleus

```
% Compute the complement of the picture  
I_eq_c = imcomplement(I);  
Setting regions containing nucleus and background to a minimum  
I_mod = imimposemin(I_eq_c, ~bw4 | mask_em);  
Applying the watershed function  
L = watershed(I_mod);  
clear I_mod;  
figure, imshow(label2rgb(L))  
figure, imshow(MyRGB);
```



Original picture



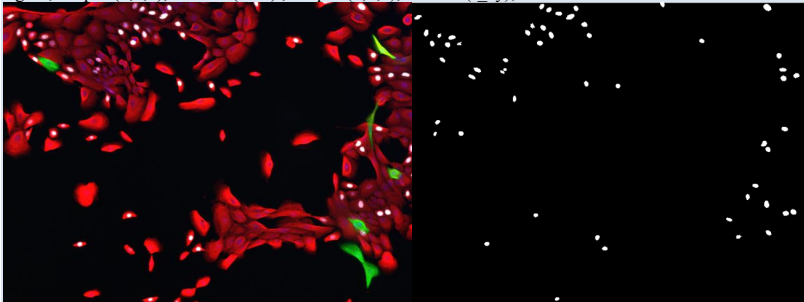
Segmented picture

```
stats = regionprops(L, 'Area', 'Perimeter');
```

```
%Green
stats_green = regionprops(L, Igreen, 'MeanIntensity', 'Area', 'Centroid');
%Red
stats_red = regionprops(L, Ired, 'MeanIntensity', 'Centroid');
%clear L_red;
```

#### Cell number 2: Segmenting cells incorporating EdU

```
%EdU
bw = im2bw(I_cy, 0.2);
bw2 = imfill(bw, 'holes');
bw3 = bwareaopen(bw2, 30);
figure, subplot(2,1,1), imshow(bw3), subplot(2,1,2), imshow(I_cy);
```



Original picture with nucleus  
incorporating EdU

Segmented nucleus  
incorporating EdU

#### Cell number 3: Computing the number of cells incorporating EdU:

Labeling each object from the segmentation with mean intensity, area and centroid properties

```
stats_cy5 = regionprops(bw3, I_cy, 'Area', 'MeanIntensity', 'Centroid');
stats_red2 = regionprops(bw3, Ired, 'MeanIntensity', 'Centroid');
stats_green2 = regionprops(bw3, Igreen, 'MeanIntensity', 'Centroid');
```

```
% The EdU function segments cells incorporating EdU and store the red/green  
% intensity ratios in a variable.
```

```
if position1==1
[EdU_cKit, n2] = EdU(EdU_cKit, n2, position2, stats_red2, stats_green2, stats_cy5);
end
```

```
if position1==2
[EdU_unso, n3] = EdU(EdU_unso, n3, position2, stats_red2, stats_green2, stats_cy5);
end
```

#### Cell number 4: Computing the results

```
m=1;
for k=1:length(stats_green)
% Apply a threshold against the background or unstained cells
if (stats_green(k).Area < 1000) && (stats_red(k).MeanIntensity > 40 ...
|| stats_green(k).MeanIntensity > 40)
if log2(stats_red(k).MeanIntensity / stats_green(k).MeanIntensity) ~= -Inf ...
```

```
&& log2(stats_red(k).MeanIntensity / stats_green(k).MeanIntensity ) ~ Inf
```

Computing the ratio of each cell and store the intensities

```
ratio(m)=log2(stats_red(k).MeanIntensity / stats_green(k).MeanIntensity );  
intensity(m,1) = stats_red(k).MeanIntensity;  
intensity(m,2) = stats_green(k).MeanIntensity;
```

```
if position1==2 %cKit  
histo_cKit(count2,1) = ratio(m);  
histo_cKit(count2,2) = position2;  
red_cKit(count2,1) = stats_red(k).MeanIntensity;  
red_cKit(count2,2) = position2;  
green_cKit(count2,1) = stats_green(k).MeanIntensity;  
green_cKit(count2,2) = position2;  
count1 = count1 +1;  
end
```

```
if position1==2 %unsorted cells  
histo_unso(count3,1) = ratio(m);  
histo_unso(count3,2) = position2;  
red_unso(count3,1) = stats_red(k).MeanIntensity;  
red_unso(count3,2) = position2;  
green_unso(count3,1) = stats_green(k).MeanIntensity;  
green_unso(count3,2) = position2;  
count2 = count2 +1;  
end  
m=m+1;  
end  
end  
end
```

Writing in different excel files

```
new_size =m;  
if exist('ratio')  
xlswrite(res_ratio,(Xia, Sakban et al.),'Sheet1', strcat('A',num2str(size)));  
xlswrite(res_intensity,{name},'Sheet1', strcat('A',num2str(size2)));  
xlswrite(res_intensity,{'Red Intensity'},'Sheet1', strcat('A',num2str(size2+1)));  
xlswrite(res_intensity,{'Green Intensity'},'Sheet1', strcat('B',num2str(size2+1)));  
  
xlswrite(res_ratio, ratio,'Sheet1', strcat('A',num2str(size+1)));  
xlswrite(res_intensity,intensity(:,1),'Sheet1', strcat('A',num2str(size2+2)));  
xlswrite(res_intensity,intensity(:,2),'Sheet1', strcat('B',num2str(size2+2)));  
xlswrite(res_ratio, position2,'Sheet1', strcat('B',num2str(size+1),',', 'B',num2str(size+new_size-1)));  
size= size + new_size;  
size2= size2 + new_size+1;  
end  
clear ratio;  
clear intensity;  
% end  
% end  
end
```

Adapted from Steve Eddins, <http://blogs.mathworks.com/steve/2006/06/02/cell-segmentation/>

## Cell feature detection with Matlab:

This function imports a directory of pictures and computes the homogeneity of each picture.

### Initializing cell:

```
input_directory = uigetdir('C:\','Select INPUT directory');
if (input_directory == 0)
error('This directory does not exist');
end
output_directory = input_directory;

%Create excel file names
res_ratio = strcat(output_directory,'/ratio.xls');
files = dir(input_directory);
size = 1;
size2=1;
```

### Cell number 1: Computing image heterogeneity

```
for i = 3:1:length(files)
% Name of the current picture must contain the population name (cKit,
% or unsorted) and the stiffness (L, M, H, VH, or G)
name = char(files(i).name);
Nmean=[];
% The directory should contain only pictures, if not, you can select for
% tif or lsm files.

%     if length(name) > 3
%         strin = char(name(length(name)-2:length(name)));
%         % Consider tif files only
%         if strcmp(strin, 'lsm') || strcmp(strin, 'LSM')

disp(strcat('Processing image ',files(i).name, ', ', num2str(i),'',...
num2str(length(files))));
```

### The coor\_cyto function finds the population (cKit or unsorted)

```
position = coor_cyto(name);
currentFile = strcat(input_directory, '/', files(i).name);

% Open the current picture
test = imread(currentFile);

% Attribute each channel to a single picture
%blue: Hoechst, red: pFAK, green: phalloidin, mag: vinculin
I_blue = test(:,:,1);
Ired = test(:,:,2);
Igreen = test(:,:,3);
I_mag = test(:,:,4);
I_black = zeros(length(I_blue),length(I_blue));
%In this example, we analyze F-actin homogeneity
MyRGB = cat(3,I_black,Igreen, I_blue);
MyGray = rgb2gray(MyRGB);
```

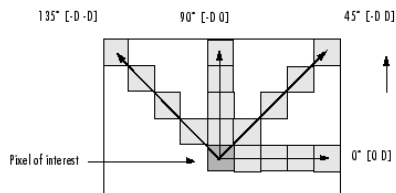
```
I = MyGray;
```

#### Filtering the picture

```
H = fspecial('unsharp');  
Ish = imfilter(Igreen,H,'replicate');  
K = rangefilter(Igreen);  
% figure, imshow(K)  
% figure, imshow(Igreen)  
% figure, imshow(Ish)
```

#### Applying the graycomatrix function

```
offsets = [ 0 1; 0 2; 0 3; 0 4;...  
-1 1; -2 2; -3 3; -4 4;...  
-1 0; -2 0; -3 0; -4 0;...  
-1 -1; -2 -2; -3 -3; -4 -4];  
glcms = graycomatrix(Ish,'Offset',offsets);  
stats = graycoprops(glcms,'Contrast Correlation Homogeneity Energy');  
Nmean=mean(stats.Homogeneity);
```



The figure illustrates the spatial relationships of pixels that are defined by this array of offsets, where  $\Delta$  represents the distance from the pixel of interest.

MathWorks

Adapted from MathWorks: <http://www.mathworks.com/help/images/analyzing-the-texture-of-an-image.html>

## Supplemental References

- Ananthanarayanan, B., Y. Kim, et al. (2011). "Elucidating the mechanobiology of malignant brain tumors using a brain matrix-mimetic hyaluronic acid hydrogel platform." *Biomaterials* **32**(31): 7913-7923.
- Ning, X., J. Guo, et al. (2008). "Visualizing metabolically labeled glycoconjugates of living cells by copper-free and fast Huisgen cycloadditions." *Angew Chem Int Ed Engl* **47**(12): 2253-2255.
- Xia, L., R. B. Sakban, et al. (2012). "Tethered spheroids as an in vitro hepatocyte model for drug safety screening." *Biomaterials* **33**(7): 2165-2176.







# High dimensional analysis of age-related phenotypic diversity in human mammary epithelial cells

Fanny A. Pelissier<sup>1,2</sup>, Denis Schapiro<sup>3</sup>, Hang Chang<sup>2</sup>, Alexander D Borowsky<sup>4</sup>, Bahram Parvin<sup>2</sup>, Bernd Bodenmiller<sup>†3</sup>, Mark A. LaBarge<sup>†2</sup> and James B. Lorens<sup>†1</sup>

<sup>1</sup>Department of Biomedicine, University of Bergen, Bergen N-5009, Norway

<sup>2</sup>Biological Systems and Engineering Division, Lawrence Berkeley National Laboratory, Berkeley, CA 94720, USA

<sup>3</sup>Institute of Molecular Life Sciences, University of Zürich, CH-8057 Zürich

<sup>4</sup>Department of Pathology, University of California Davis, Sacramento, California

<sup>†</sup> Equal contribution

## Correspondence

Prof. James Lorens

Department of Biomedicine, UiB, Jonas Lies Vei 91, 5009 Bergen, Norway

Jim.Lorens@uib.no, phone +47 55 58 67 76

Prof. Bernd Bodenmiller, Institute of Molecular Life Sciences, Winterthurerstrasse 190, 8057 Zürich, Switzerland, Bernd.Bodenmiller@imls.uzh.ch, phone +41 791798029

Dr. Mark LaBarge, Lawrence Berkeley National Laboratory, Berkeley CA USA

MALabarge@lbl.gov

## Running title

The Shape of Aging Mammary Epithelia

## Keywords

Human mammary epithelia, aging, mass cytometry, single cell analysis, heterogeneity, breast cancer

## **Summary**

The accumulation of defective stem and progenitor cells may be common in aging tissues. This skewed differentiation potential is thought to impair maintenance of healthy homeostasis in tissues and may increase susceptibility to oncogenic events. There is not a strong age-dependent association with particular mutations in mammary epithelia to explain age-related cancer susceptibility, but there is reduction of tumor suppressive cell types and accumulation of defective luminal and epithelial progenitors with age. However, a quantitative understanding of the phenotypic and functional heterogeneity within aged tissues is lacking, which would allow us to pinpoint subpopulations of cells that are changing during the aging process and that may be missed in population-average experiments. We profiled the phenotype of primary human mammary epithelial cells from forty-four women from 16 to 91 years old using high-dimensional (30-parameter) mass cytometry single cell analysis. Unsupervised population partitioning identified a subset of luminal cells that acquired a more basal-like phenotype and accumulated with age. The presence of luminal cells with that basal-like phenotype enabled robust classification of a tissue age-group. Further, increased in cytokeratin 14 and decrease in cytokeratin 19 with age in luminal epithelia was a specific phenotype from mass cytometry analysis, which we used to validate our findings by categorizing a separate cohort of normal breast tissue sections by age, using image analysis. We show that the etiology of these age-related luminal cell changes was due to altered mammary luminal progenitor cells. Examination of a subset of the primary strains that were pushed down the malignant progression revealed that

specific marker expression signatures found in age-altered luminal cell subpopulations were characteristic of immortalized derivatives of older HMEC. This study presents the first high-resolution examination of age-related phenotypic diversity of human epithelial cells and pinpoints specific luminal and progenitor subpopulations that are changing and accumulating with age.

## Introduction

Stem cells regulate tissue homeostasis and their activity is altered with age (Biteau et al., 2008; Mansilla et al., 2011). There is increasing evidence that dampened function of adult stem cells plays a role in the susceptibility to diseases of aging (reviewed in (Sharpless and DePinho, 2007; Signer and Morrison, 2013)). In human mammary gland, differentiation defective cKit-expressing multipotent progenitors (MPP) accumulate with age, and the proportions of their daughter myoepithelial cells (MEP) and luminal epithelial cells (LEP) shift with age (Garbe et al., 2012). The majority of age-related breast cancers are of luminal subtype (Carey et al., 2006; Jenkins et al., 2014) and the causes for this phenotype remain elusive. We have hypothesized that these age-associated changes may make aged breast tissue more susceptible to malignant progression. We previously demonstrated that post-menopausal LEP frequently express low levels of cytokeratin 14 (K14), as well as other markers typically associated with MEP and progenitors that express both K14 and K19. Moreover, age-dependent changes in the efficiency of YAP/TAZ-mediated mechano-transduction may help drive that phenotype of aging, as older progenitors do not respond to mechanical cues and more YAP has been observed in the nucleus of older LEP *in vivo* (Pelissier et al., 2014) which homolog TAZ is associated with a basal differentiation transcription program (Skibinski et al., 2014). We hypothesized that with age the luminal population retains distinct attributes reflective of an incomplete cell differentiation. Thus, with age, luminal cells may acquire a phenotypic divergence that is the result of age-related cell-to-cell variability in protein levels in luminal cells.

Analysis of this cellular heterogeneity requires a multiparametric single cell-level approach to quantify marker proteins and intracellular cell signaling changes representative of different cell states. Standard immunofluorescence and flow cytometry methods are limited to

relatively few parameters (Bendall et al., 2012). Mass cytometry is a recent technology that allows high-dimensional analysis of single cells in complex heterogeneous biological systems (Bandura et al., 2009). Signaling pathways, cell cycle state, cell viability, using platinum-based viability reagent (Fienberg et al., 2012) and many other cellular pathways can be simultaneously interrogated (Bendall et al., 2011). Mass cytometry increases the number of parameters that can be measured, reduces overlap between channels and eliminates background fluorescence (Bandura et al., 2009) due to the use of isotopically pure metal labelled antibodies (Lou et al., 2007).

In this study, we applied mass cytometry methods to measure the phenotypic heterogeneity in forty-four primary human mammary epithelial cell (HMEC) samples from women aged 16 to 91 years old (y). We developed a panel of twenty-nine antibodies recognizing proteins and protein-modifications reflective of the epithelial phenotypic cell hierarchy together with markers of cell migration, cell growth, proliferation and apoptosis. To analyze the vast data, a dimensionality-reduction strategy using t-distributed stochastic neighbor embedding (tSNE) (Amir el et al., 2013) and PhenoGraph were run to visualize and partition high-dimensional single-cell data into subpopulations (Levine et al., 2015). Additionally, unsupervised identification of stratifying subpopulations that changed with age were analyzed using Citrus (Bruggner et al., 2014). This comprehensive analysis revealed an unprecedented high definition determination of lineage-dependent heterogeneity in normal HMEC. Strikingly, unsupervised population partitioning revealed age-dependent clusters only within the luminal compartment. The aged luminal cells manifested a marker expression signature that correlated with an enhanced basal phenotype. Using this data-set we built an unsupervised classification model that correctly assigned more than 80% of the samples into their correct age-group. Further, we found age-related changes in luminal progenitor cells, supporting the notion of accumulated age-altered

stem/progenitor cell populations during aging. Hence, high-dimensional analysis of normal human mammary epithelial cells revealed a remarkable age-related phenotypic divergence in the luminal and luminal progenitor cells.

## Results

### High dimensional analysis of human mammary epithelia from women <30y

We used mass cytometry to obtain single-cell proteomic profiles of cryopreserved normal primary human mammary epithelial tissue (HMEC) at passage 4 from forty-four women from 16 to 91 years old (y) (Fig 1 and Table S1). We selected 10 highly informative luminal, myoepithelial and progenitor surface markers that captured the lineage-heterogeneity in HMEC according to previous work (Asiedu et al., 2014; dos Santos et al., 2013; Hebbard et al., 2000; LaBarge et al., 2007; Lim et al., 2009b; Louderbough et al., 2011; Rubin and Yarden, 2001; Taylor-Papadimitriou et al., 1989; Villadsen et al., 2007). We added 12 antibody probes against intracellular protein phosphorylation-epitopes, 4 antibody probes against proteins of the Hippo pathway and 3 antibody probes against cell cycle and apoptosis proteins, thus allowing simultaneous measurement of surface phenotype and signaling behavior in single HMEC cells (Figure S1 and Table S2). The complete data-set contained single cells from women from three age-groups (<30y N=16, >30<50y N=13 and >50y N=15) measured in 29 simultaneous protein epitope dimensions (D) (Fig 1A). To visualize the single cell relationships, we used tSNE to project all 29 dimensions in 2D by a non-linear dimensionality reduction. Each dot on the tSNE map represents a single cell with similarity represented by a geometrical distance, such that phenotypically related cells are close together (Fig 1B). Highlighting each marker expression revealed distinct LEP (K19+/K7+/K8/18+/CD133+) and MEP (K14+/K5/6+) populations in woman <30y (Fig 2A). Several signaling markers were perceptibly lineage-dependent: CD44, YAP, phospho-(p)EGFR, pStat1, pS6 and p-Phospholipase C Gamma 2 (pPLC $\gamma$ 2) that have been previously implicated in myoepithelial function and contractility (Chan et al., 2012; Fu et al., 2015; Haricharan and Li, 2014; Hebbard et al., 2000; Louderbough et al., 2011; Pasic et al., 2011; Paszek et al., 2005; Raymond et al., 2011; Reversi et al., 2005; Vlug et al., 2013; Zhao et al.,

2010). In order to exhibit lineage-dependent markers in younger women, LEP and MEP populations were manually gated (gating strategy is depicted in Fig 1B). As expected, K19, K7, K8/18, CD133 and cKit expression was higher in LEP and K14, K5/6 expression was higher in MEP (Figure 2B). LEP had also higher MST1, LATS1, and MST2 expression correlating with a decreased YAP expression. Interestingly, LEP exhibited higher pNFκB, which has been shown to be involved in mammary epithelial proliferation and branching in a mouse model (Brantley et al., 2001). MEP showed higher marker expression of Ax1, pS6, pPLGγ2, pEGFR, CD44, pGsk3, pCreb, pMEK1/2, pErk1/2, pAkt pStat1, pStat3 and pStat5 which have been implicated in myoepithelial homeostasis (Barash, 2006; Dembowy et al., 2015; Dietze et al., 2005; Gallego et al., 2001; Tumaneng et al., 2012; Watson, 2006). Similar phenotypic space representation was observed in older women (Fig S2 and S3) although qualitative differences were already perceptible. The most prominent age-related difference was observed in the LEP population where YAP expression increased significantly (Fig S3A, linear regression  $p=0.0179$ , data not shown). Thus, high dimensional reduction analysis revealed inter-lineage heterogeneity with an unprecedented dimensional level and a qualitatively perceptible age-related phenotypic divergence between HMEC from women <30y and HMEC from older women.

### **Intra-lineage and age-related phenotypic divergence in the HMEC landscape**

Next we delved further into the phenotypic heterogeneity within each LEP and MEP population. We noted “patches” of K14, K5/6, pRb and CyclinB1 expression within the MEP lineage suggesting the existence of distinct subpopulations (Fig 2A). To better investigate this, we applied PhenoGraph to automatically identify intra-lineage subpopulations (Fig 3A). The PhenoGraph analysis generated distinct phenotypic clusters within each lineage. LEP and MEP cell subpopulations (clusters) were identified by characteristic cytokeratin expression and tSNE

phenotypic projection (Fig 3B). One population, denoted double positive (DP), that co-expressed K14 and K19 was identified between LEP and MEP populations in a separate phenotypic space. This DP population represents multipotent progenitors as previously observed *in vivo* (Villadsen et al., 2007). The last subpopulation consisted of unknown cells with low marker expression (<0.52 ion counts per cell). Only LEP3 was more proliferative than the others according to higher levels of pRb and/or CyclinB1 (Giacinti and Giordano, 2006; Jin et al., 1998), while clusters MEP 2, 4, 7 and 8 expressed higher levels of pRb and/or CyclinB1 that correlated with higher DNA content (data not shown) than the other MEP subpopulations. Similar gene expression profiles were observed in older women (data not shown). However, increased K14 expression and decreased K19 expression was observed with age in the LEP subpopulations (Fig 3C and 3D). Age-related changes in marker expression were observed, mainly in the LEP subpopulations (Fig 3D). In addition, the abundance of each LEP subpopulation increased, while the abundance of each MEP subpopulation decreased with age (Fig 3E). This trend was observed at the individual level, although we observed high inter-sample heterogeneity (Fig 3F). Thus, high dimensional analysis revealed age-specific phenotypic divergence in specific subpopulations comprising both cell number and marker expression.

### **Evidence of age-dependent phenotypic divergence in the luminal population**

As the number of clusters obtained by PhenoGraph analysis was user-defined, we sought to further investigate age-dependent changes in an unsupervised manner. We used a hierarchical agglomerative clustering, characterization and regression tool (Citrus) to identify age-dependent clusters. Briefly, the Citrus algorithm combines all samples into one aggregate data-set before identifying cell populations by hierarchical clustering of phenotypically similar cells. Cells are assigned back to the individual samples and cluster abundance is calculated. Citrus identified

seven subpopulations that were more abundant with age (Fig 4A and Fig S4). These subpopulations were all projected within the luminal compartment of the tSNE phenotypic landscape. Each had a specific marker expression signature (Fig 4B): all of them were K14<sup>high</sup>, cluster A was K19<sup>low</sup> and was at the apex of the hierarchy. Thus, with age there is an overall accumulation of luminal cells with basal characteristics. Clusters B, C and D had the highest YAP, HER2, cKit, Axl, pS6, pPLC $\gamma$ 2, pEGFR, CD44, pGSK3, MST1, MST2, LATS1, pNF $\kappa$ B, pAkt, pERK1/2, pMEK1/2, pStat1, pStat3, and pStat5 expression. Most of these markers are associated with proliferation, migration and are mainly expressed in young MEP. Cluster B with the highest pRb and CyclinB1 expression which correlated with higher DNA content (data not shown) was “Proliferative LEP”, Cluster C was labeled “basal LEP” while cluster D, “pS6 luminal” had the highest pS6 expression. Cluster E was all “Keratin<sup>low</sup>” and Cluster F was labeled “Keratin-low S” with respect to its southern spatial position in the tSNE map. Finally, cluster G had the highest Axl expression and was named “Axl<sup>high</sup>”. Interestingly, no evidence for age-dependent subpopulations was observed in the myoepithelial population by this unsupervised analysis.

### **Evidence of an age-dependent functional divergence in the luminal population**

Next we investigated the functional consequences of the age-related changes in the mammary luminal compartment. The increased basal characteristics of the older luminal cells would be expected to affect cell adhesion and migration characteristics. LEP and MEP were FACS-sorted from different HMEC strains and analyzed for cell migration kinetics by real-time impedance measurements. LEP isolated from women <30y migrated faster than isogenic MEP (Fig 4C) as expected from their less adhesive properties as compared to MEP (Cerchiari et al., 2015). LEP

isolated from women >50y migrated much slower and a rate comparable to MEP (Fig 4C and D). This is consistent with enhanced basal properties of aged LEP.

### **Derivation of an age classification model**

We used the age-related phenotypic divergence to build a classification model to test the hypothesis that age-related changes in marker expression from our previous statistical analysis will generalize to an independent data-set. More importantly, a classification model uses cross-validation which is important in guarding against testing hypotheses suggested by the data (called type III errors). Using a training-set of five strains from each <30 and >50y age-group, we successfully assigned 13/16 women <30y, and 12/15 women >50y (Fig 4E). The classification performance was increased with the number of training samples (Fig S4B). Three strains <30y were incorrectly classified as “old”. One of them, 407P is a sample obtained from peripheral mastectomy tissue. 172L and 240L are samples with a high proportion of LEP compared to other strains from young women (240L is noticeable on Fig 3F). From the >30 and <50y age-group, 6 strains were assigned to “old”: 250MK which come from milk and has a luminal phenotype, 245AT which has an ATM heterozygote mutation, 173T which comes from a tumor, 173P and 42P which are samples from peripheral mastectomy. Finally, 60R is a sample from a 47y woman, thus close to the older age-group. From the >50y age-group, 3 strains were assigned to “young”. 153L is a sample with a low proportion of LEP compared to other strains from older women. 117R, and 881P might be classification errors. Thus, most of the incorrectly assigned strains have a particular phenotype that likely contributed to incorrect assignment. Hence, the classification model validated the hypothesis that subsets of luminal cells are changing with age and their alterations in phenotypic diversity are a hallmark of aging.

Considering that the K14<sup>high</sup>K19<sup>low</sup> cluster was at the hierarchy apex amongst age-dependent clusters, we hypothesized that these two markers were sufficient to be used as classifiers to build a classification model *in vivo*. Human breast sections were immunostained for K14, K19 and DAPI (<30y N=52, >30<50y N=86 and >50y N=33) (Fig 4F), and a classification model was built using morphometric context (Chang et al., 2013). This computational model relies on cell segmentation to define different epithelial cells, which then allows assessment of single cell K14 and K19 levels, as well as a number of morphometric features. Next, a machine learning-based classification model was trained for the three age-groups (<30y, >30 <50y and >50y) and could correctly assign more than 50% of the samples into their correct age-group as compared with a random guess of 33.3% (Fig 4G). In conclusion, a subpopulation of LEP accumulating with age with basal characteristics *in vitro* was identified *in vivo* and age-related markers could be used to perform a morphometric context classification.

### **Evidence of age-dependent phenotypic divergence in the cKit-progenitor population**

Collectively, the evidence above supported the notion that the age-related changes in the human mammary gland strongly affected the LEP population. We hypothesized that these age-dependent traits are the result of concomitant changes in LEP progenitors. To test this hypothesis, cKit-expressing luminal-biased progenitors (Lim et al., 2009a) were FACS-enriched from HMEC strains derived from three women <30y and three women >50y, and analyzed by mass cytometry using twelve progenitor and lineage markers (Fig 5A). Unsupervised agglomerative clustering identified two clusters that were more abundant with age (Fig 5B and Fig S5). These clusters were projected in the luminal compartment in the tSNE phenotypic space and had a specific marker signature (Fig 5C): cluster A was K7<sup>high</sup> while Cluster B was K19<sup>high</sup>. Both of these displayed high expression of CD133, cKit, HER2 and YAP. Thus, subpopulations of luminal

progenitors were more abundant with age and were identifiable via a specific marker signature. These data support the notion that age-dependent alterations in luminal progenitors are the etiology of the observed changes in the luminal population.

### **Age-related functional response to EGF activation**

To reveal age-dependent functional differences, HMEC from three <30y and three >50y women were treated with EGF and vanadate for 60min. At, t=0, 10, 30 and 60min cells were harvested and analyzed with mass cytometry using MCB and a panel of 23 antibody probes (Fig S6). LEP and MEP manually gated showed an activation of MEK/ERK pathway within the time-course (Fig S1B). However, pStat, pEGFR, pErk and pMEK and pPLC $\gamma$ 2 signaling marker expression were higher in LEP from women >50y. Dimensionality reduction using tSNE revealed pEGFR activation at the bottom-right corner of the phenotypic map with time (Fig S6B). Thus, in both age-groups, a cell activation wave from the top-left to the-bottom right corner in the phenotypic map was observed (Fig S6C). However in HMEC derived from older women, this effect was enhanced, suggesting increased responsiveness to EGF. We observed that pEGFR, pMEK1/2 and pErk expression was higher in MEP (Fig 2A) and in the clusters of older LEP (Fig 4B). Hence, MEK/ERK pathway activation response was reinforced in HMEC from older women due to functional changes in the LEP population.

### **Chronological age influenced immortalization into luminal breast cancer subtypes**

Normal epithelial cells must bypass tumor-suppressive barriers to give rise to malignancies. Pre-stasis HMEC can be efficiently immortalized in a two-step process that bypasses Rb function (by *CCND1* expression or *CDKN2A* knockdown) and reinstates telomerase activity (by *MYC* expression) (Garbe et al., 2014). HMEC from four women of different ages were immortalized to

assess the outcome of breast cancer-relevant changes (Lee et al., 2015). High dimensional analysis of six immortalized HMEC cell lines with tSNE revealed that immortalization using overexpression of *CCND1* to bypass stasis was associated with a luminal subtype while that immortalization using knock-down of *CDKN2A* was associated with a basal subtype. Strikingly, increased HMEC age resulted in a bias toward a luminal breast cancer subtype (Fig 6A). HMEC immortalization is associated with large-scale changes in gene expression, genomic instability and epigenetic reprogramming (Garbe et al., 2009; Garbe et al., 2014) that accounted for the inter-sample divergence in marker expression signature (Fig 6C). Strikingly, only the older luminal strain (122LD1MY) but not the younger luminal strain (240D1MY), exhibited also high expression of basal markers YAP, Axl, pS6, pPLC $\gamma$ 2, pEGFR, CD44 and pGSK3. These markers were also found highly expressed in the subset of LEP that accumulated with age (Fig 4B). Collectively, these results indicate that the specific marker expression signatures found in age-altered luminal cell subpopulations were characteristic of immortalized derivatives of older HMEC. This is consistent with the hypothesis that accumulation of altered luminal progenitors and luminal cells with basal traits during mammary gland aging reflect a breast cancer susceptibility phenotype.

## **Discussion**

In this study we described the first high-dimensional phenotypic heterogeneity of normal human mammary epithelial cell states. Our comprehensive single cell analysis of age-related phenotypic divergence revealed specific protein expression changes reflecting age-related changes in mammary epithelial cells.

The strongest risk factor for breast cancer is age yet there is no genetic evidence that fully explains this increased incidence (LaBarge et al., 2015; Stephens et al., 2012). However, there are age-dependent intrinsic changes in the breast epithelia. We have shown previously that multipotent progenitors have a differentiation defect that leads to their accumulation with age (Garbe et al., 2012). Their daughter LEP are not fully lineage committed and acquire a basal phenotype. Using a test-set with appreciable size and appropriate computational tools, we revealed a subset of LEP that accumulated with age with skewed differentiation and a basal phenotype. The older LEP are functionally more adherent to a substrate and more responsive to EGF stimulation.

Age-related signatures in the luminal clusters accumulating with age show a high expression of the basal marker K14. Decreased luminal K19 expression with age was a second marker forming the basis for a classification model that robustly assigned most samples into their correct age-group.

Specific markers in the age-related signatures were found in clusters of progenitors accumulating with age: cKit, CD133, YAP and HER2. This finding correlates with the fact that *cKit* over-expression prevents normal differentiation (Regan et al., 2012) and may explain the accumulation of cKit progenitors with age. CD133 was the marker which changed the most with age. CD133 was found to be a luminal progenitor marker (Hilton et al., 2014; Raouf et al., 2008). In addition, CD133 is expressed in certain types of breast cancer, in which CD133-positivity

seems to identify a restricted subgroup of tumor stem cells (Wright et al., 2008). As previously described, YAP expression in luminal biased-progenitors might result in a luminal differentiation with basal traits. Moreover, over-expression of HER2 has been shown to play an important role in the development and progression of certain aggressive types of breast cancer (Menard et al., 2000). More recently, a group showed that in luminal breast cancer, hormonal treatment lead to a reduction in estrogen receptor alpha levels promoting cancer stem cell phenotype (CD133<sup>high</sup> and CD44<sup>low</sup>) (Sansone et al., 2016). This results correlate well with the fact estradiol serum concentration decreases with age (van Landeghem et al., 1985) and we observed an increase in CD133<sup>high</sup> and CD44<sup>low</sup> cell proportion. These cells are highly suspected for the implication as cells-of-origin for breast cancers. The accumulation of these cells with age represents a high susceptibility factor for oncogenic events.

Collectively, we identified age-related markers that were used to build a classification model. Further investigation will be needed to determine those that are implicated in breast cancer progression. Thus with age, progenitors and their luminal progenies appear in altered phenotypic states, and accumulate. Altogether, the reciprocal dynamic between the microenvironment and the progenitor is altered, leading to an increase selection for adaptive mutations and a decrease in tumor suppressive mechanisms (Henry et al., 2011).

A functional decline in stem cells is not necessarily caused by a loss of the ability to self-renew but may also reflect an inability of stem cell progeny to properly differentiate, resulting in the accumulation of mis-differentiated cells and an increased potential for neoplastic transformation. For instance, elevated Jun N-terminal kinase (JNK) activity in intestinal stem cells causes a dysregulation of cell differentiation leading to a stem cell pool accumulation (Biteau et al., 2008). As a comparison, the number of HSCs in the bone marrow increases with age (Beerman et al., 2010; Beerman et al., 2013; Challen et al., 2010) with no difference in

cycling activity (Geiger et al., 2013) and aging skews differentiation potential toward myeloid lineages. Intuitively, increased stem cells may seem beneficial. However, this accumulating pool of stem cells is functionally impaired and may be more susceptible to oncogenic events.

In addition, the age-related marker expression signature were observed in the basal immortalized strains and only in the older luminal immortalized strain which have overcome major barriers to carcinogenesis. In conclusion, we speculate that the cells' epigenetic states that are associated with aging explain these differentiation biases in young and old progenitors. If we assume that the epigenetic states precede malignant transformation it would help to explain the distribution of intrinsic subtypes described previously (Jenkins et al., 2014).

## **Experimental Procedures**

**Cell Culture** – All cell culture was in M87A medium with 0.1nM oxytocin (X) and cholera toxin (CT) at 0.5ng/mL (Garbe et al., 2009). Primary HMEC strains were generated and maintained as described (Labarge et al., 2013) all tissues were obtained with proper oversight from the Lawrence Berkeley National Laboratory institutional review board. All the pre-stasis strains were used at 4<sup>th</sup> passage. Table S1 shows the strains used. For the EGF treatment time course, HMEC from three <30y and three >50y women were treated with EGF (Sigma E-9644 0.1µg/mL) and sodium orthovanadate (Sigma 13721-39-6 12.5mM) for one hour. Samples at time 0, 10min, 30min and 60min were harvested with TrypLE, fixed with 1.6% paraformaldehyde (PFA) for 10min at room temperature (RT) and frozen at -80°C for further analysis.

**Generation of immortal cell lines** – Finite lifespan HMEC from specimens 184, 240L, 122L, and 805P were obtained from reduction mammoplasty tissues or peripheral to mastectomy tissues (i.e. 805P). HMEC were grown in M87A supplemented with CT at 0.5 ng/ml, and X (Bachem) at 0.1 nM. Retroviral vectors: The p16 shRNA was in the MSCV vector, c-Myc was in the pBabe-hygro (BH2) or LXSXN vector. Retroviral stocks were generated from supernatants collected in M87A medium. Strains 240L, 122L, and 805P at passage 3 or and 184 at passage 4 were transduced with MSCV-p16sh or MSCV control and selected with puromycin. At the next passage, after puromycin selection, the p16sh transduced cells were transduced with c-Myc pBabe-hygro (c-myc LXSXN for 184) and selected with hygromycin. Vector only control pre-stasis cells entered stasis at passage 12-15, whereas the immortalized lines continued to grow.

**Antibodies used for analysis.** Antibodies were obtained in carrier protein-free PBS and then prepared using the MaxPAR antibody conjugation kit (DVS Sciences) according to the manufacturer's protocol. After determining the percent yield by measurement of absorbance at 280 nm, the metal-labeled antibodies were diluted in Candor PBS Antibody Stabilization solution (Candor Bioscience GmbH) for long-term storage at 4 °C. Antibodies used in this study are listed in Table S2. Antibodies were titrated and validated beforehand using both positive and negative cell controls.

**Flow Cytometry** – HMEC at fourth passage were trypsinized and resuspended in their media. For enrichment of luminal epithelial, myoepithelial and progenitor lineages, anti-CD227-FITC (Becton Dickinson, clone HMPV, 1:50), anti-CD10-PE, (BioLegend, clone HI10a, 1:100) or anti-CD117-PE (BioLegend, clone 104D2, 1:50), respectively were added to the media for 25 minutes on ice, washed in PBS, and sorted using FACS Vantage DIVA (Becton Dickinson). After sorting, progenitor cells were fixed in 1.6% PFA for 10min at RT and frozen at -80°C for further analysis.

**Cell barcoding and antibody staining.** HMEC strains were incubated with cisplatin (WR International, Radnor, PA, Cat# 89150-634, 25µM) for one minute to assess cell viability (Fienberg et al., 2012), were fixed in 1.6% PFA for 10min at RT and washed once with Cell Staining Media (CSM, PBS with 0.5% BSA, 0.02% NaN<sub>3</sub> with 0.03% saponin). The cells were then resuspended in PBS, and DMSO stocks of the barcoding reagent were added as described (Bodenmiller et al., 2012; Zivanovic et al., 2014). The cells were incubated at room temperature for 30 min, washed three times with CSM, and then pooled into a single FACS tube for staining with metal-labeled antibodies for 1h at RT. A staining volume of 800 µl was used ( $\sim 1 \times 10^8$

cells/ml). After antibody staining, the cells were washed twice with CSM and once with PBS, and then incubated for 20 min at room temperature or overnight at 4°C with an iridium-containing intercalator (DVS Sciences) in PBS with 1.6% PFA. The cells were then washed three times with CSM and once with PBS, diluted with water to  $\sim 10^6$  cells per ml, and filtered through a 40- $\mu$ m membrane just before analysis by mass cytometry.

**Mass cytometry analysis.** The age of the strains were not known at the time of the experiment. Cells were analyzed on a CyTOF mass cytometer (DVS Sciences) at an event rate of  $\sim 500$  cells per second. The settings of the instrument and the initial post-processing parameters were described previously (Bandura et al., 2009). For each barcoded sample several data files were recorded. The files were concatenated using the Cytobank concatenation tool, normalized (Finck et al., 2013) and debarcoded (Zunder et al., 2015).

**Data analysis-** After gating out viable and iridium labeled events, the data were analyzed by applying t-Distributed Stochastic Neighbor Embedding (tSNE). This non-linear dimensionally reduction technique is implemented via Barnes-Hut approximations in the Matlab toolbox *cyt* (Amir el et al., 2013). In tSNE, each cell is represented as a point in high-dimensional space. Each dimension is one parameter (the expression level of each protein in our case). An optimization algorithm searches for a projection of the points from the high-dimensional space into two dimensions such that pairwise distances between the points are best conserved between the high- and low-dimensional spaces.

The unsupervised PhenoGraph algorithm in *cyt* has been used to group cells which are phenotypically similar and cluster these subpopulations using modularity optimization (Levine et al., 2015). tSNE and PhenoGraph were performed only on surface markers.

The Citrus toolbox in R was used to identify clusters and markers that changed in abundance with age (Bruggner et al., 2014) in an unsupervised manner. Therefore, clusters were identified using a hierarchical clustering and linked to clinical data for characterization. The minimal selected cluster size was 0.1% of the total analyzed data. Stratifying clusters were learned by using regularized supervised learning methods.

Heatmaps were obtained with Cytobank.

**Classification-** Using a training-set of HMEC from 5 women <30y and 5 women >50y, Citrus efficiently assigned most of the test-set to “young” or “old”. The training-set was changed to N=8 to N=12 with an increased efficiency. After randomization of the training-set Citrus was not able to do the classification anymore, thus validating the system (data not shown).

Citrus uses nearest shrunken centroids as a predictive model to identify properties that are predictive of sample class. This method is implemented in the PAM package for R.

The prediction model is based on the initial training data model. Therefore, new samples are mapped and later assigned to the initial clusters for prediction.

**Model significance-** The optimal model regularization threshold was identified by using a fixed range of regularization thresholds. Cross-validation at each regularization threshold was used to estimate model error rates which were used to assess the quality of the models. Further details on result assessment and selection of a final regularization threshold can be found in the Citrus publication (Bruggner et al., 2014).

**xCELLigence analysis-** The lower xCELLigence chambers were filled with M87A media with 10% FPS and the upper chamber were filled with  $4 \times 10^5$  cells in serum-free M87 media. Cell Index (CI) and slopes were measured using the RTCA-DP instrument.

**In vivo section staining-** Paraffin-embedded tissue sections were deparaffinized and antigen-retrieved (Vector Labs). For immunofluorescence, sections were blocked with PBS/5% normal goat serum/0.1% Triton X-100, and incubated with anti-K14 (1:1,000, Covance, polyclonal rabbit) and anti-K19 (1:20, Developmental Studies Hybridoma Bank, clone Troma-III) overnight at 4°C, then visualized with fluorescent secondary antibodies (Invitrogen) and imaged with a 710LSM microscope (Carl Zeiss). Each image was represented as its Cellular Morphometric Context (Chang et al., 2013), which was constructed as the histogram of cellular morphometric subtypes derived from the cellular morphometric features (K14/K19 signals) through K-Means (dictionary size =1024). Homogeneous kernel map (Vedaldi and Zisserman, 2012) was then applied on the Cellular Morphometric Context representation, so that linear support vector machine (SVM) (Yang et al., 2009) could be adopted for efficient and effective differentiation among age groups.

Amir el, A.D., Davis, K.L., Tadmor, M.D., Simonds, E.F., Levine, J.H., Bendall, S.C., Shenfeld, D.K., Krishnaswamy, S., Nolan, G.P., and Pe'er, D. (2013). viSNE enables visualization of high dimensional single-cell data and reveals phenotypic heterogeneity of leukemia. *Nat Biotechnol* *31*, 545-552.

Asiedu, M.K., Beauchamp-Perez, F.D., Ingle, J.N., Behrens, M.D., Radisky, D.C., and Knutson, K.L. (2014). AXL induces epithelial-to-mesenchymal transition and regulates the function of breast cancer stem cells. *Oncogene* *33*, 1316-1324.

Bandura, D.R., Baranov, V.I., Ornatsky, O.I., Antonov, A., Kinach, R., Lou, X., Pavlov, S., Vorobiev, S., Dick, J.E., and Tanner, S.D. (2009). Mass cytometry: technique for real time single cell multitarget immunoassay based on inductively coupled plasma time-of-flight mass spectrometry. *Analytical chemistry* *81*, 6813-6822.

Barash, I. (2006). Stat5 in the mammary gland: controlling normal development and cancer. *Journal of cellular physiology* *209*, 305-313.

Beerman, I., Bhattacharya, D., Zandi, S., Sigvardsson, M., Weissman, I.L., Bryder, D., and Rossi, D.J. (2010). Functionally distinct hematopoietic stem cells modulate hematopoietic lineage potential during aging by a mechanism of clonal expansion. *Proceedings of the National Academy of Sciences of the United States of America* *107*, 5465-5470.

Beerman, I., Bock, C., Garrison, B.S., Smith, Z.D., Gu, H., Meissner, A., and Rossi, D.J. (2013). Proliferation-dependent alterations of the DNA methylation landscape underlie hematopoietic stem cell aging. *Cell stem cell* *12*, 413-425.

Bendall, S.C., Nolan, G.P., Roederer, M., and Chattopadhyay, P.K. (2012). A deep profiler's guide to cytometry. *Trends in immunology* *33*, 323-332.

Bendall, S.C., Simonds, E.F., Qiu, P., Amir el, A.D., Krutzik, P.O., Finck, R., Bruggner, R.V., Melamed, R., Trejo, A., Ornatsky, O.I., *et al.* (2011). Single-cell mass cytometry of differential immune and drug responses across a human hematopoietic continuum. *Science* *332*, 687-696.

Biteau, B., Hochmuth, C.E., and Jasper, H. (2008). JNK activity in somatic stem cells causes loss of tissue homeostasis in the aging *Drosophila* gut. *Cell stem cell* *3*, 442-455.

Bodenmiller, B., Zunder, E.R., Finck, R., Chen, T.J., Savig, E.S., Bruggner, R.V., Simonds, E.F., Bendall, S.C., Sachs, K., Krutzik, P.O., *et al.* (2012). Multiplexed mass cytometry profiling of cellular states perturbed by small-molecule regulators. *Nat Biotechnol* *30*, 858-867.

Brantley, D.M., Chen, C.L., Muraoka, R.S., Bushdid, P.B., Bradberry, J.L., Kittrell, F., Medina, D., Matrisian, L.M., Kerr, L.D., and Yull, F.E. (2001). Nuclear factor-kappaB (NF-kappaB) regulates proliferation and branching in mouse mammary epithelium. *Molecular biology of the cell* *12*, 1445-1455.

Bruggner, R.V., Bodenmiller, B., Dill, D.L., Tibshirani, R.J., and Nolan, G.P. (2014). Automated identification of stratifying signatures in cellular subpopulations. *Proceedings of the National Academy of Sciences of the United States of America* *111*, E2770-2777.

Carey, L.A., Perou, C.M., Livasy, C.A., Dressler, L.G., Cowan, D., Conway, K., Karaca, G., Troester, M.A., Tse, C.K., Edmiston, S., *et al.* (2006). Race, breast cancer subtypes, and survival in the Carolina Breast Cancer Study. *Jama* *295*, 2492-2502.

Cerchiari, A.E., Garbe, J.C., Jee, N.Y., Todhunter, M.E., Broaders, K.E., Peehl, D.M., Desai, T.A., LaBarge, M.A., Thomson, M., and Gartner, Z.J. (2015). A strategy for tissue self-organization that is robust to cellular heterogeneity and plasticity. *Proceedings of the National Academy of Sciences of the United States of America* *112*, 2287-2292.

Challen, G.A., Boles, N.C., Chambers, S.M., and Goodell, M.A. (2010). Distinct hematopoietic stem cell subtypes are differentially regulated by TGF-beta1. *Cell stem cell* *6*, 265-278.

Chan, S.R., Vermi, W., Luo, J., Lucini, L., Rickert, C., Fowler, A.M., Lonardi, S., Arthur, C., Young, L.J., Levy, D.E., *et al.* (2012). STAT1-deficient mice spontaneously develop estrogen receptor alpha-positive luminal mammary carcinomas. *Breast cancer research : BCR* *14*, R16.

Chang, H., Borowsky, A., Spellman, P., and Parvin, B. (2013). Classification of Tumor Histology by Morphometric Context. *Proceedings / CVPR, IEEE Computer Society Conference on Computer Vision and Pattern Recognition IEEE Computer Society Conference on Computer Vision and Pattern Recognition 2013*.

Dembowy, J., Adissu, H.A., Liu, J.C., Zacksenhaus, E., and Woodgett, J.R. (2015). Effect of glycogen synthase kinase-3 inactivation on mouse mammary gland development and oncogenesis. *Oncogene* *34*, 3514-3526.

Dietze, E.C., Bowie, M.L., Mrozek, K., Caldwell, L.E., Neal, C., Marjoram, R.J., Troch, M.M., Bean, G.R., Yokoyama, K.K., Ibarra, C.A., *et al.* (2005). CREB-binding protein regulates apoptosis and growth of HMECs grown in reconstituted ECM via laminin-5. *Journal of cell science* *118*, 5005-5022.

dos Santos, C.O., Rebbeck, C., Rozhkova, E., Valentine, A., Samuels, A., Kadiri, L.R., Osten, P., Harris, E.Y., Uren, P.J., Smith, A.D., *et al.* (2013). Molecular hierarchy of mammary differentiation yields refined markers of mammary stem cells. *Proceedings of the National Academy of Sciences of the United States of America* *110*, 7123-7130.

Fienberg, H.G., Simonds, E.F., Fantl, W.J., Nolan, G.P., and Bodenmiller, B. (2012). A platinum-based covalent viability reagent for single-cell mass cytometry. *Cytometry A* *81*, 467-475.

Finck, R., Simonds, E.F., Jager, A., Krishnaswamy, S., Sachs, K., Fantl, W., Pe'er, D., Nolan, G.P., and Bendall, S.C. (2013). Normalization of mass cytometry data with bead standards. *Cytometry Part A : the journal of the International Society for Analytical Cytology* *83*, 483-494.

Fu, N.Y., Rios, A.C., Pal, B., Soetanto, R., Lun, A.T., Liu, K., Beck, T., Best, S.A., Vaillant, F., Bouillet, P., *et al.* (2015). EGF-mediated induction of Mcl-1 at the switch to lactation is essential for alveolar cell survival. *Nature cell biology* *17*, 365-375.

Gallego, M.I., Binart, N., Robinson, G.W., Okagaki, R., Coschigano, K.T., Perry, J., Kopchick, J.J., Oka, T., Kelly, P.A., and Hennighausen, L. (2001). Prolactin, growth hormone, and epidermal growth factor activate Stat5 in different compartments of mammary tissue and exert different and overlapping developmental effects. *Developmental biology* *229*, 163-175.

Garbe, J.C., Bhattacharya, S., Merchant, B., Bassett, E., Swisshelm, K., Feiler, H.S., Wyrobek, A.J., and Stampfer, M.R. (2009). Molecular distinctions between stasis and telomere attrition senescence barriers shown by long-term culture of normal human mammary epithelial cells. *Cancer research* *69*, 7557-7568.

Garbe, J.C., Pepin, F., Pelissier, F.A., Sputova, K., Fridriksdottir, A.J., Guo, D.E., Villadsen, R., Park, M., Petersen, O.W., Borowsky, A.D., *et al.* (2012). Accumulation of multipotent progenitors with a basal differentiation bias during aging of human mammary epithelia. *Cancer research* *72*, 3687-3701.

Garbe, J.C., Vrba, L., Sputova, K., Fuchs, L., Novak, P., Brothman, A.R., Jackson, M., Chin, K., LaBarge, M.A., Watts, G., *et al.* (2014). Immortalization of normal human mammary epithelial cells in two steps by direct targeting of senescence barriers does not require gross genomic alterations. *Cell Cycle* *13*, 3423-3435.

Geiger, H., de Haan, G., and Florian, M.C. (2013). The ageing haematopoietic stem cell compartment. *Nature reviews Immunology* *13*, 376-389.

Giacinti, C., and Giordano, A. (2006). RB and cell cycle progression. *Oncogene* *25*, 5220-5227.

Haricharan, S., and Li, Y. (2014). STAT signaling in mammary gland differentiation, cell survival and tumorigenesis. *Molecular and cellular endocrinology* *382*, 560-569.

Hebbard, L., Steffen, A., Zawadzki, V., Fieber, C., Howells, N., Moll, J., Ponta, H., Hofmann, M., and Sleeman, J. (2000). CD44 expression and regulation during mammary gland development and function. *Journal of cell science* *113 ( Pt 14)*, 2619-2630.

Henry, C.J., Marusyk, A., and DeGregori, J. (2011). Aging-associated changes in hematopoiesis and leukemogenesis: what's the connection? *Aging* *3*, 643-656.

Hilton, H.N., Santucci, N., Silvestri, A., Kantimm, S., Huschtscha, L.I., Graham, J.D., and Clarke, C.L. (2014). Progesterone stimulates progenitor cells in normal human breast and breast cancer cells. *Breast cancer research and treatment* *143*, 423-433.

Jenkins, E.O., Deal, A.M., Anders, C.K., Prat, A., Perou, C.M., Carey, L.A., and Muss, H.B. (2014). Age-specific changes in intrinsic breast cancer subtypes: a focus on older women. *The oncologist* *19*, 1076-1083.

Jin, P., Hardy, S., and Morgan, D.O. (1998). Nuclear localization of cyclin B1 controls mitotic entry after DNA damage. *The Journal of cell biology* *141*, 875-885.

Labarge, M.A., Garbe, J.C., and Stampfer, M.R. (2013). Processing of human reduction mammoplasty and mastectomy tissues for cell culture. *Journal of visualized experiments* : JoVE.

LaBarge, M.A., Mora-Blanco, E.L., Samson, S., and Miyano, M. (2015). Breast Cancer beyond the Age of Mutation. *Gerontology*.

LaBarge, M.A., Petersen, O.W., and Bissell, M.J. (2007). Of microenvironments and mammary stem cells. *Stem cell reviews* *3*, 137-146.

Lee, J.K., Garbe, J.C., Vrba, L., Miyano, M., Futscher, B.W., Stampfer, M.R., and LaBarge, M.A. (2015). Age and the means of bypassing stasis influence the intrinsic subtype of immortalized human mammary epithelial cells. *Frontiers in cell and developmental biology* *3*, 13.

Levine, J.H., Simonds, E.F., Bendall, S.C., Davis, K.L., Amir el, A.D., Tadmor, M.D., Litvin, O., Fienberg, H.G., Jager, A., Zunder, E.R., *et al.* (2015). Data-Driven Phenotypic Dissection of AML Reveals Progenitor-like Cells that Correlate with Prognosis. *Cell* *162*, 184-197.

Lim, E., Vaillant, F., Wu, D., Forrest, N.C., Pal, B., Hart, A.H., Asselin-Labat, M.L., Gyorki, D.E., Ward, T., Partanen, A., *et al.* (2009a). Aberrant luminal progenitors as the candidate target population for basal tumor development in BRCA1 mutation carriers. *Nature medicine* *15*, 907-913.

Lim, E., Vaillant, F., Wu, D., Forrest, N.C., Pal, B., Hart, A.H., Asselin-Labat, M.L., Gyorki, D.E., Ward, T., Partanen, A., *et al.* (2009b). Aberrant luminal progenitors as the candidate target population for basal tumor development in BRCA1 mutation carriers. *Nature medicine* *15*, 907-913.

Lou, X., Zhang, G., Herrera, I., Kinach, R., Ornatsky, O., Baranov, V., Nitz, M., and Winnik, M.A. (2007). Polymer-based elemental tags for sensitive bioassays. *Angewandte Chemie* *46*, 6111-6114.

Louderbough, J.M., Brown, J.A., Nagle, R.B., and Schroeder, J.A. (2011). CD44 Promotes Epithelial Mammary Gland Development and Exhibits Altered Localization during Cancer Progression. *Genes & cancer* *2*, 771-781.

Mansilla, E., Diaz Aquino, V., Zambon, D., Marin, G.H., Martire, K., Roque, G., Ichim, T., Riordan, N.H., Patel, A., Sturla, F., *et al.* (2011). Could metabolic syndrome, lipodystrophy, and aging be mesenchymal stem cell exhaustion syndromes? *Stem cells international* *2011*, 943216.

Menard, S., Tagliabue, E., Campiglio, M., and Pupa, S.M. (2000). Role of HER2 gene overexpression in breast carcinoma. *Journal of cellular physiology* *182*, 150-162.

Pasic, L., Eisinger-Mathason, T.S., Velayudhan, B.T., Moskaluk, C.A., Brenin, D.R., Macara, I.G., and Lannigan, D.A. (2011). Sustained activation of the HER1-ERK1/2-RSK signaling pathway controls myoepithelial cell fate in human mammary tissue. *Genes & development* *25*, 1641-1653.

Paszek, M.J., Zahir, N., Johnson, K.R., Lakins, J.N., Rozenberg, G.I., Gefen, A., Reinhart-King, C.A., Margulies, S.S., Dembo, M., Boettiger, D., *et al.* (2005). Tensional homeostasis and the malignant phenotype. *Cancer Cell* *8*, 241-254.

Pelissier, F.A., Garbe, J.C., Ananthanarayanan, B., Miyano, M., Lin, C., Jokela, T., Kumar, S., Stampfer, M.R., Lorens, J.B., and LaBarge, M.A. (2014). Age-related dysfunction in mechanotransduction impairs differentiation of human mammary epithelial progenitors. *Cell reports* *7*, 1926-1939.

Raouf, A., Zhao, Y., To, K., Stingl, J., Delaney, A., Barbara, M., Iscove, N., Jones, S., McKinney, S., Emerman, J., *et al.* (2008). Transcriptome analysis of the normal human mammary cell commitment and differentiation process. *Cell stem cell* *3*, 109-118.

Raymond, K., Cagnet, S., Kreft, M., Janssen, H., Sonnenberg, A., and Glukhova, M.A. (2011). Control of mammary myoepithelial cell contractile function by alpha3beta1 integrin signalling. *The EMBO journal* 30, 1896-1906.

Regan, J.L., Kendrick, H., Magnay, F.A., Vafaizadeh, V., Groner, B., and Smalley, M.J. (2012). c-Kit is required for growth and survival of the cells of origin of Brca1-mutation-associated breast cancer. *Oncogene* 31, 869-883.

Reversi, A., Cassoni, P., and Chini, B. (2005). Oxytocin receptor signaling in myoepithelial and cancer cells. *Journal of mammary gland biology and neoplasia* 10, 221-229.

Rubin, I., and Yarden, Y. (2001). The basic biology of HER2. *Annals of oncology : official journal of the European Society for Medical Oncology / ESMO* 12 Suppl 1, S3-8.

Sansone, P., Ceccarelli, C., Berishaj, M., Chang, Q., Rajasekhar, V.K., Perna, F., Bowman, R.L., Vidone, M., Daly, L., Nnoli, J., et al. (2016). Self-renewal of CD133(hi) cells by IL6/Notch3 signalling regulates endocrine resistance in metastatic breast cancer. *Nature communications* 7, 10442.

Sharpless, N.E., and DePinho, R.A. (2007). How stem cells age and why this makes us grow old. *Nature reviews Molecular cell biology* 8, 703-713.

Signer, R.A., and Morrison, S.J. (2013). Mechanisms that regulate stem cell aging and life span. *Cell stem cell* 12, 152-165.

Skibinski, A., Breindel, J.L., Prat, A., Galvan, P., Smith, E., Rolfs, A., Gupta, P.B., Labaer, J., and Kuperwasser, C. (2014). The Hippo transducer TAZ interacts with the SWI/SNF complex to regulate breast epithelial lineage commitment. *Cell reports* 6, 1059-1072.

Stephens, P.J., Tarpey, P.S., Davies, H., Van Loo, P., Greenman, C., Wedge, D.C., Nik-Zainal, S., Martin, S., Varela, I., Bignell, G.R., et al. (2012). The landscape of cancer genes and mutational processes in breast cancer. *Nature* 486, 400-404.

Taylor-Papadimitriou, J., Stampfer, M., Bartek, J., Lewis, A., Boshell, M., Lane, E.B., and Leigh, I.M. (1989). Keratin expression in human mammary epithelial cells cultured from normal and malignant tissue: relation to in vivo phenotypes and influence of medium. *Journal of cell science* 94 ( Pt 3), 403-413.

Tumaneng, K., Schlegelmilch, K., Russell, R.C., Yimlamai, D., Basnet, H., Mahadevan, N., Fitamant, J., Bardeesy, N., Camargo, F.D., and Guan, K.L. (2012). YAP mediates crosstalk between the Hippo and PI(3)K-TOR pathways by suppressing PTEN via miR-29. *Nature cell biology* 14, 1322-1329.

van Landeghem, A.A., Poortman, J., Nabuurs, M., and Thijssen, J.H. (1985). Endogenous concentration and subcellular distribution of estrogens in normal and malignant human breast tissue. *Cancer research* 45, 2900-2906.

Vedaldi, A., and Zisserman, A. (2012). Efficient additive kernels via explicit feature maps. *IEEE transactions on pattern analysis and machine intelligence* 34, 480-492.

Villadsen, R., Fridriksdottir, A.J., Ronnov-Jessen, L., Gudjonsson, T., Rank, F., LaBarge, M.A., Bissell, M.J., and Petersen, O.W. (2007). Evidence for a stem cell hierarchy in the adult human breast. *The Journal of cell biology* 177, 87-101.

Vlug, E.J., van de Ven, R.A., Vermeulen, J.F., Bult, P., van Diest, P.J., and Derksen, P.W. (2013). Nuclear localization of the transcriptional coactivator YAP is associated with invasive lobular breast cancer. *Cellular oncology* 36, 375-384.

Watson, C.J. (2006). Involution: apoptosis and tissue remodelling that convert the mammary gland from milk factory to a quiescent organ. *Breast cancer research : BCR* 8, 203.

Wright, M.H., Calcagno, A.M., Salcido, C.D., Carlson, M.D., Ambudkar, S.V., and Varticovski, L. (2008). Brca1 breast tumors contain distinct CD44+/CD24- and CD133+ cells with cancer stem cell characteristics. *Breast cancer research : BCR* 10, R10.

Yang, J., Yu, K., Gong, Y., and Huang, T. (2009). Linear Spatial Pyramid Matching using Sparse Coding for Image Classification. *Proceedings of the Conference on Computer Vision and Pattern Recognition*, 1794-1801.

Zhao, B., Li, L., Lei, Q., and Guan, K.L. (2010). The Hippo-YAP pathway in organ size control and tumorigenesis: an updated version. *Genes & development* 24, 862-874.

Zivanovic, N., Jacobs, A., and Bodenmiller, B. (2014). A practical guide to multiplexed mass cytometry. *Curr Top Microbiol Immunol* 377, 95-109.

Zunder, E.R., Finck, R., Behbehani, G.K., Amir el, A.D., Krishnaswamy, S., Gonzalez, V.D., Lorang, C.G., Bjornson, Z., Spitzer, M.H., Bodenmiller, B., *et al.* (2015). Palladium-based mass tag cell barcoding with a doublet-filtering scheme and single-cell deconvolution algorithm. *Nat Protoc* 10, 316-333.

## Figure legends

### **Figure 1. Mass Cytometry Analysis of Human Mammary Epithelial Cells (HMEC).** (A)

Summary of experimental design. (B) Strategy to analyze high-dimensional single-cell data and identify lineage and age-related phenotypic divergence. See also Figure S1.

### **Figure 2. Luminal and Myoepithelial Lineages Exhibit a Phenotypic Divergence.** (A) tSNE

maps from HMEC from women <30y (merged, N=16). Each dot represents one cell in the phenotypic space. The closer the distance between two cells, the more phenotypically similar. The marker expression is ranged from the lowest (blue) to the highest (red). (B) Log<sub>2</sub> fold change in marker expression of LEP over MEP manually gated from tSNE projection map. Student t-test \* p<0.05 N=16. See also Figure S2 and S3.

### **Figure 3. Age-Related Phenotypic Divergence in the Landscape of HMEC.** (A) Heatmaps of

marker expression in each clusters identified with automatic cell partitioning with PhenoGraph of HMEC from women <30y (merged, N=16). A stronger color indicates a higher marker expression. (B) tSNE projection of the clusters identified with PhenoGraph. Each cluster is color-coded, and the same color code is used in the other figure panels. (C) Heatmaps of marker expression in each clusters identified with PhenoGraph of HMEC from women >30 and <50y and women >50y (D). Data was normalized to values from <30y women to highlight age-related changes. Four abnormal samples were excluded from the analysis: a sample from milk fluid (250MK), two samples bearing BRCA1 or ATM mutation (90P and 245AT), and one sample from a tumor (173T). The fold change of marker expression is ranged from the lowest (blue) to the highest (red). (E) Plots of cell percentage in each cluster. Four abnormal samples we excluded: 250MK, 90P and 245AT, 173T. (F) Intra-sample heterogeneity for each woman is represented graphically by a horizontal bar in which segment lengths represent the proportion of

the sample assigned to each cluster, colored accordingly. The two horizontal bars represent the age of 30 and 50y. 250MK was excluded from the analysis.

**Figure 4. Evidence of Age-Dependent Phenotypic Divergence in the Luminal Population.**

The Citrus algorithm combines all samples into one aggregate data-set before identifying cell populations by hierarchical clustering of phenotypically similar cells. Next, cells are assigned back to the individual samples and cluster abundance is calculated. Four abnormal samples were excluded: a sample from milk fluid (250MK), two samples bearing BRCA1 or ATM mutation (90P and 245AT), and one sample from a tumor (173T). (A) Boxplots of cell abundance in each cluster for each age-group and its representative tSNE phenotypic projection. (B) Heatmaps of marker expression in each cluster normalized to LEP from <30y women. (C) Graphs show cell migration index (CI) measured with xCELLigence instrument in FACS sorted LEP and MEP from women <30y and women >50y (N=3, p=0.045). (D) Plots show the fold change of LEP CI migration slope normalized to MEP CI migration slope in women <30y and >50y (N=3, Student t-test p=0.024). (E) Citrus classification using a training-set of five women <30y and five women >50y. (F) Representative human breast sections immunostained for K14 (red), K19 (green) and DAPI (blue) from a 32y woman (left panel) and a 67y woman (right panel). The arrows point to 2 clusters of K14+/K19+ cells (G) Plots show classification performance of breast sections from 171 women (<30y N=52, >30<50y N=86 and >50y N=33) analyzed using morphometric context with increasing training set size. See also Figure S4.

**Figure 5. Evidence of Age-dependent Phenotypic Divergence in HMEC progenitors. (A)**

tSNE maps from cKit FACS-enriched HMEC progenitors from three women <30y and three women >50y. The marker expression is ranged from the lowest (blue) to the highest (red). (B)

Boxplots of cell abundance in age-dependent clusters identified with Citrus and their representative tSNE spatial projection. (C) Heatmaps of marker expression in each cluster compared to the background. See also Figure S5.

**Figure 6. Chronological age influenced immortalization into luminal subtype.** (A) tSNE maps of eight immortalized strains are shown. Each color represents a strain. (B) Five selected marker are shown (K19, K4, K7, Axl and YAP) to illustrate phenotypic diversity. The marker expression is ranged from the lowest (blue) to the highest (red). (C) Heatmap of marker expression of each strain.

**Table S1. Cell strains analyzed.** HMEC strains were derived from reduction mammaplasty (RM), peripheral non-tumor regions from mastectomy (P) tissues, milk fluids (Milk) and a tumor (T). The name of the strain, the age at the time of surgery and the characteristics are indicated.

**Table S2. Antibody panel.** A panel of 29 antibodies is shown, comprising 10 highly informative surface markers, 12 antibody probes against intracellular phosphorylation, 4 antibody probes against the Hippo pathway and 3 antibody probes against cell cycle and apoptosis pathway. Each antibody clone, supplier, epitope and conjugated isotope is indicated. All the antibodies have been previously validated and titrated. References for relevant pathways in the regulation of HMEC are indicated.

**Figure S1. Validation of the Antibody Panel.** The antibody panel has been extensively validated and titrated (data not shown). (A) Scatter plots show the antibody staining in women <30y (merged, N=16) to reveal the signal quality of each marker, ranging from  $10^0$  to  $10^4$  ion counts per cell. (B) Heatmaps of marker expression in HMEC from three <30y and >50y women

treated with EGF and vanadate for 60min, then manually gated after tSNE projection. At,  $t=0$ , 10, 30 and 60min cells were harvested and analyzed with mass cytometry using MCB and a panel of 23 antibody probes. The fold change of marker expression is ranged from the lowest (green) to the highest (red). This experiment validates the signaling pathway antibodies.

**Figure S2. Luminal and Myoepithelial Lineages Exhibit a Phenotypic Divergence in women >30 and <50y.** (A) tSNE maps from HMEC from women >30y and <50y (merged, N=9). Four abnormal samples we excluded: a sample from milk fluid (250MK), two samples bearing BRCA1 or ATM mutation (90P and 245AT), and one sample from a tumor (173T). The marker expression is ranged from the lowest (blue) to the highest (red). (B)  $\text{Log}_2$  fold change in marker expression of LEP over MEP manually gated from tSNE. Some differential marker expression were not significant due to a lower sample number (N=9) in addition to age-related changes. Student t-test \*  $p<0.05$  N=9.

**Figure S3. Luminal and Myoepithelial Lineages Exhibit a Phenotypic Divergence in women >50y.** (A) tSNE maps from HMEC from women >50y (merged, N=15). The marker expression is ranged from the lowest (blue) to the highest (red). (B)  $\text{Log}_2$  fold change in marker expression of LEP over MEP manually gated from tSNE. Student t-test \*  $p<0.05$  N=15.

**Figure S4. Evidence of Age-Dependent Phenotypic Divergence in Luminal Subpopulations.** (A) Hierarchical tree of agglomerative clusters. A circle represents a cell cluster. Bubbles show main marker expression in the different parts of the tree. Clusters accumulating with age were in the luminal branch of the tree. (B) Citrus classification performance using 8, 10 or 12 training samples.

**Figure S5. Evidence of Age-Dependent Phenotypic Divergence in the in the cKit-progenitor population.** Hierarchical tree of agglomerative clusters. A circle represents a cell cluster. Bubbles show main marker expression in the different parts of the tree. The two clusters accumulating with age are shown.

**Figure S6. Age-related functional response to EGF activation.** HMEC from three <30y and >50y women were treated with EGF and vanadate for 60min. At, t=0, 10, 30 and 60min cells were harvested and analyzed with mass cytometry using MCB and a panel of 23 antibody probes. (A) Heatmaps of marker expression in LEP and MEP manually gated after tSNE projection. Data was normalized to values from <30y women to highlight age-related changes. The  $\log_2$  fold change is ranged from the lowest (blue) to the highest (red). (B) tSNE maps of HMEC from women <30y at t=0, 10, 30 and 60min. pEGFR expression is shown to highlight the movement of HMEC in the phenotypical space upon EGF activation. (C) Density plots in the tSNE phenotypic space exhibited a stronger response in women >50y upon EGF activation.

Figure 1

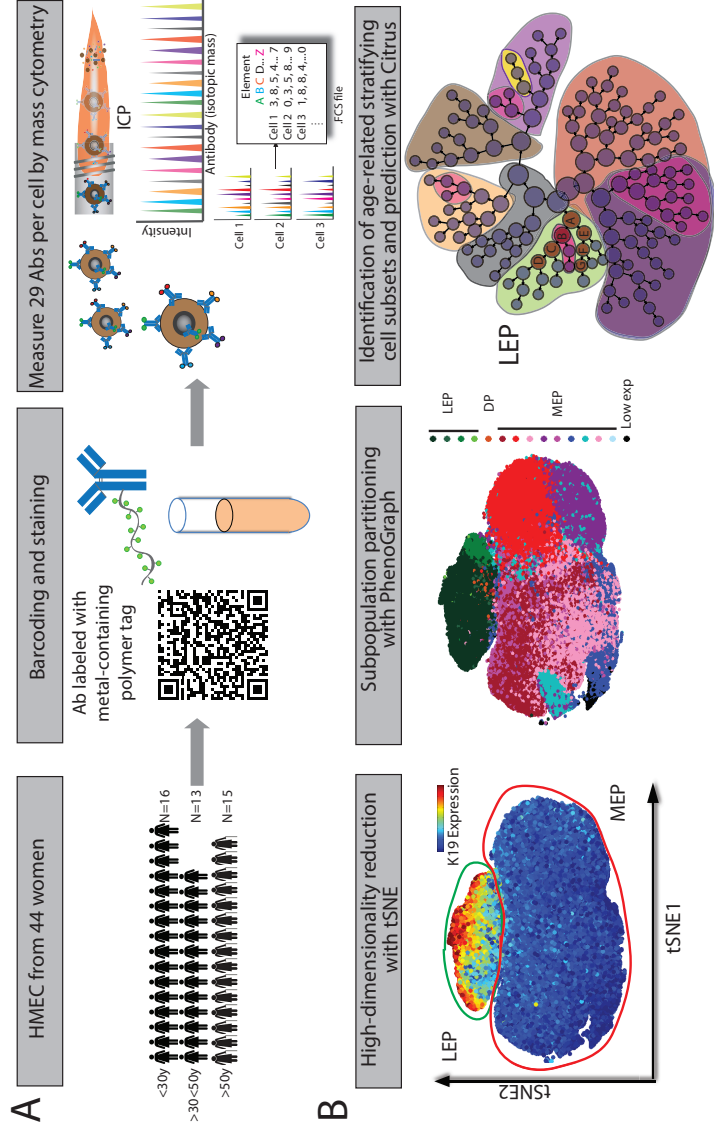
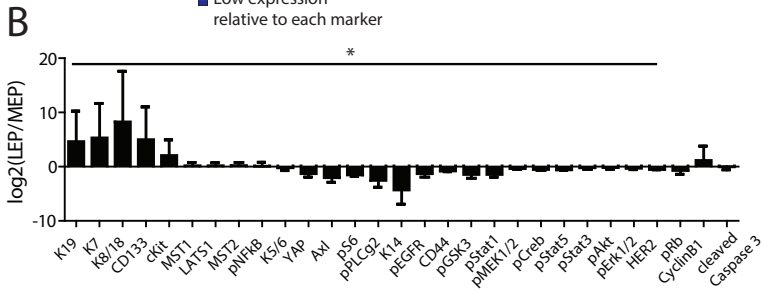
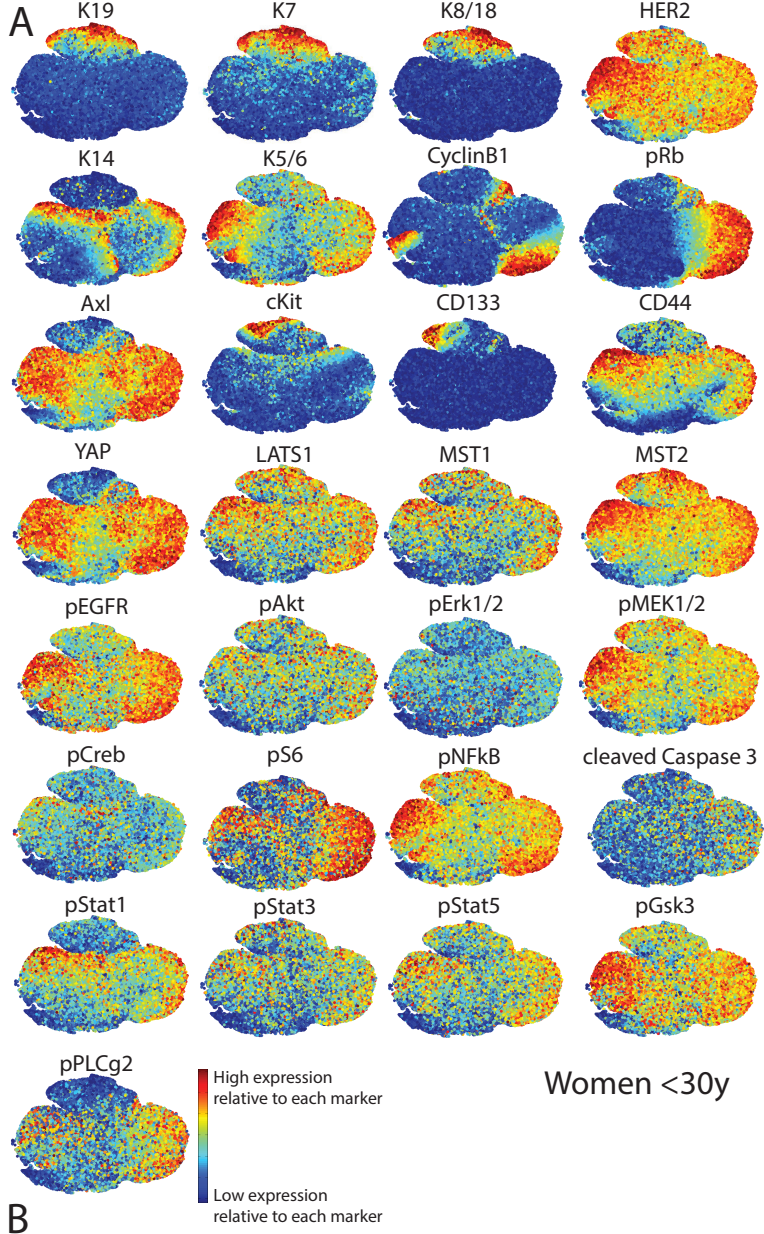
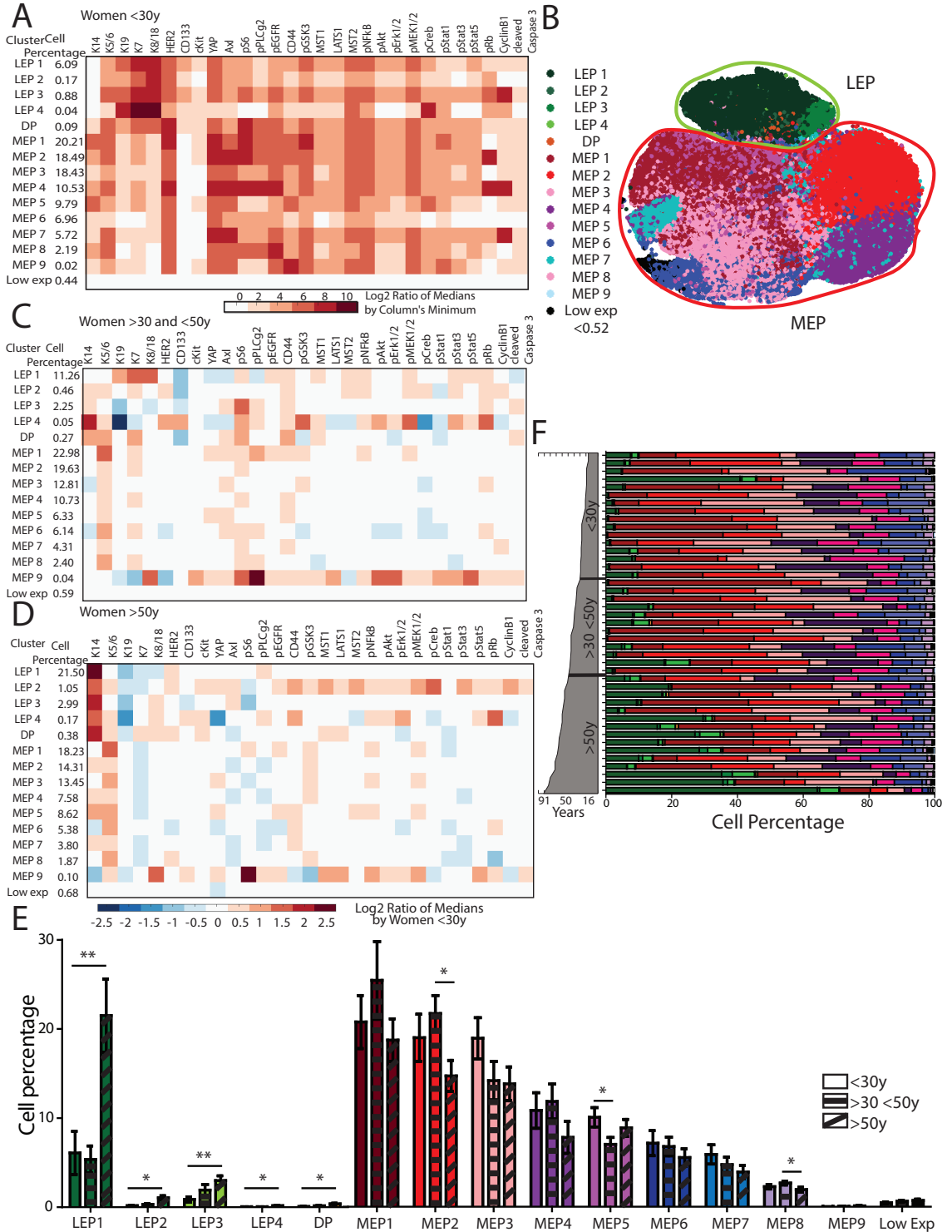


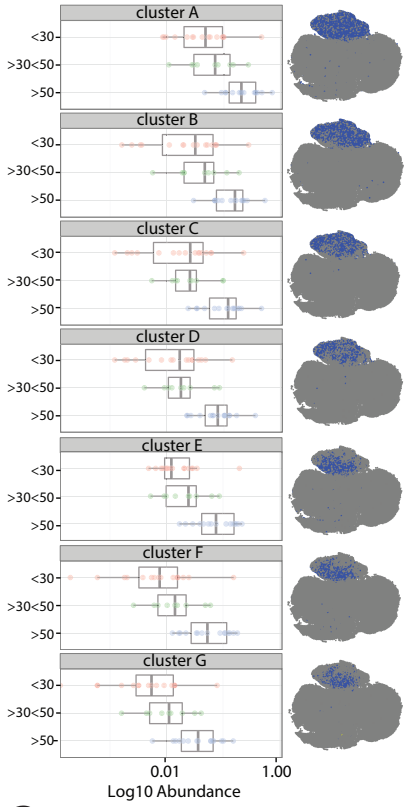
Figure 2



# Figure 3



# A Figure 4



# B Hierarchical Clusters

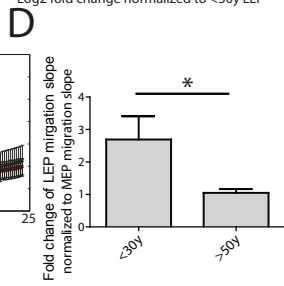
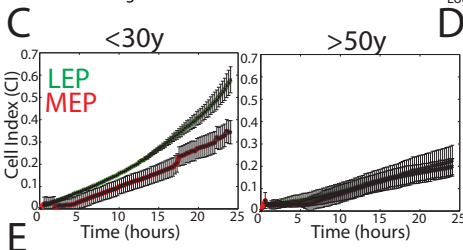
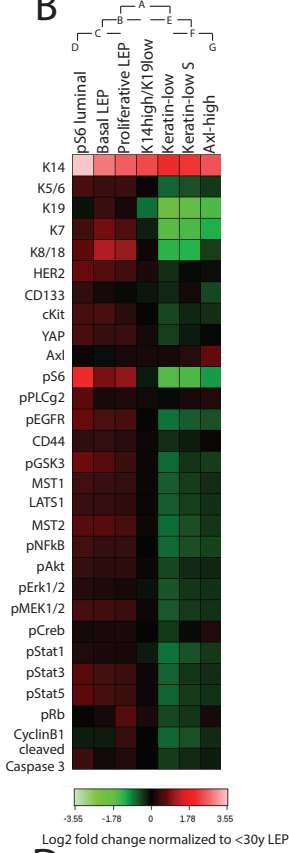


Figure 4E: Table showing Predictions and Correctly Assigned for three age groups.

Predictions	Correctly Assigned
<30	13/16 (81.25%)
>30<50	7/13*
>50	12/15 (80%)

\*7/13 assigned to "Young"  
6/13 assigned to "Old"

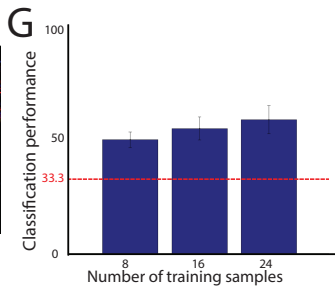
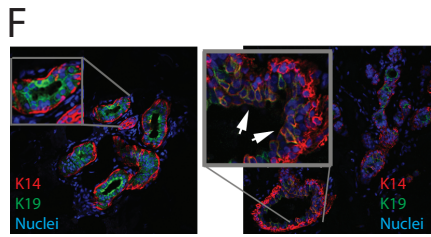


Figure 5

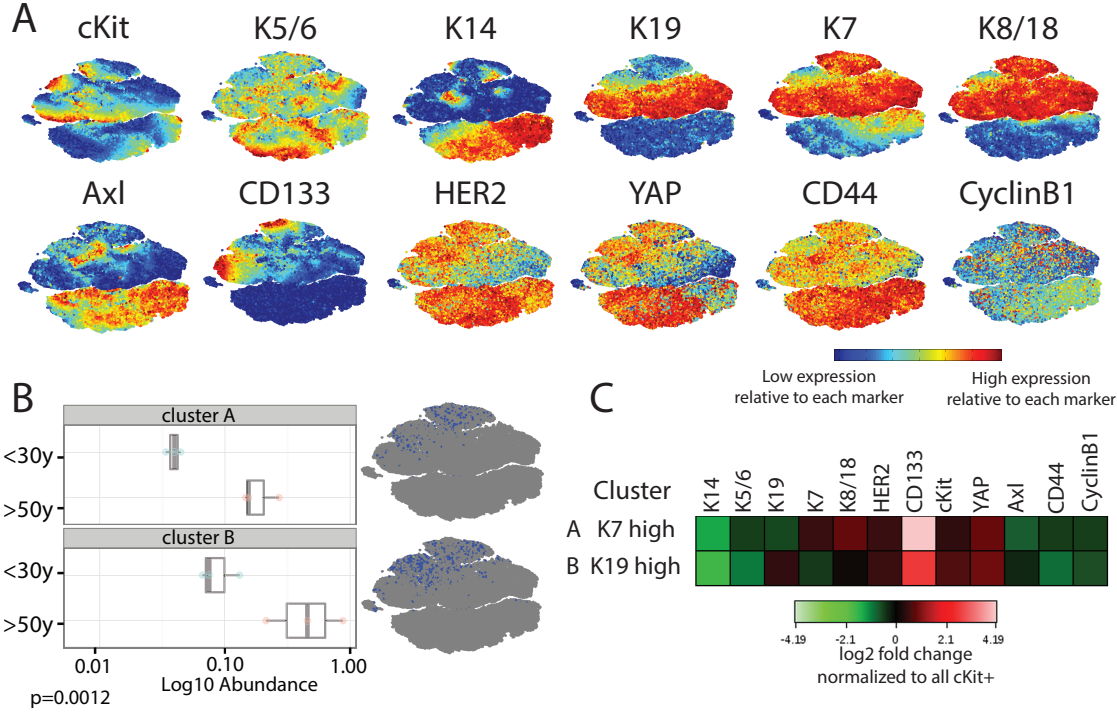
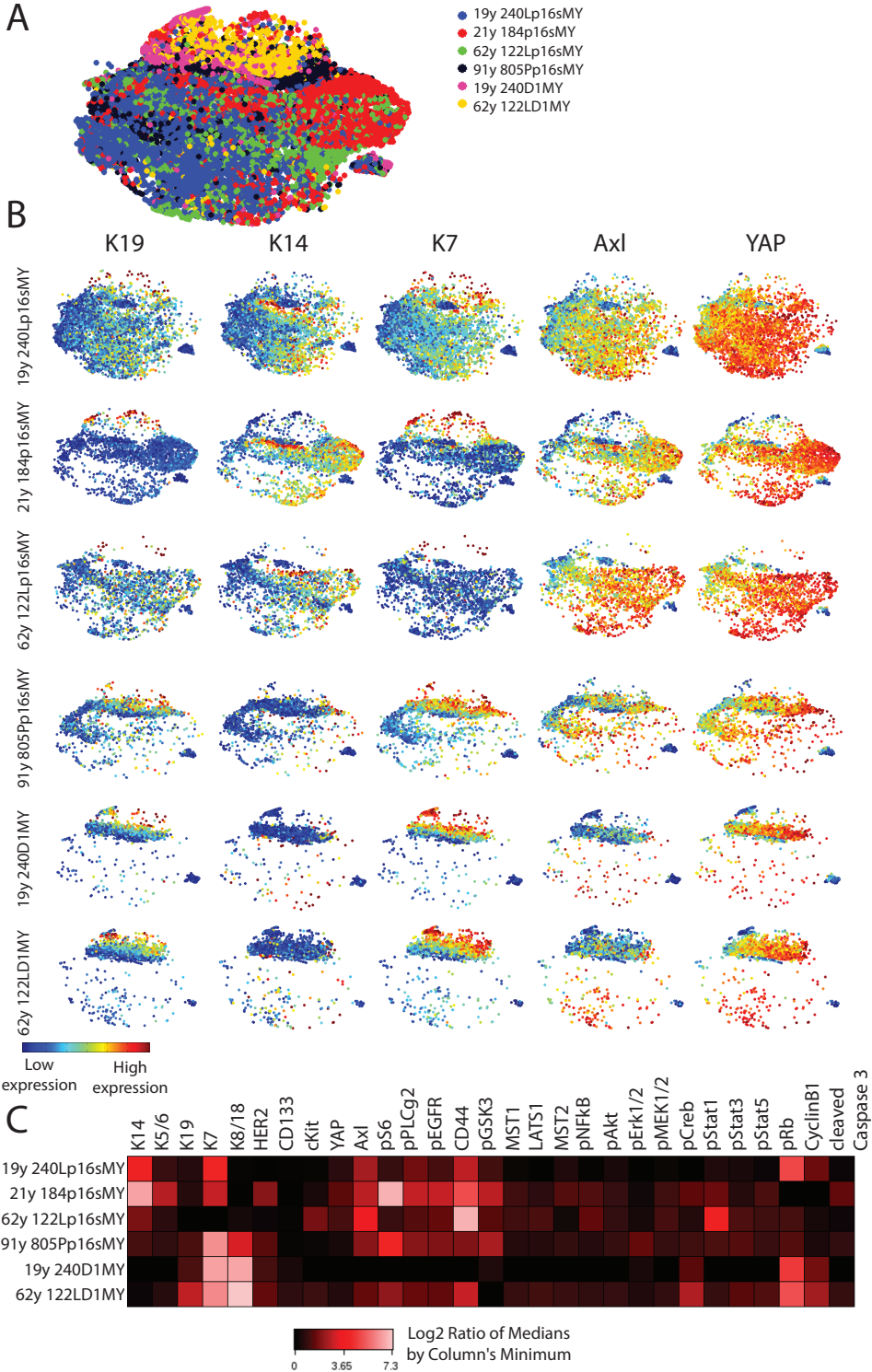


Figure 6



# Table S1

Women <30y			
Sample	Age, y	Source	Known characteristics/ pathology notes
48R	16	RM	African-American
160	16	RM	
407P	19	P	IDC, lymph node+, ER+, PR+
240L	19	RM	Mildly hyperplastic
168R	19	RM	African-American
399E	20	RM	Benign
184	21	RM	
356E	21	RM	Normal
001P	24	P	IDC, lymph node-
123	27	RM	African-American, mammary hyperplasia
195L	27	RM	
97	27	RM	
51L	28	RM	Mild periductal mastitis (R+L), focal microcalcification (R.)
172L	28	RM	Minimal phase of fibrocystic disease
676P	29	P	
124	29	RM	

Women >30y and <50y			
Sample	Age, y	Source	Known characteristics/ pathology notes
42P	30	P	IDC, lymph node-
169L	35	RM	
90P	36	P	BRCA-1 mut (185delAG)
250MK	37	Milk	
100P	39	P	Noninvasive ductal carcinoma, ER-, PR-
6	40	RM	
245AT	41	RM	ATM heterozygote, tissue was clinically normal tissue
173P	45	P	
173T	45	Tumor	IDC, ER-, PR-
208	45	RM	
2	46	RM	
60R	47	RM	
30	49	RM	

Women >50y			
Sample	Age, y	Source	Known characteristics/ pathology notes
178R	51	RM	
191L	56	RM	Slight fibrocystic disease, hypertrophy, stromal fibrosis, and adenosis present in mammary parenchyma
117R	56	RM	Patchy stromal fibrosis (R.), fibrocystic disease (L.)
335R	58	P	Infiltrating adenocarcinoma, ER+, PR+/-
153L	60	RM	Benign fibrocystic disease
639P	60	P	
122L	62	RM	Fibrocystic disease, hypertrophy, apocrine metaplasia of ductal epithelium, cystic dilatation of ducts, and focal areas of intraductal hyperplasia
881P	65	P	
96R	66	RM	Slight focal fibrocystic change
29	68	RM	
353P	72	P	Colloid (mucinous) carcinoma, ER+/-, PR-
429ER	72	RM	
464P	80	P	
451P	83	P	
805P	91	P	

Table S2

Isotope	Antigen	Antibody raised against	Pathway	References	Clone	Supplier
ER 170	K14	Total	Myoepithelial marker	(Villadsen et al., 2007)	polyclonal	Thermo
PR 141	K5/6	Total	Myoepithelial marker	(LaBarge et al., 2007)	D5	Millipore
DY 163	K19	Total	Luminal marker	(Villadsen et al., 2007)	Tromalll	DSHB
DY164	K7	Total	Luminal marker	(Taylor-Papadimitriou et al., 1989)	RCK105	BD
YB 174	K8/18	Total	Luminal marker	(Villadsen et al., 2007)	C51	CST
YB 173	CD133	Total, epitope 1	Luminal marker	(dos Santos et al., 2013)	AC133	Miltenyi
GD 161	cKit	Total	Progenitor marker	(Lim et al., 2009; Regan et al., 2012)	104D2	Biogen
ER 168	Axl	Total	Stemness	(Asiedu et al., 2014)	1H12	BerGenBio
GD 160	CD44	Total, surface	Stemness, migration	(Hebbard et al., 2000; Louderbough et al., 2011)	IM7	BD
HO 165	HER2	C terminal 1242-1255	Proliferation	(Rubin, Yarden, 2001; Yarden, 2011)	3B5	BD
ER 167	YAP	C terminal 379-407	Hippo	(Zhao et al., 2010; Vlugg et al., 2013)	H9	Santa Cruz
ND148	MST1	aa475-505	Hippo	(Zhao et al., 2010)	polyclonal	LS-Bio
SM149	LATS1	N-terminus	Hippo	(Zhao et al., 2010)	polyclonal	LS-Bio
DY 162	MST2	Total	Hippo	(Zhao et al., 2010)	polyclonal	LS-Bio
LA 139	pCreb	pS133	Survival	(Dietze et al., 2005)	J151-21	BD
ND 144	pMEK1/2	pS221	Myoepithelial contractility	(Pasic et al., 2011)	166F8	CST
ND 145	pStat3	pY705	Involution	(Haricharan and Li, 2014)	4/pStat3	BD
ND 146	pStat5	pY694	Lobuloalveolar development	(Gallego et al., 2001; Barash, 2006)	47	BD
ND150	pNFkB	pS529	Mammary gland morphogenesis	(Brantley et al., 2001)	K10-895.12.50	BD
EU 151	pEGFR	pY1068	Myoepithelial contractility	(Pasic et al., 2011; Paszek et al., 2005)	Y38	Abcam
SM152	pStat1	pY701	Tumor suppressor	(Chan et al., 2012; Haricharan and Li, 2014).	4a	BD
EU 153	pAkt	pS473	Survival	(Watson, 2006)	D9E	CST
SM 154	pErk1/2	pT202/pY204	Myoepithelial contractility	(Pasic et al., 2011)	20A	BD
GD 158	pGsk3	pS9 (Inactivation)	Milk synthesis and cell proliferation	(Demboway et al., 2015)	D85E12	CST
TM169	pPLCgamma2	pY759	Myoepithelial contractility	(Raymond et al., 2011; Reversi et al., 2005)	K86-689.37	BD
YB 171	pS6	pS235/pS236	Survival	(Fu et al. 2015; Tumaneng et al. 2012)	N7-548	BD
GD156	Cyclin B1	Total	Proliferation	(Jin et al., 1998)	GNS-11	BD
LU 175	pRb	pS807/811	Proliferation	(Giacinti and Giordano, 2006)	D20B12	CST
YT 172	Cleaved caspase3	Cleaved@D175	Apoptosis	(Watson, 2006)	5A1E	CST

Figure S1

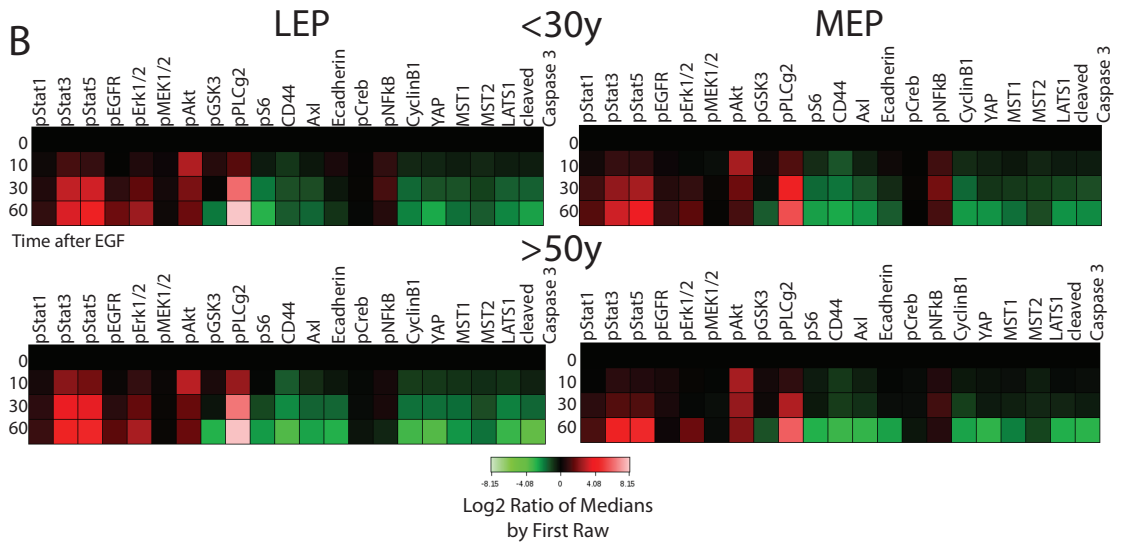
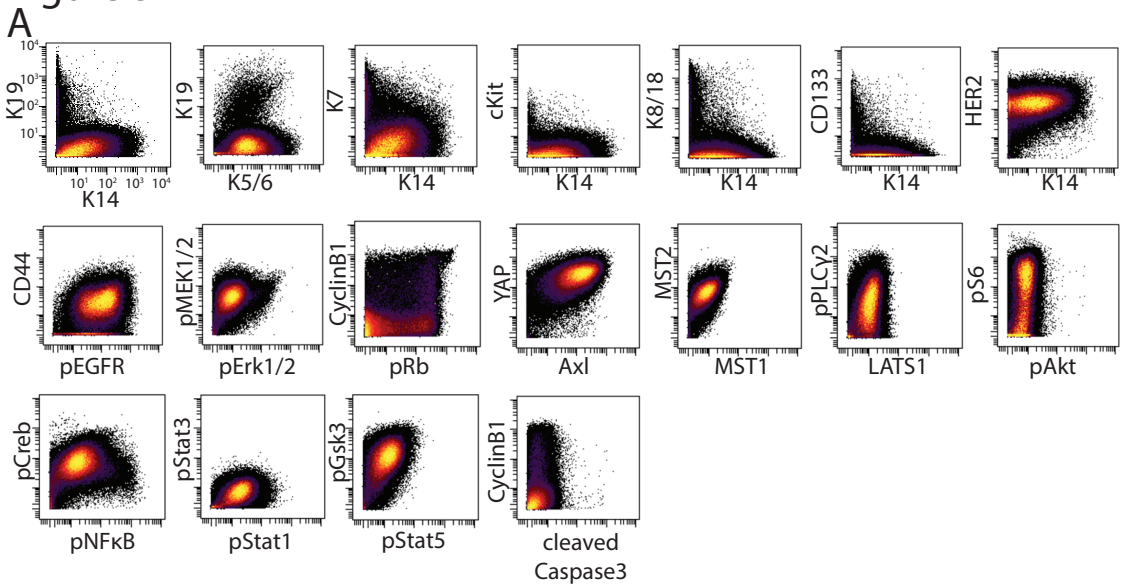


Figure S2

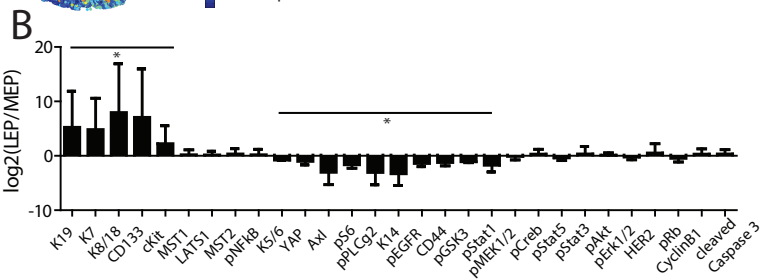
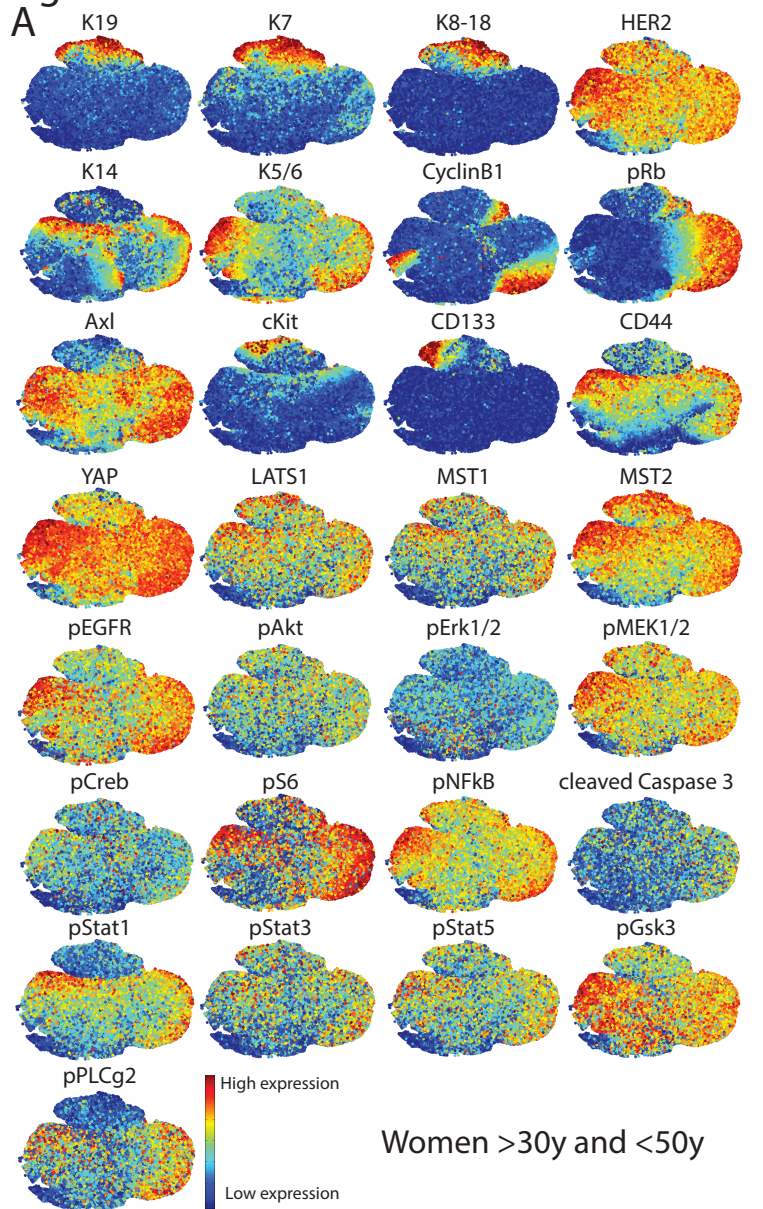


Figure S3

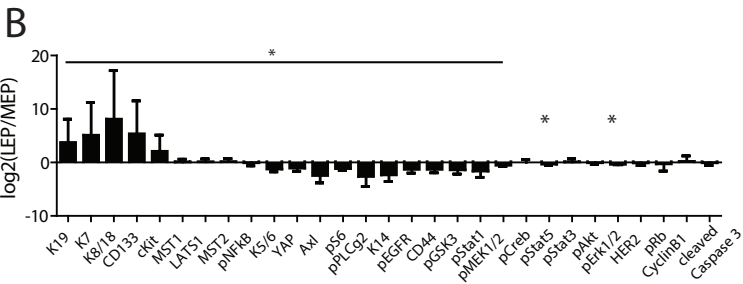
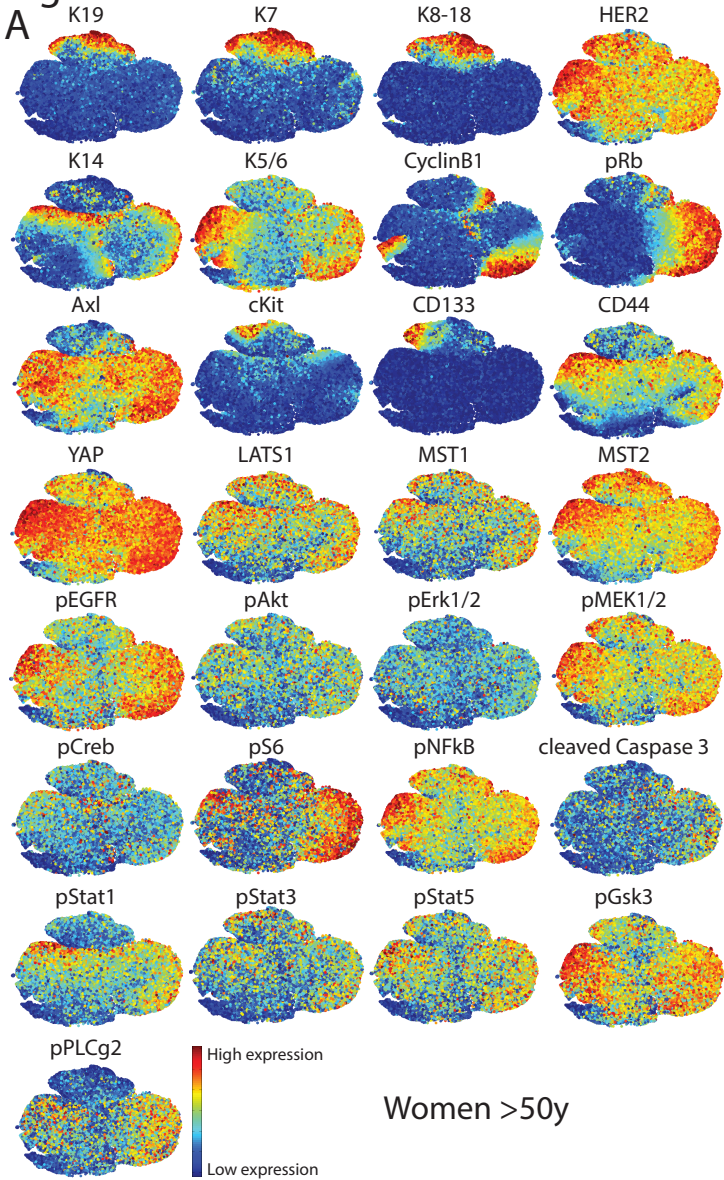


Figure S4

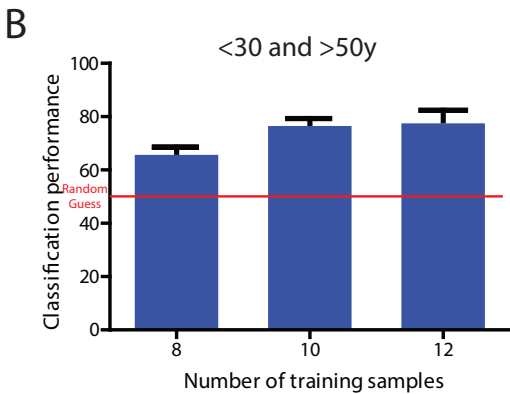
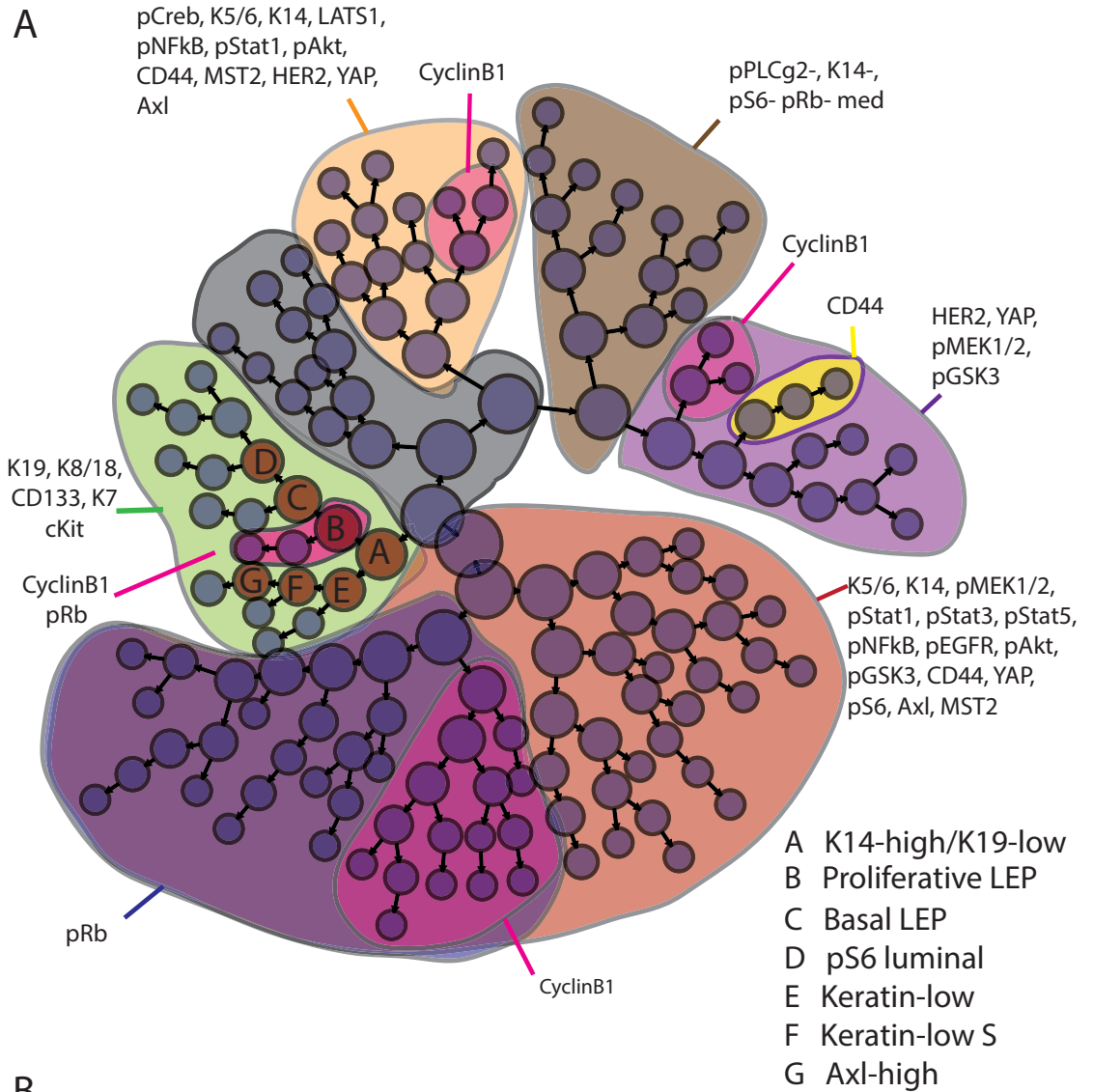


Figure S5

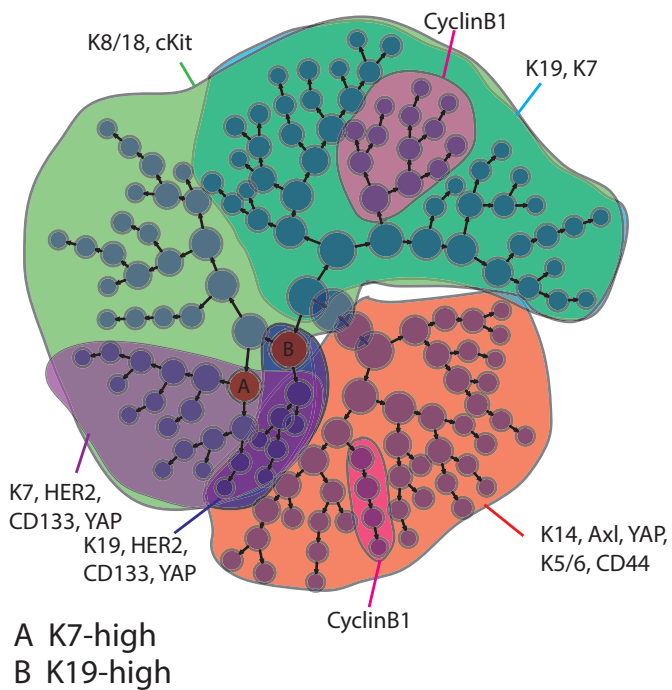


Figure S6

